



University
of Glasgow

Ali, Imran (2010) *Spacecraft nonlinear attitude control with bounded control input*. PhD thesis.

<http://theses.gla.ac.uk/1717/>

Copyright and moral rights for this thesis are retained by the author

A copy can be downloaded for personal non-commercial research or study, without prior permission or charge

This thesis cannot be reproduced or quoted extensively from without first obtaining permission in writing from the Author

The content must not be changed in any way or sold commercially in any format or medium without the formal permission of the Author

When referring to this work, full bibliographic details including the author, title, awarding institution and date of the thesis must be given.

SPACECRAFT NONLINEAR ATTITUDE CONTROL WITH BOUNDED CONTROL INPUT

Imran Ali

A thesis submitted for the degree of Doctor of Philosophy (PhD)

Department of Aerospace Engineering

Faculty of Engineering

University of Glasgow

November 2009

© Copyright 2009 by Imran Ali

All Rights Reserved

Dedication

To my parents and my family

Author's Declaration

Attention is drawn to the fact that copyright of this thesis rests with its author. This copy of the thesis has been supplied on the condition that anyone who consults it is understood to recognise that its copyright rests with the author and that no quotation from the thesis and no information derived from it may be published, without prior written consent of the author. This thesis may not be consulted, photocopied or lent by any library without the permission of the author for a period of six months from the date of acceptance of the thesis.

Abstract

The research in this thesis deals with nonlinear control of spacecraft attitude stabilization and tracking manoeuvres and addresses the issue of control torque saturation on a *priori* basis. The cascaded structure of spacecraft attitude kinematics and dynamics makes the method of integrator backstepping preferred scheme for the spacecraft nonlinear attitude control. However, the conventional backstepping control design method may result in excessive control torque beyond the saturation bound of the actuators. While remaining within the framework of conventional backstepping control design, the present work proposes the formulation of analytical bounds for the control torque components as functions of the initial attitude and angular velocity errors and the gains involved in the control design procedure. The said analytical bounds have been shown to be useful for tuning the gains in a way that the guaranteed maximum torque upper bound lies within the capability of the actuator and, hence, addressing the issue of control input saturation. Conditions have also been developed as well as the generalization of the said analytical bounds which allow for the tuning of the control gains to guarantee prescribed stability with the additional aim that the control action avoids reaching saturation while anticipating the presence of bounded external disturbance torque and uncertainties in the spacecraft moments of inertia. Moreover, the work has also been extended blending it with the artificial potential function method for achieving autonomous capability of avoiding pointing constraints for the case of spacecraft large angle slew manoeuvres. The idea of undergoing such manoeuvres using control moment gyros to track commanded angular momentum rather than a torque command has also been studied. In this context, a gimbal position command generation algorithm has been proposed for a pyramid-type cluster of four single gimbal control moment gyros. The proposed algorithm not only avoids the

saturation of the angular momentum input from the control moment gyro cluster but also exploits its maximum value deliverable by the cluster along the direction of the commanded angular momentum for the major part of the manoeuvre. In this way, it results in rapid spacecraft slew manoeuvres. The ideas proposed in the thesis have also been validated using numerical simulations and compared with results already existing in the literature.

Acknowledgements

First of all, I am grateful to Almighty Allah for blessing me with life and everything the greatest of what is His guidance through His Prophets (a.s.) and His Books with Imam u'l Anbiya Sayyidina Muhammad (may peace and blessings of Allah be upon His Prophet and the Prophet's Family (a.s.)) being the last Prophet and Umm Al-Kitab the Holy Quran the last Book.

Then, I would like to express my gratitude to my father and mother for praying for me all the time, missing me so hard and keeping my morale high during hard times of my research. I acknowledge the support of my wife Saira and my children Muhammad Bashir, Hifza and Dua who sacrificed a lot for the successful completion of my research and whose love kept me relaxed during tough times of my studies. I also want to thank my parents-in-law, my brothers Ali and Adnan, my sisters Humera, Sadaf and Najaf, my nephews Aun and Muhammad, my nieces Fatima and Momina, my brothers-in-laws Bilal and Blawal, sisters-in-law Samra and Saba and all my relatives for wishing me success.

I am also thankful to the government of Pakistan for funding my research. I would thank my supervisor Dr. Gianmarco who was supportive during my stay for PhD. I would acknowledge him and Charles Wallace Trust, Pakistan for supporting me for last few months of my research. I would thank Dr. Jongrae, Dr. Giulio, Dr. McQuade, Dr. Maruthi, and many others for the discussions with them and their comments regarding my research.

Table of Contents

Author's Declaration	3
Abstract	4
Acknowledgements	6
Table of Contents	7
List of Tables.....	9
List of Figures	11
Thesis Contributions	14
Publications	16
Nomenclature	17
1 Introduction	26
1.1 Spacecraft Attitude Control Issues.....	26
1.2 Open-Loop Control	27
1.3 Lyapunov-based Control.....	28
1.4 Nonlinear PID-based Control.....	30
1.5 Notion of Almost Global Stability	31
1.6 Attitude Parameterizations Related Issues	32
1.7 Quaternions as Attitude Parameterization.....	33
1.8 Variable Structure Sliding Mode Control	33
1.9 Integrator Backstepping-based Control.....	37
1.10 Other Miscellaneous Control Schemes	37
1.11 Potential Function Method for Constrained Attitude Manoeuvres	39
1.12 Actuators for Spacecraft Attitude Control	45
1.13 Control Moment Gyros as Actuators	47
1.14 Research Objectives	51

1.15	Thesis Outlines.....	53
2	Spacecraft Attitude Control with Bounded Torque Input.....	55
2.1	Rigid Spacecraft Attitude Motion.....	56
2.2	Control Design and Torque Bound.....	58
2.3	Robustness Analysis.....	63
2.4	Attitude Stabilization Specialization.....	68
2.5	Numerical Simulation.....	69
2.5.1	Stabilization Case.....	69
2.5.2	Tracking Case.....	81
3	Spacecraft Constrained Slew Manoeuvres with Bounded Control Torque.....	92
3.1	Pointing Constraint Avoidance.....	93
3.2	Control Design and Torque Bound.....	94
3.3	Robustness Analysis.....	99
3.4	Numerical Simulation.....	102
4	Spacecraft Rapid Slew Manoeuvres Using Control Moment Gyros.....	112
4.1	Attitude Motion of Rigid Spacecraft Equipped with CMGs.....	113
4.2	Gimbal Rate Steering Logic.....	115
4.3	Gimbal Position Steering Logic.....	116
4.4	Gimbal Position Steering Logic for Maximum Angular Momentum.....	119
4.5	Numerical Simulation.....	128
4.6	Summary.....	137
5	Conclusions and Future Work.....	138
	Appendix.....	143
	Bibliography.....	145

List of Tables

Table 2.1 Stabilization Example Nominal Case by Trial and Error	70
Table 2.2 Stabilization Example Nominal Case with Minimized Analytical Bound for Control Torque Norm.....	72
Table 2.3 Stabilization Example Nominal Case Simulation Results Comparison: All values taken from (Kim and Kim, 2003) except the ones for the proposed controller	74
Table 2.4 Stabilization Example Nominal Case with Minimized Analytical Bound for Control Torque Norm while Robustness Ensured	75
Table 2.5 Stabilization Example Non-nominal Case with Constant External Disturbance Torque	78
Table 2.6 Stabilization Example Non-nominal Case with Time Varying External Disturbance Torque.....	79
Table 2.7 Tracking Example Nominal Case by Trial and Error	85
Table 2.8 Tracking Example Nominal Case with Minimized Analytical Bound for Control Torque Norm.....	86
Table 2.9 Tracking Example Nominal Case with Minimized Analytical Bound for Control Torque Norm while Robustness Ensured.....	88
Table 2.10 Tracking Example Non-nominal Case with Constant External Disturbance Torque	90
Table 2.11 Tracking Example Non-nominal Case with Time Varying External Disturbance Torque	91
Table 3.1 Constrained Slew Manoeuvre Nominal Case by Trial and Error	103
Table 3.2 Constrained Slew Manoeuvre Nominal Case with Minimized Analytical Bound for Control Torque Norm	105

Table 3.3 Constrained Slew Manoeuvre Nominal Case with Minimized Analytical Bound for Control Torque Norm while Robustness Ensured.....	108
Table 3.4 Constrained Slew Manoeuvre Non-nominal Case with Time Varying External Disturbance Torque.....	111
Table 4.1 Data for the spacecraft equipped with pyramid-like cluster of four single-gimbal CMGs.....	128
Table 4.2 Data for the attitude manoeuvre examples for spacecraft equipped with pyramid-like cluster of four single-gimbal CMGs.....	128

List of Figures

Fig. 1.1 Sun vector avoidance	41
Fig. 1.2 Phase plane visualization of Lyapunov function	43
Fig. 1.3 Phase plane visualization of artificial potential function.....	44
Fig. 1.4 Single Gimbal Control Moment Gyro Unit	48
Fig. 2.1 Relations between the used frames: The reference frame \mathbf{R} is rigidly connected to the reference frame $\tilde{\mathbf{R}}$ and is misaligned with it in the same way as the principle-axis frame \mathbf{P} with the body frame \mathbf{B}	56
Fig. 2.2 Simulation results for the stabilization case example with the control gains tuned by trial and error.....	71
Fig. 2.3 Simulation results for the stabilization case example with the control gains tuned to minimize the analytical bound for control torque norm	73
Fig. 2.4 Simulation results for the stabilization case example with the control gains tuned to ensure robustness against bounded external disturbance and uncertain moments of inertia.....	76
Fig. 2.5 Simulation results for the stabilization case example under the action of constant bounded external disturbance and non-nominal moments of inertia	78
Fig. 2.6 Simulation results for the stabilization case example under the action of time varying bounded external disturbance and non-nominal moments of inertia.....	80
Fig. 2.7 Reference manoeuvre for the tracking case example	83
Fig. 2.8 Simulation results for the tracking case example with the control gains tuned by trial and error.....	85
Fig. 2.9 Simulation results for the tracking case example with the control gains optimized for the minimum analytical bound of control torque norm.....	86

Fig. 2.10 Simulation results for the tracking case example with the control gains tuned to ensure robustness against bounded external disturbance and uncertain moments of inertia	89
Fig. 2.11 Simulation results for the tracking case example under the action of constant bounded external disturbance and non-nominal moments of inertia	90
Fig. 2.12 Simulation results for the tracking case example under the action of time varying bounded external disturbance and non-nominal moments of inertia	91
Fig. 3.1 Simulation results for the constrained slew manoeuvre example with the control gains tuned by trial and error	104
Fig. 3.2 Simulation results for the constrained slew manoeuvre example with the control gains optimized for the minimum analytical bound of control torque norm	106
Fig. 3.3 Simulation results for the constrained slew manoeuvre example with the control gains optimized for the minimum analytical bound for control torque norm while ensuring robustness against bounded external disturbance and uncertain moments of inertia.....	109
Fig. 3.4 Simulation results for the constrained slew manoeuvre example under the action of time varying bounded external disturbance and non-nominal moments of inertia.....	110
Fig. 4.1 Pyramid mounting for a cluster of four single-gimbal CMGs.....	114
Fig. 4.2 Gimbal state with the direction $\hat{\mathbf{h}}_s$ considered as singular (Yoon, 2004)	121
Fig. 4.3 Singular surface for pyramid-type CMG cluster with $\hat{\mathbf{h}}_s \cdot \hat{\mathbf{s}}_i > 0$ for $i = 1, 2, 3, 4$ (Yoon, 2004)	121
Fig. 4.4 Singular surface for pyramid-type CMG cluster with $\hat{\mathbf{h}}_s \cdot \hat{\mathbf{s}}_i > 0$ for $i = 2, 3, 4$ and $\hat{\mathbf{h}}_s \cdot \hat{\mathbf{s}}_1 < 0$ (Yoon, 2004).....	122
Fig. 4.5 Angular momentum envelope for pyramid-type CMG cluster (Yoon, 2004)	122
Fig. 4.6 Singular surface for pyramid-type CMG cluster with $\hat{\mathbf{h}}_s \cdot \hat{\mathbf{s}}_i > 0$ for all i (i.e. $i = 1, 2, 3, 4$) and with $\hat{\mathbf{h}}_s \cdot \hat{\mathbf{s}}_i > 0$ for all i except one value for which $\hat{\mathbf{h}}_s \cdot \hat{\mathbf{s}}_i < 0$ (Yoon, 2004)	123
Fig. 4.7 Block diagram.....	127
Fig. 4.8 Simulation results for the benchmark roll manoeuvre with the gimbal position steering logic exploiting the maximum available angular momentum	129

Fig. 4.9 Simulation results for the benchmark roll manoeuvre with nonlinear approximate gimbal position steering logic	130
Fig. 4.10 Simulation results for the benchmark roll manoeuvre with the gimbal position steering logic exploiting the maximum available angular momentum while avoiding a pointing constraint.....	132
Fig. 4.11 Simulation results for the benchmark roll manoeuvre with nonlinear approximate gimbal position steering logic while avoiding a pointing constrain	134
Fig. 4.12 Simulation results for the three-axis slew manoeuvre with gimbal position steering logic for maximum angular momentum while incorporating two pointing constraints	136

Thesis Contributions

- The use of a generic class K_∞ function has been proposed within the framework of conventional integrator backstepping based nonlinear control of spacecraft attitude stabilization and tracking manoeuvres. A simple form of that function has introduced a new gain which proved to be useful for reducing the peak control torque. Moreover, the backstepping scheme has also been exploited for formulating the bounds for the control torque components analytically as a function of the initial attitude and angular velocity errors and the gains involved in the control design procedure. The said analytical bounds have been shown to be useful for tuning the gains in a way that the guaranteed maximum torque upper bound lies within the capability of the actuator and, hence, addressing the issue of control input saturation. Conditions have also been developed as well as the generalization of the said analytical bounds which allow for the tuning of the control gains to guarantee prescribed stability with the additional aim that the control action avoids reaching saturation in the presence of bounded external disturbance torque and uncertainties in the spacecraft moments of inertia.
- Integrator backstepping scheme has been blended with the artificial potential function method to propose a control law for the spacecraft large angle slew manoeuvres with autonomous ability of avoiding pointing constraints. The developments proposed for the general spacecraft attitude control problem guiding the tuning of the control gains to ensure stability while avoiding control torque saturation in the presence of bounded external disturbance torque and prescribed uncertain variations in the spacecraft moments of inertia have also been adapted for the case of aforesaid constrained slew manoeuvres.

- A gimbal position command generation algorithm has been proposed for a pyramid-type cluster of four single gimbal control moment gyros. The proposed algorithm exploits the maximum angular momentum deliverable by the control moment gyro cluster corresponding to the direction of the commanded angular velocity for the major part of the spacecraft reorientation manoeuvre and, hence, results in rapid slew manoeuvres.

Publications

[1] Ali, I., Radice, G., and Kim, J., "Backstepping Control Design with Actuator Torque Bound for Spacecraft Attitude Manuever", *Journal of Guidance, Control and Dynamics*, Vol. 33, No. 1, 2010, pp. 254-259, DOI: 10.2514/1.45541

[2] Ali, I., Kim, J., and Radice, G., "Large Angle Reorientation Manoeuvre of Spacecraft Using Robust Backstepping Control", *The 59th International Astronautical Congress*, Glasgow, UK, Sept. 29 - Oct. 3, 2008

[3] Ali, I., and Radice, G., "Autonomous Attitude Control Using Potential Function Method Under Control Input Saturation", *The 59th International Astronautical Congress*, Glasgow, UK, Sept. 29 - Oct. 3, 2008

[4] Avanzini, G., Radice, G., and Ali, I., "Potential Approach for Constrained Autonomous Manoeuvres of a Spacecraft Equipped with a Cluster of Control Moment Gyroscopes", *The 18th AAS/AIAA Space Flight Mechanics Meeting*, Galveston, Texas, USA, Jan. 27-31, 2008

[5] Avanzini, G., Radice, G., and Ali, I., "Potential Approach for Constrained Autonomous Manoeuvres of a Spacecraft Equipped with a Cluster of Control Moment Gyroscopes", *Advances in the Astronautical Sciences*, Vol. 130, No. 2, 2009, pp. 550-570

[6] Avanzini, G., Radice, G., and Ali, I., "Potential Approach for Constrained Autonomous Manoeuvres of a Spacecraft Equipped with a Cluster of Control Moment Gyroscopes", *Proceedings of the Institution of Mechanical Engineers, Part G: Journal of Aerospace Engineering*, Vol. 223, No. 3, 2009, pp. 285-296, DOI: 10.1243/09544100JAERO375

Nomenclature

Roman symbols

$\mathbf{b} = [b_v^T, b_4]^T =$ Unit quaternion describing the attitude of the principal-axis frame \mathbf{P} with respect to the constraint attitude represented by the quaternion $\mathbf{q}_c = [q_{cv}^T, q_{c4}]^T$

$\tilde{\mathbf{b}} = [\tilde{b}_v^T, \tilde{b}_4]^T =$ Unit quaternion describing the attitude of the body frame \mathbf{B} with respect to the constraint attitude represented by the quaternion $\tilde{\mathbf{q}}_c = [\tilde{q}_{cv}^T, \tilde{q}_{c4}]^T$

Control gains $(A, B, g, K_\delta, s, \alpha, \beta, \eta) =$ Positive constants where $(A, B, g, s, \alpha, \beta, \eta)$ are considered as optimizing parameters

$D_i =$ An upper bound for the components of external disturbance torque vector $\mathbf{T}_d = [T_1^d, T_2^d, T_3^d]^T$ where $|T_i^d| \leq D_i$ for $i = 1, 2, 3$

$\mathbf{e} = [e_1, e_2, e_3]^T =$ Angular velocity error vector where $e_i = \delta\omega_i - \delta\omega_i^s$ for $i = 1, 2, 3$

$\hat{\mathbf{g}}_i =$ Unit vector along the gimbal axis of the i th CMG of the pyramid-type cluster (expressed in the body frame \mathbf{B})

$\mathbf{h} = [h_1, h_2, h_3]^T =$ Total angular momentum vector due to the pyramid-type cluster of four single-gimbal control moment gyros

(expressed in the body frame \mathbf{B})

$h_{CMG} =$ Angular momentum magnitude due to each CMG of the pyramid-type cluster

$\mathbf{h}_i =$ Angular momentum vector due to the i th CMG of the pyramid-type cluster (expressed in the body frame \mathbf{B})

$\mathbf{h}_n =$ Maximal total angular momentum deliverable by the CMG cluster corresponding to the direction of \mathbf{h}_s

$\mathbf{h}_{np} =$ Component of \mathbf{h}_n perpendicular to \mathbf{h}_s

$\mathbf{h}_{nr} =$ Component of \mathbf{h}_n parallel to \mathbf{h}_s

$\mathbf{h}_s = [h_{s1}, h_{s2}, h_{s3}]^T =$ Commanded $\mathbf{h} = [h_1, h_2, h_3]^T$

$\hat{\mathbf{h}}_s =$ Unit vector parallel to \mathbf{h}_s (expressed in the body frame \mathbf{B})

$\dot{\mathbf{h}}_s =$ Commanded $\dot{\mathbf{h}}$

$\mathbf{H} =$ Total angular momentum vector of the spacecraft (expressed in the body frame \mathbf{B})

$\mathbf{J} =$ Principal-axis frame \mathbf{P} referenced nominal inertia matrix of the spacecraft where $\mathbf{J} = \mathbf{S}\mathbf{J}_B\mathbf{S}^T$ and $\mathbf{J} = \text{diag}(J_1, J_2, J_3)$

$\mathbf{J}_a =$ Principal-axis frame \mathbf{P} referenced non-nominal inertia matrix of the spacecraft where $\mathbf{J}_a = \text{diag}(J_1^a, J_2^a, J_3^a)$

$\mathbf{J}_B =$ Body frame \mathbf{B} referenced inertia matrix of the spacecraft

$\mathbf{M} =$ Jacobian matrix $\partial\mathbf{h}/\partial\boldsymbol{\delta}$

$p_i = (J_j - J_k)/J_i$ for $(i, j, k) \in \text{Id}$

$\mathbf{q} = [\mathbf{q}_v^T, q_4]^T =$ Unit quaternion describing the attitude of the principal-axis frame \mathbf{P} with respect to the inertial frame $\tilde{\mathbf{N}}$ where $\mathbf{q}_v = \mathbf{S}\tilde{\mathbf{q}}_v$ and $q_4 = \tilde{q}_4$

$\tilde{\mathbf{q}} = [\tilde{\mathbf{q}}_v^T, \tilde{q}_4]^T =$ Unit quaternion describing the attitude of the body frame \mathbf{B} with respect to the inertial frame \mathbf{N} where $\tilde{\mathbf{q}}_v = [\tilde{q}_1, \tilde{q}_2, \tilde{q}_3]^T$ is the vector part of $\tilde{\mathbf{q}}$ so that $\tilde{\mathbf{q}} = [\tilde{q}_1, \tilde{q}_2, \tilde{q}_3, \tilde{q}_4]^T$

$\mathbf{q}_c = [\mathbf{q}_{cv}^T, q_{c4}]^T =$ Unit quaternion describing the constraint attitude relative to the inertial frame $\tilde{\mathbf{N}}$ to be avoided by the principal-axis frame \mathbf{P} where $\mathbf{q}_{cv} = \mathbf{S}\tilde{\mathbf{q}}_{cv}$ and $q_{c4} = \tilde{q}_{c4}$

$\tilde{\mathbf{q}}_c = [\tilde{\mathbf{q}}_{cv}^T, \tilde{q}_{c4}]^T =$ Unit quaternion describing the constraint attitude relative to the inertial frame \mathbf{N} to be avoided by the body frame \mathbf{B}

$\mathbf{q}_r = [\mathbf{q}_{rv}^T, q_{r4}]^T =$ Unit quaternion describing the attitude of the frame $\tilde{\mathbf{R}}$ with respect to the inertial frame \mathbf{N} where $\mathbf{q}_{rv} = [q_{r1}, q_{r2}, q_{r3}]^T$ is the vector part of \mathbf{q}_r so that $\mathbf{q}_r = [q_{r1}, q_{r2}, q_{r3}, q_{r4}]^T$

$\Re =$ Set of real numbers

Reference frame $\mathbf{B} =$ A set of three mutually perpendicular axes fixed in spacecraft with origin at the centre of mass of the spacecraft also called as body frame

Reference frame $\mathbf{N} =$ An inertial frame

Reference frame $\tilde{\mathbf{N}} =$ An inertial frame represented by the reference frame \mathbf{R} for the case when the reference frame $\tilde{\mathbf{R}}$ becomes coincident with the inertial frame \mathbf{N}

Reference frame $\mathbf{P} =$ Spacecraft principal-axis frame

Reference frame \mathbf{R} = Reference frame which is rigidly connected to the reference frame $\tilde{\mathbf{R}}$ and is misaligned with it in the same way as the principal-axis frame \mathbf{P} with the body frame \mathbf{B}

Reference frame $\tilde{\mathbf{R}}$ = Reference frame corresponding to the commanded motion for the spacecraft attitude tracking problem

$\hat{\mathbf{s}}_i$ = Unit vector along the spin axis of the i th CMG of the pyramid-type cluster (expressed in the body frame \mathbf{B})

\mathbf{S} = Direction cosine matrix of the principal-axis frame \mathbf{P} relative to the body frame \mathbf{B}

Subscripts i, j, k = $(i, j, k) \in \text{Id}$ where $\text{Id} = \{(1, 2, 3), (2, 3, 1), (3, 1, 2)\}$

t = Time

t_f = Final time

$\hat{\mathbf{t}}_i$ = Unit vector along the gyroscopic torque axis of the i th CMG of the pyramid-type cluster where $\hat{\mathbf{t}}_i = \hat{\mathbf{g}}_i \times \hat{\mathbf{s}}_i$ (expressed in the body frame \mathbf{B})

t_0 = Starting time

t_{settling} = Settling time defined as the time at and after which the norm of the error state vector $[\boldsymbol{\sigma}_v^T, \boldsymbol{\delta\omega}^T]^T$ is bounded by 1% error from the steady state being zero

$\mathbf{T} = [T_1, T_2, T_3]^T$ = Spacecraft control torque vector expressed in the principal-axis frame \mathbf{P} where $\mathbf{T} = \mathbf{S}\mathbf{T}_B$

$\|\mathbf{T}_{\text{analytical}}\|$ = Analytical bound for the Euclidean norm of control torque vector

$\mathbf{T}_B =$ Spacecraft control torque vector expressed in the body frame
B

$\mathbf{T}_d = [T_1^d, T_2^d, T_3^d]^T =$ External disturbance torque vector expressed in the
principal-axis frame **P**

$\tilde{\mathbf{T}}_d =$ External disturbance torque vector expressed in the body
frame **B**

$U =$ Lyapunov function for the stabilization of complete
spacecraft attitude system comprising the attitude kinematics
and dynamics subsystems

$u_i = T_i / J_i$ for $i = 1, 2, 3$

$V =$ Lyapunov function for the spacecraft attitude kinematics
subsystem stabilization

$V_r =$ Repulsive potential to be added to the Lyapunov function V
for constructing the artificial potential function W

$\bar{V}_r =$ Lower bound of V_r corresponding to the minimum value of
the constraint separation angle $\Delta\theta$

$W =$ Artificial potential function for the spacecraft attitude
kinematics subsystem stabilization with constraints on
admissible attitudes

Greek symbols

$\gamma =$ An upper bound for the components of $\dot{\boldsymbol{\omega}}_r = [\dot{\omega}_1^r, \dot{\omega}_2^r, \dot{\omega}_3^r]^T$
where $|\dot{\omega}_i^r| \leq \gamma$ for $i = 1, 2, 3$

$\Gamma_e = (\delta_{s_2} + \delta_{s_4})/2$

$$\Gamma_o = (\delta_{s1} + \delta_{s3})/2$$

$\boldsymbol{\delta}$ = Gimbal angles vector for the pyramid-type cluster of four CMGs where $\boldsymbol{\delta} = [\delta_1, \delta_2, \delta_3, \delta_4]^T$

$\dot{\boldsymbol{\delta}}$ = Time rate of the gimbal angles vector for the CMG cluster

δ_i = Gimbal angle for the i th CMG of the pyramid-type cluster

$\dot{\delta}_{\max}$ = Gimbal angle rate limit for each CMG of the pyramid-type cluster

$\boldsymbol{\delta}_s$ = Commanded $\boldsymbol{\delta}$ (known as gimbal position command for the CMG cluster) where $\boldsymbol{\delta}_s = [\delta_{s1}, \delta_{s2}, \delta_{s3}, \delta_{s4}]^T$

$\dot{\boldsymbol{\delta}}_s$ = Commanded $\dot{\boldsymbol{\delta}}$ (known as gimbal rate command for the CMG cluster)

δ_{si} = Commanded gimbal angle for the i th CMG of the pyramid-type cluster

$\boldsymbol{\delta\omega} = [\delta\omega_1, \delta\omega_2, \delta\omega_3]^T$ = Angular velocity of the spacecraft with respect to the reference frame \mathbf{R} expressed in the principal-axis frame \mathbf{P}

$\frac{P}{dt}(\boldsymbol{\delta\omega}) = [\delta\dot{\omega}_1, \delta\dot{\omega}_2, \delta\dot{\omega}_3]^T$ = Angular acceleration of the spacecraft with respect to the reference frame \mathbf{R} expressed in the principal-axis frame \mathbf{P}

$\boldsymbol{\delta\omega}_s = [\delta\omega_1^s, \delta\omega_2^s, \delta\omega_3^s]^T$ = Pseudo control input for the stabilization of the kinematics subsystem corresponding the spacecraft attitude tracking problem (expressed in the principal-axis frame \mathbf{P})

$\Delta\theta$ = Eigen-axis rotation angle separating the spacecraft current attitude from the inadmissible (or constraint) attitude

$(\theta_1, \theta_2, \theta_3)$ = 3-2-1 Euler angles describing the attitude of the body frame

B with respect to the inertial frame **N**

$\lambda =$ Allowed normalized percentage variation for moments of inertia with respect to their nominal values

$\Lambda =$ Eigen-axis rotation angle separating the spacecraft current attitude from the desired one

$\Lambda_T =$ Threshold value of the angle Λ before which the gimbal position command transferring the maximum angular momentum is employed

$\mu =$ Pyramid skew angle for the CMG cluster

$\xi =$ An upper bound for the components of $\boldsymbol{\omega}_r = [\omega_1^r, \omega_2^r, \omega_3^r]^T$ where $|\omega_i^r| \leq \xi$ for $i = 1, 2, 3$

$$\Pi_e = (\delta_{s_2} - \delta_{s_4})/2$$

$$\Pi_o = (\delta_{s_1} - \delta_{s_3})/2$$

$\boldsymbol{\sigma} = [\sigma_v^T, \sigma_4]^T =$ Unit quaternion describing the attitude of the principal-axis frame **P** with respect to the reference frame **R** where $\boldsymbol{\sigma}_v = \mathbf{S}\tilde{\boldsymbol{\sigma}}_v$, $\sigma_4 = \tilde{\sigma}_4$ and $\boldsymbol{\sigma}_v = [\sigma_1, \sigma_2, \sigma_3]^T$ is the vector part of $\boldsymbol{\sigma}$ so that $\boldsymbol{\sigma} = [\sigma_1, \sigma_2, \sigma_3, \sigma_4]^T$

$\tilde{\boldsymbol{\sigma}} = [\tilde{\boldsymbol{\sigma}}_v^T, \tilde{\sigma}_4]^T =$ Unit quaternion describing the attitude of the body frame **B** with respect to the reference frame $\tilde{\mathbf{R}}$ where $\tilde{\boldsymbol{\sigma}}_v = [\tilde{\sigma}_1, \tilde{\sigma}_2, \tilde{\sigma}_3]^T$ is the vector part of $\tilde{\boldsymbol{\sigma}}$ so that $\tilde{\boldsymbol{\sigma}} = [\tilde{\sigma}_1, \tilde{\sigma}_2, \tilde{\sigma}_3, \tilde{\sigma}_4]^T$

$\phi(\sigma_i) =$ Nonlinear tracking function for designing $\delta\omega_i^s$ for $i = 1, 2, 3$ where a possible choice is $\phi(\sigma_i) = \alpha \tan^{-1}(\beta\sigma_i)$ for

$i = 1, 2, 3$ with α and β as positive constants

$\tilde{\phi}_i(\mathbf{q}) =$ Nonlinear tracking function for designing ω_i^s with $i = 1, 2, 3$ for constrained attitude stabilization problem where a possible choice is $\tilde{\phi}_i(\mathbf{q}) = q_i - BV_r b_i$ for $i = 1, 2, 3$ with V_r based on a Gaussian function being $V_r = A \exp\left(-\frac{1}{2} B \left[b_1^2 + b_2^2 + b_3^2 + (1-b_4)^2 \right]\right)$ and A and B as positive constants

$\boldsymbol{\omega} = [\omega_1, \omega_2, \omega_3]^T =$ Angular velocity of the spacecraft with respect to the inertial frame \mathbf{N} expressed in the principal-axis frame \mathbf{P} where $\boldsymbol{\omega} = \mathbf{S} \tilde{\boldsymbol{\omega}}$

$\tilde{\boldsymbol{\omega}} = [\tilde{\omega}_1, \tilde{\omega}_2, \tilde{\omega}_3]^T =$ Angular velocity of the spacecraft with respect to the inertial frame \mathbf{N} expressed in the body frame \mathbf{B}

$\boldsymbol{\omega}_r = [\omega_1^r, \omega_2^r, \omega_3^r]^T =$ Angular velocity of the reference frame \mathbf{R} with respect to the inertial frame \mathbf{N} expressed in the principal-axis frame \mathbf{P}

$\dot{\boldsymbol{\omega}}_r = [\dot{\omega}_1^r, \dot{\omega}_2^r, \dot{\omega}_3^r]^T =$ Angular acceleration of the reference frame \mathbf{R} with respect to the inertial frame \mathbf{N} expressed in the principal-axis frame \mathbf{P}

$\boldsymbol{\omega}_s = [\omega_1^s, \omega_2^s, \omega_3^s]^T =$ Pseudo control input for the stabilization of the kinematics subsystem corresponding the spacecraft attitude stabilization problem (expressed in the principal-axis frame \mathbf{P})

$\tilde{\boldsymbol{\omega}}_s =$ Pseudo control input for the stabilization of the kinematics subsystem corresponding the spacecraft attitude stabilization problem (expressed in the body frame \mathbf{B})

$\Omega(\cdot) =$ A class κ_∞ function which is defined to be zero at zero, strictly increasing and becomes unbounded as its argument

does so where a possible simple choice is $\Omega(x) = \eta x$ with $\eta > 0$

Acronyms

CMG = Control Moment Gyro

FEEP = Field Emission Electric Propulsion

ISO = Infrared Space Observatory

SAMPEX = Solar, Anomalous, and Magnetospheric Particle Explorer

Chapter 1

Introduction

Rigid body attitude control has been studied since long ago because of having many mechanical systems applications such as pointing and slewing of aircraft, helicopter, spacecraft, underwater vehicle and several other applications in robot manipulation. Future generations of these applications are expected to have more stringent requirements in terms of highly accurate pointing, fast slewing, and other rapid manoeuvres from large initial conditions under the action of large external disturbances, measurement noise and modelling uncertainties in conjunction with fault detecting, tolerating and isolating capabilities. Newly emerged idea of coordinated control of multiple agents or formation of agents (e.g. spacecraft) has imposed additional demand of controlling the attitudes of all the individuals tightly to follow the formation coordination commands rapidly and accurately.

1.1 Spacecraft Attitude Control Issues

Spacecrafts commonly function in the presence of different disturbances, including gravitational torque, aerodynamic torque, radiation torque, and other environmental and non-environmental torques. The problem of disturbance attenuation is predominantly

pronounced in the case of low-Earth-orbiting satellites that operate in the altitude ranges where their performance is significantly influenced by most of the above mentioned disturbances. Moreover, the facts that the inertia matrix of spacecraft is usually not known precisely and the movement of payload and appendages like telescope, camera and solar array causes the change of moments of inertia, especially for the case of microsattellites, render addressing the issue of parametric uncertainties an important consideration in the context of spacecraft attitude control design. Hence, disturbance attenuating control strategies that also ensure robustness against parametric uncertainties are of great importance. The control torques provided by the typical actuating devices for spacecraft attitude control are generally classified as being external or internal to the spacecraft. Actuators pertaining to the former kind such as thrusters can change the overall angular momentum of the spacecraft and the ones belonging to the latter type such as reaction wheels or control moment gyros (CMGs) can exchange angular momentum with it while the overall momentum remains constant. Now, there is an upper bound on the torque producible by the former onto the spacecraft or the angular momentum exchangeable by the latter with it. So, accounting for saturation of control input either in the form of torque or as exchangeable angular momentum is also of tremendous significance. Moreover, if the spacecraft is relatively stiff and does not use liquid fuels that can slosh then its approximation as a rigid body is sufficient for control design purposes. Otherwise, if the frequency of the lowest vibration or slosh mode is less than about six times the desired control bandwidth then flexibility or fuel slosh must be taken into account (Bryson, 1994).

1.2 Open-Loop Control

The rigid spacecraft attitude control problem has been studied quite widely (Hughes, 1986). A broad division of spacecraft attitude control algorithms can be classified as open-loop systems and closed-loop or feedback systems. Open-loop systems, usually based upon a pre-computed pointing manoeuvre trajectory, are typically determined using optimal control techniques involving the solution of a two-point-boundary-problem. The time-optimal attitude manoeuvre is an example of open-loop control. Works by Junkins and Turner (1980), Skaar and Kraige (1984), Vadali and Junkins (1984) and Bilimoria and Wie

(1993) are the examples of this kind of solutions to the spacecraft attitude control problem. Survey paper by Scrivener and Thompson (1994) provides an excellent account of such results. Lai, Yang and Wu (2007) recently proposed to use constrained nonlinear programming for time-optimal rest-to-rest manoeuvres of spacecraft while considering the actuator (reaction wheels) constraints. However, as open loop schemes lack any corrective measures based on the difference between desired and actual performance resulting from modelling uncertainties and external disturbances so these are generally sensitive to stated factors as well as non-nominal initial conditions. One of the key uses of feedback is to provide robustness against such uncertainties by supplying a corrective action. If the system undergoes some change that affects the performance then the closed-loop schemes sense this change and try to force the system back to the desired operating point. In the following, various closed-loop approaches that have been employed in the literature for spacecraft attitude control problem are reviewed.

1.3 Lyapunov-based Control

The necessity of highly precise slewing and/or pointing manoeuvres making the spacecraft rotate along relatively large-angle amplitude trajectories call for the utilization of a nonlinear dynamic spacecraft model for control system design. Among the various nonlinear control design methods that have been employed to solve the problem of spacecraft attitude stabilization/tracking, the main contributors are those based upon Lyapunov stability theory (Lyapunov, 1892, 1992).

The stability of a nonlinear dynamical system about a given equilibrium state or nominal reference trajectory refers to the behaviour of the system when displaced from the said desired state/states. Lyapunov proposed two theorems to deal with this property of dynamical systems. Lyapunov's first theorem, also called Lyapunov's linearization method or Lyapunov's indirect method, talks of the stability property of the nonlinear dynamical system by studying the stability of the system linearized about the equilibrium state or the nominal reference trajectory. However, the stability claims, if available, that can be made with the help of this theorem are valid only for a neighbourhood around the desired state/states. Lyapunov's second theorem, also known as Lyapunov's direct method, does

not rely on local linear approximations. It is based upon the existence of a scalar energy-like function for the dynamical system (Junkins and Bang, 1993b) which possesses continuous partial derivatives and is positive definite about the desired state/states whereas its time-rate is negative semidefinite/definite. Existence of such a function, called Lyapunov function, fulfilling the mentioned properties either locally around the desired state/states or globally, proves the local/global stability of the system. The selection of Lyapunov functions can be performed simultaneously with the design of controllers for the dynamical systems resulting in the stability claims for the closed-loop system (Junkins and Kim, 1993).

The work by Kalman and Bertram (1960a, 1960b) exemplifies the early uses of Lyapunov stability theory for the synthesis of feedback controllers. Starting from the research by Meyer (1966, 1971), a number of works (Creamer et al., 1996; Joshi, Kelkar and Wen, 1995; Reyhanoglu et al., 1999; Schaub, Robinett and Junkins, 1996; Schaub and Junkins, 1996; Schaub, Robinett and Junkins, 1997; Schaub and Junkins, 2003; Slotine and Li, 1991; Tsiotras, 1996; Wen and Kreutz-Delgado, 1991; Wie and Barba, 1985; Wie, Weiss and Arapostathis, 1989; Wie, 1998) followed the path of first selecting a candidate Lyapunov function and then extracting the nonlinear feedback control law for the spacecraft attitude stabilization/tracking problem. Creamer et al. (1996) demonstrated the on-orbit success of Lyapunov stability theory-based control law for the Clementine mission which used reaction wheels as the actuators in conjunction with a Kalman filter-based estimator for the spacecraft inertia. However, Robinett et al. (1997a, 1997b) were the first to use the Lyapunov's direct method to arrive at a saturated control design that was found to be effective in simulation studies. In particular, they employed the idea of Lyapunov optimality where the time derivative of the given Lyapunov function is made as negative as possible during the intervals where one or more of the control devices are saturated (Anderson and Grantham, 1989; Lee and Grantham, 1989; Junkins and Bang, 1993a; Schaub and Junkins, 2003). Nevertheless, Robinett et al. (1997a, 1997b) proved stability for the case of spacecraft angular velocity stabilization only and the stability analysis in the case of simultaneous stabilization of spacecraft attitude and angular velocity and more general spacecraft attitude tracking problem under control input saturation was

not carried out. They also did not carry out the robustness analysis of the approach for the later case against disturbances and model uncertainty. A similar problem was considered by Seywald (2001) also in the disturbance-free case, and the control law again needs the information about the inertia matrix.

1.4 Nonlinear PID-based Control

Wie and Lu (1995) addressed the problem of rapid reorientation under sensor and actuator constraints for the XTE spacecraft (Bauer, Femiano and Mosier, 1992). In the paper, only the rest-to-rest manoeuvres are investigated without considering the existence of external disturbances. Moreover, the controller robustness against uncertainties in the spacecraft inertia matrix is not explored. Wie, Heiberg and Bailey (2002) expanded upon the quaternion feedback based nonlinear proportional-integral-derivative (PID) type controllers in (Wie, and Barba, 1985; Wie, Weiss and Arapostathis, 1989; Wie, and Lu, 1995; Wie, 1998) to design a formulation which can be employed for rapid retargeting control of an agile spacecraft under the action of various physical constraints like actuator saturation, slew rate limit, control bandwidth limit and/or eigenaxis slew constraints. However, the authors acknowledged that, like any PID-type controller under control input saturation, their control logic is vulnerable to the so-called phenomenon of integrator windup resulting in large transient overshoot and control effort (Franklin, Powell and Emami-Naeini, 1994; Friedland, 1996) and it needs to be used in conjunction with the so-called integrator anti-windup or integrator synchronization which, in the case of a digital computer implementation, is realized by the simple turning off the integral action as soon as the actuator or any other limiter in the control loop saturates. Indeed, control input saturation resulting from the integral action is a classical issue in control engineering and various promising approaches in the name of anti-windup controller (AWC) have been proposed in the literature (Hanu, Kinnaert and Henrotte, 1987; Kothare, Campo, Morari and Nett, 1994; Teel and Kapoor, 1997; Choi, Bang and Kim, 1998). In general, windup is related to large oscillations and possible instability induced by saturation only. The integral element is sometimes provided by the dynamics of the system itself, rather than the controller, or being simply not present in the system. Considering integral effect as the

primary source of actuator saturation, (Bang, Tahk and Choi, 2003) investigated the modification of the conventional nonlinear PID-type controllers for spacecraft large angle manoeuvres to accommodate the anti-windup control and intelligent integrator (Krikelis, 1980) schemes. However, the stability analysis while incorporating the anti-windup control is not performed and a systematic way for choosing the feedback gains is also not mentioned.

1.5 Notion of Almost Global Stability

There exist some short comings with the aforementioned approach of solving the spacecraft attitude control problem using Lyapunov stability theory. Firstly, the natural state space for the spacecraft attitude control problem involves the special orthogonal group of 3×3 rotation matrices that describe spacecraft orientation in three dimensions, that is, $SO(3)$ and the compactness of $SO(3)$ presents difficulties with regards to global asymptotic stabilization, i.e. Lyapunov stability of a desired equilibrium point along with global convergence. To gain an insight into this problem, one can think of rotation of a rigid body about a fixed axis. The configuration space of the system can be represented by the unit circle in the complex plane. The unit circle can be transformed into a Euclidean vector space given by the real line where the origin 0 is seen as distinct from 2π . A controller designed using the real line parameterization for the actual configuration space rotate the rigid body needlessly from 2π to 0 . This is because of the fact that the same reference physical configuration is being represented on the real line by two distinct values 0 and 2π . The resulting unwinding can be eliminated by replacing the angular position to be used by the controller with the principle value in $[-\pi, \pi)$. Then, the resulting feedback control is discontinuous. More details of this example of unwinding phenomenon can be found in (Bhat and Bernstein, 2000). Indeed, the global asymptotic stabilization under continuous control is impossible due to this inherent nature of $SO(3)$ and the related unwinding phenomenon regardless of the adopted parameterization for attitude representation (Koditschek, 1988; Bhat and Bernstein, 2000; Sanyal, Fosbury, Chaturvedi and Bernstein, 2009; Wen and Kreutz-Delgado, 1991). The objective of global asymptotic stability then has to be relaxed to ‘almost’ global asymptotic stability. The standard

terminology of ‘almost’ global asymptotic stability for the spacecraft attitude control problem means asymptotic stability over an open and dense set in the set of the special group of rotation matrices $SO(3)$ (Seo and Akella, 2007; Tsiotras, 1998). This means that all the solutions apart from those starting in a nowhere dense set of measure zero converge asymptotically to the desired equilibrium point. A nowhere dense set of measure zero is considered thin and negligible in both a measure-theoretical and a topological sense. In practical terms and from an asymptotic point of view, this relaxation is fairly mild, since disturbances and sensor noise will prevent system trajectories from remaining on this thin set (Angeli, 2004; Chaturvedi, Bloch and McClamroch, 2006). However, close vicinity to that set may cause the convergence of the system trajectories to the desired equilibrium to be arbitrarily slow (Chaturvedi, McClamroch and Bernstein, 2007; Chaturvedi and McClamroch, 2007).

1.6 Attitude Parameterizations Related Issues

A further complicating factor in the way of developing globally asymptotically stabilizing continuous controls pertains to the choice of parameterization for the representation of the orientation of the rigid spacecraft relative to an inertial frame. Among the various parameterizations that can be employed for deriving the feedback controls are Euler angles (Slotine and Li, 1991), quaternions (also called Euler parameters (Hughes, 1986)), angle-axis representation, Rodrigues parameters, modified Rodrigues parameters (Marandi and Modi, 1987), direction cosine matrices, and rotation matrices (the transpose of direction cosine matrices) (Shuster, 1993). Some of the parameterizations like Euler angles and Rodrigues parameters possess singularities and thus the stability results accompanied with their use are only of a local nature as the system trajectories may evolve to one of the singularities of such parameterizations. Other parameterizations, such as quaternions (or Euler parameters) and the angle-axis representation are not one-to-one, that is, they cover the Special Orthogonal group $SO(3)$ multiple times which results in ambiguities. Such attitude representations may result in control laws that are generally not well-defined and may cause the closed-loop systems to exhibit the phenomenon of unwinding. Dwyer (1984, 1986) employed a reduced quaternion representation of attitude which helped to transform

the complete equations of rotational motion into a linear model accompanied with attitude singularities.

1.7 Quaternions as Attitude Parameterization

Quaternions cover the $SO(3)$ twice leading to two distinct quaternions for every single physical attitude. Hence, quaternion based control law may give rise to two different control torques for the same physical orientation of the spacecraft, a property manifesting inconsistency. Despite this apparent discrepancy, continuous quaternion-based controllers that ensure convergence to a desired equilibrium point from every point except the remaining equilibrium point can be designed (Luo, Chu and Ling, 2005b). Here, the two equilibrium points represent the same desired physical attitude. The existence of two equilibrium points may cause the spacecraft to exhibit unwinding in the sense that one of these is chosen as the desired equilibrium point and the initial condition being close to the other would entail a large-angle physical rotation away from and then back to the desired physical orientation, thus showing the deficiency of Lyapunov stability on the physical space $SO(3)$. Hence, small perturbations can make the spacecraft exhibit the phenomenon of unwinding even though it may be possible to go for smaller angle manoeuvres. These discrepancies arise in continuous quaternion-based controllers such as those derived in (Ahmed, Coppola and Bernstein, 1998; Joshi, Kelkar and Wen, 1995; Wie and Barba, 1985). A discontinuous quaternion-based controller with a switch at the 180 deg error condition overcomes unwinding (Crassidis, Vadali and Markley, 2000; Schaub and Junkins, 2003) and the same is true for the case of modified Rodrigues parameters-based attitude control laws (Schaub and Junkins, 2003). However, the resulting discontinuous dynamics may involve pathological problems (Cortes, 2008) and may lead to chattering in the vicinity of the discontinuity.

1.8 Variable Structure Sliding Mode Control

The aforementioned hardships hindering the achievement of continuous control laws with the help of Lyapunov stability theory for the spacecraft attitude stabilization and tracking

problems, lead to the use of variable structure control methodology for this purpose. The methodology has been widely used in the literature for the said problem and is especially advisable for the attitude control of the spacecraft having on–off thrusters as actuation devices. The variable structure control approach takes advantage of the useful characteristics of different structures while designing appropriate algorithms for changing the structure of the control system during its course of operation. Much frequent switching between the selected structures, under certain conditions, results in a new behaviour of the system known as sliding mode. The method was first proposed by Emelyanov in the early 1950s and elaborated by his group and a number of other researchers (DeCarlo, Zak and Matthews, 1988; Emelyanov, 1967; Utkin, 1997; Hung, Gao and Hung, 1993). Under sliding mode, the states of the dynamical system are confined to a hypersurface, also called sliding surface, in the system state space where the behaviour of the system is dominated by lower-order dynamics and invariant to external disturbances and parameter variations. In the case when the achievement of a sliding mode cannot be assured, the discontinuous controller is referred to as the variable structure control algorithm. The property of finite time response is also attributed to the use of variable structure controller with/without a sliding mode. These features have been widely exploited to develop exceedingly robust controllers for both linear and nonlinear systems and have proved to be useful for a broad range of engineering systems (DeCarlo, Zak and Matthews, 1988; Hung, Gao and Hung, 1993). As the variable structure controllers employ high-frequency switching to maintain the solutions of the system on the sliding manifold and because of the imperfection of the actuating devices, the phenomenon of chattering of the signals in the system occurs in practice particularly in the presence of sensor noise or disturbances. This undesirable feature can be removed by changing the sign function commonly used to implement such controllers by either the saturation function (DeCarlo, Zak and Matthews, 1988), or by an approximate sign function (Bošković, 1997; Narendra and Bošković, 1990; Narendra and Bošković, 1992). This remedy results in the solutions of the closed-loop system being restricted to a boundary layer around the switching surface rather than to the surface itself so that the error remains bounded rather than converging to zero. The extent of the resulting set of uniform ultimate boundedness can be attuned with the appropriate selection of the free design parameters.

The variable structure control (VSC) has been used for spacecraft attitude control problem in a number of works. Singh and Iyer (1989), Dwyer and Sira-Ramirez (1988) and Crassidis and Markley (1996) used VSC for spacecraft attitude manoeuvres but their use of Euler angles and Rodrigues parameters as the attitude parameterizations rendered the proposed control algorithms nonglobal. Lo and Chen (1995) and McDuffie and Shtessel (1997) used quaternions, a global representation of spacecraft orientation, for the development of their control formulations. The controllers proposed by them, however, are also not global as the reciprocal of one of the quaternion components is used in the control law implementation. Vadali (1986) was the first to design a global VSC algorithm for attitude stabilization control. The sliding surface is determined by the use of optimal control theory for a quadratic performance index in the quaternion and angular velocity components. However, the analysis seems to be incomplete as only a simplified spacecraft model is used. This work was generalized to control of spacecraft tracking manoeuvres by Crassidis, Vadali and Markley (2000). Terui (1998) augmented this approach to include the control of spacecraft translational motion.

The mentioned VSC related research for the most part employed the equivalent control part in the control law to keep the system dynamics in the sliding mode. None of these works went for an explicit study of the issue of control input saturation. Bošković, Li and Mehra (2001) designed several formulations for global stabilization of spacecraft attitude dynamics. The proposed controllers rely on variable structure control and explicitly cater for the problem of control input saturation. The control algorithms are proved to guarantee fast and accurate response and be highly robust to bounded external disturbance torque and inertia matrix uncertainty. Moreover, these control algorithms have the property of computational simplicity and straightforward tuning. Bošković, Li and Mehra (1999) extended the algorithms to the case of spacecraft attitude tracking control. However, the Lyapunov-like function employed in the stability analysis was not global in the sense of covering the entire state space of the system. Also, the control algorithms, for the cases of both attitude stabilization and tracking, guarantee the convergence of the errors to zero only when they are discontinuous. This can induce the chattering of the signals in the system. The provision of an approximate sign function in the control law can circumvent

the issue of chattering but for this case the stabilization and tracking errors can be proved to be bounded rather than asymptotically converge to zero. Further, the proposed dynamic controllers for the cases of both attitude stabilization and tracking, relies on an adaptable control gain whose value can either decrease or remain constant. This constraint can lead to a situation when the value of the adaptable gain approaches zero. This is the main shortcoming of the work as in that situation it would not be possible to achieve the convergence of the error quaternion to zero. Bošković, Li and Mehra (2004) augmented the previous results (Bošković, Li and Mehra, 1999; Bošković, Li and Mehra, 2001) to propose a robust and continuous algorithm for the spacecraft attitude tracking control. The algorithm is basically a continuous version of the variable structure control design approach. The use of an appropriate Lyapunov function helped to demonstrate the global stability for the overall system. The proposed controller ensures asymptotic tracking and disturbance rejection under control input saturation and robustness to the spacecraft inertia matrix uncertainties. However, to achieve the global asymptotic stability, the proposed smooth controller needs to ensure a nonzero value of the adaptable control gain all the time and for the realization of that objective a condition is imposed in the formulation. To meet this explicit condition is the major technical hardship associated with the proposed scheme. Li and Wang (2006) have identified some of the disturbances in the presence of which the explicit condition, accompanied with the solution proposed by (Bošković, Li and Mehra, 2004), cannot be satisfied. Wallsgrove and Akella (2005) proposed another smooth version of the variable structure control of the spacecraft attitude stabilization problem. They used a hyperbolic tangent function for this purpose. Although, the angular velocity error converges to zero, the asymptotic convergence of the attitude error to zero is not guaranteed. Further, this control algorithm introduces numerical problems in simulations of long duration, a fact that was acknowledged by the authors. Following the steps of (Bošković, Li and Mehra, 2001), Li and Wang (2007) proposed an attitude tracking controller which guarantees global asymptotic stability in the presence of disturbances providing robustness against bounded parametric uncertainties, accounting for actuator saturation constraint under mild conditions and ensuring chattering avoidance. The authors, however, did not support their theoretical findings with a realistic numerical example.

1.9 Integrator Backstepping-based Control

Integrator Backstepping is a popular nonlinear control design technique that has been widely studied in the literature (Kanellakopoulos, Kokotovic and Morse, 1992; Khalil, 2002; Kokotovic, 1992; Krstić, Kanellakopoulos, and Kokotovic, 1995). It is a systematic control design method in which a subset of the state space is regarded as virtual control to the dynamics of another subset of the state space. These virtual controls are designed to asymptotically stabilize the subset of the dynamics. The next step of the control design procedure is to select the next series of virtual controls to make the previous virtual controls track to the desired value. The process is then applied repeatedly through all subsets of the dynamics until the actual controls are designed. The term backstepping refers to this recursive nature of the control design procedure where a control law as well as a control Lyapunov function is recursively constructed to guarantee stability. Generating a family of globally asymptotically stabilizing control laws is the main advantage of this method that can be exploited for addressing robustness issues and solving adaptive problems. The sliding mode control design technique is similar to backstepping control design technique in the sense that the model takes the form of a cascaded nonlinear system, but differs in that the error between the actual and desired virtual controls is made to converge to zero (or a neighborhood of zero) in finite time rather than asymptotically (Karlgaard, 2006). Backstepping has been considered for the spacecraft manoeuvres (Kim and Kim, 2003; Krstić and Tsiotras, 1999). The cascaded structure of spacecraft kinematics and dynamics makes the integrator backstepping a preferred approach for the spacecraft attitude manoeuvre problem resulting in smooth feedback controls (Sontag and Sussmann, 1989). The simple or conventional backstepping control method, however, may result in excessive control input beyond saturation bound of the actuators used for the spacecraft attitude control problem.

1.10 Other Miscellaneous Control Schemes

Adaptive nonlinear controllers proposed for spacecraft attitude stabilization/tracking problem include those in (Ahmed, Coppola and Bernstein, 1998; Cristi, and Burl, 1993;

Junkins, Akella and Robinett, 1997) using classical adaptive control theory (Narendra and Annaswamy, 1989; Sastry and Bodson, 1989) as well as the ones by (Paielli and Bach, 1993; Schaub, Akella and Junkins, 2000, 2001) which also hinge on the desired closed loop dynamics. In another related study (Di Gennaro, 1997), the author used dynamic state feedback to design a stabilizing controller for the spacecraft in a central gravitational field. The proposed controller realizes the goal of attitude stabilization under input saturation, inertia-matrix uncertainty, and external disturbance. Here, only gravity-gradient torque like disturbance has been considered. In particular, the control term involving the derivative action is multiplied with a factor being a continuous nonlinear function of the said control term. The factor, for higher values of its argument, assumes smaller values and, hence, addresses the saturation of the control input. The control law presents implementation difficulties in the sense that two simultaneous nonlinear equations have to be solved numerically for determining the values of estimated parameters to be used in the control law. Also, tracking of desired trajectories was not considered. Loria and Nijmeijer (1998) proposed a dynamic tracking controller for the Euler–Lagrange systems. The information of the system inertia matrix is required to implement the controller. In addition, the asymptotic stability result is non-global. The proposed solution addresses the situation when the velocities are not available. The effect of the absence of the stated constraint regarding the removal of the mentioned shortcomings of the approach, however, needs further clarification.

The problem has also been addressed by passivity-based angular velocity-free control strategies (Akella, Valdivia and Kotamraju, 2005; Caccavale and Villani, 1999; Egeland and Godhavn, 1994; Lizarralde and Wen, 1996; Tsiotras, 1998) employing a dynamic filter driven by the attitude measurements (e.g. the modified Rodrigues parameters or the vector part of the quaternion) whereas Tayebi (2008) proposed an auxiliary unit-quaternion dynamical system to make use of the passivity property. Akella, Valdivia and Kotamraju (2005) also exploited the choice of unit quaternion as attitude parameterization in conjunction with the use of hyperbolic trigonometric functions to find upper bounds for the control inputs and their rates. Some important developments for spacecraft attitude tracking with input constraints are reported in (Arambel, Manikonda and Mehra, 2000;

Tsiotras and Luo, 2000) while some findings regarding the general problem of controller design with input rate and magnitude constraints have been presented in (Esfandiari and Khalil, 1992; Teel and Praly, 1995). Optimal nonlinear control approaches involving the solution of Hamilton-Jacobi-Bellman equation (Krstić and Tsiotras, 1999; Tewari, 2002; Sharma and Tewari, 2004) and Hamilton-Jacobi-Isaacs equation (Huang and Lu, 1996; Luo, Chu and Ling, 2005a, 2005b) have also been explored for the spacecraft attitude stabilization/tracking problem. Some of the results in this direction have introduced the inverse optimal formulations which avoid the challenging job of solving the said equations while still resulting in the feedback controllers that are optimal with respect to a set of meaningful cost functionals. Nonlinear Model Predictive Control has also been employed for the subject problem (Crassidis et al., 1997) where the current control action is obtained by solving on-line, at each sampling instant, a finite horizon open-loop optimal control problem, using the current state of the plant as the initial state. The optimization, while minimizing a desired cost function using the system model, yields an optimal control sequence over the prediction horizon and the first control in this sequence is applied to the plant until the next sampling instant (Allgöwer, Findeisen and Nagy, 2004).

1.11 Potential Function Method for Constrained Attitude Manoeuvres

Manoeuvre planning in translational and rotational degrees of freedom is an important part of autonomous onboard operations for most spacecraft missions. For space science missions with heat or light sensitive payloads like cryogenically cooled infrared telescopes (Ximénez de Ferrán, 1991), star trackers, and low energy ion composition analyzers, the spacecraft is required to perform large angle reorientation/slew manoeuvres in a way that the sensitive instruments avoid exposure to bright or heat generating objects in the sky, such as Sun, by a specified minimum angle. For such missions, the attitude control system of the spacecraft has the additional task of applying the necessary control torque on the spacecraft such that the cones (defined by the minimum avoidance angles) emanating from these sensitive optical devices exclude the bright or heat generating objects during the reorientation manoeuvre (Fig. 1.1). The ISO (Infrared Space Observatory) (Ximénez de

Ferrán, 1991), Cassini mission to Saturn (Frakes et al., 1992), FIRST/Planck (Ahmed et al., 1998; Singh et al., 1997), and SAMPEX (Solar, Anomalous, and Magnetospheric Particle Explorer) (Collaudim and Passvogel, 1998) are examples of such missions involving reorientation and retargeting manoeuvres in the presence of different variations of pointing constraints.

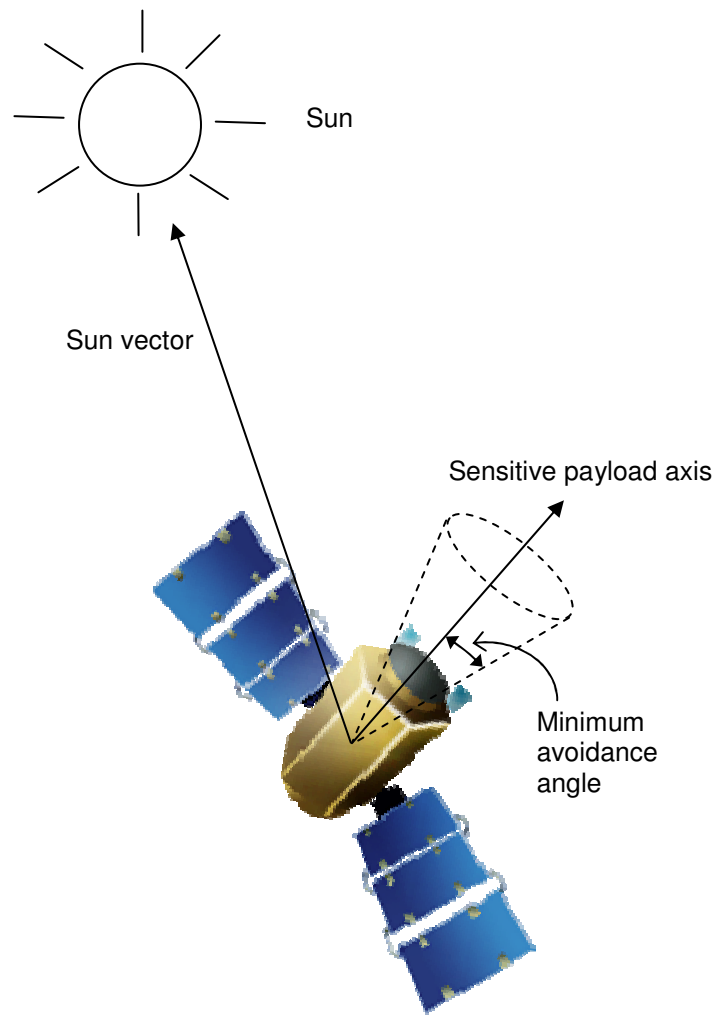


Fig. 1.1 Sun vector avoidance

Various techniques have been explored in the literature for the planning of spacecraft attitude manoeuvres in the presence of pointing constraints. Kim and Mesbahi (2004) used semidefinite programming to solve this problem. Sorenson (1993) proposed differential geometry-based approach for modelling the pointing constraints and seeking the feasible attitude trajectories which avoid such constraints. Hablani (1999) also made use of the vectorial kinematics approach and developed attitude commands for the spacecraft undergoing slew manoeuvres while avoiding bright objects through a prescribed minimum angle. The same approach has also been employed for constraint violation detection/avoidance (Singh et al., 1997) and velocity avoidance (Frakes et al., 1992) algorithms involving similar applications. Frazzoli et al. (2001) introduced random search method based path planning scheme to address the problem.

McInnes (1994) proposed to use the artificial potential field method for the control of large angle constrained slew manoeuvres borrowing the idea from robotics where it has been used for developing motion planning algorithms for manipulators and mobile agents (Ge and Cui, 2002; Khatib, 1986). Development of feedback controls in closed form happens to be an important advantage of this method that facilitates the on-board implementation with reduced software requirements. The method has also been used for other space applications such as proximity manoeuvring (Roger and McInnes, 2000), spacecraft guidance and control (McInnes, 1995a), formation flying (Badawy and McInnes, 2009; McQuade, Ward and McInnes, 2002), autonomous and distributed motion planning for satellite swarm (Izzo and Pettazi, 2007), on-orbit assembly of large and complex space structures (Badawy and McInnes, 2008; Izzo, Pettazzi and Ayre, 2005; McQuade and McInnes, 1997), and terminal descent on a planetary surface (McInnes, 1995b).

The artificial potential function method is a variation of the Lyapunov-based control design procedure mentioned briefly in Section 1.3. Unlike the Lyapunov function which ensures only convergence to the desired state/states of the nonlinear dynamical system (Fig. 1.2), an artificial potential function extends the methodology for avoiding the undesired system states by assigning higher artificial potential to the regions surrounding the undesired states (Fig. 1.3). In this way, the new variant of Lyapunov function, called artificial potential function, for the system now consists of two parts: one corresponding to the attraction

towards the desired state/states while the other relates to the repulsion against the undesired state/states. These parts may be added linearly, however, this process may result in local minima on the potential topology which may lead to trapping the system in the states other than the desired one. Various heuristics like adding noise may help to escape from such local minima. The difficulty can be also be circumvented by using the Laplace equation to numerically generate the artificial potential function (Roger and McInnes, 2000).

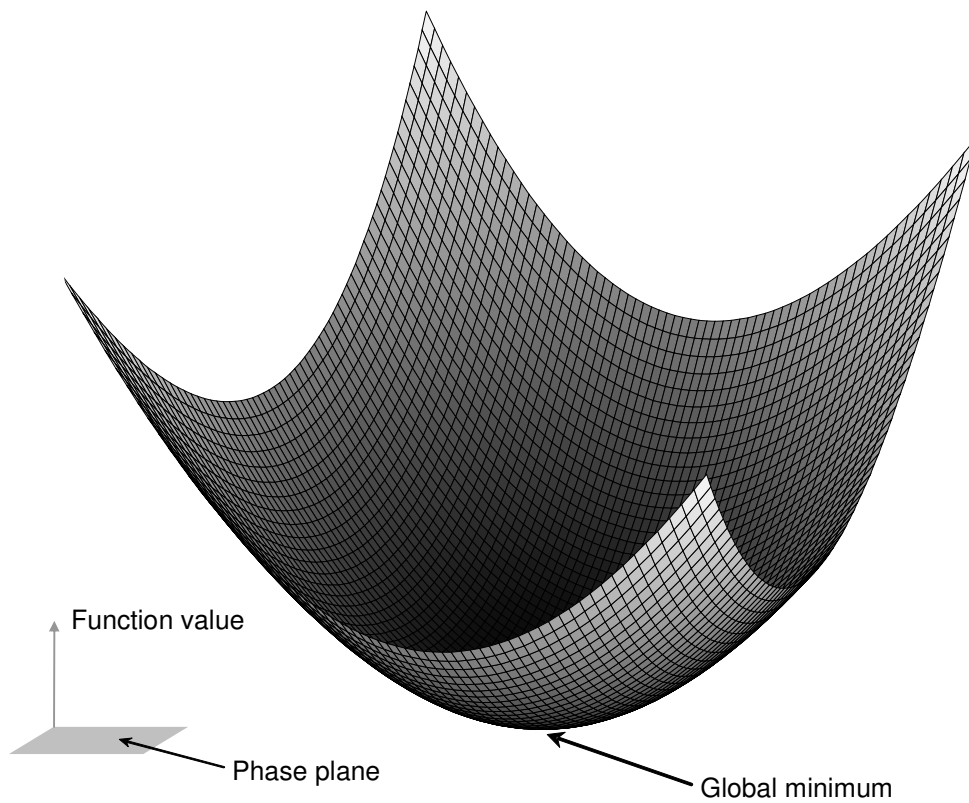


Fig. 1.2 Phase plane visualization of Lyapunov function

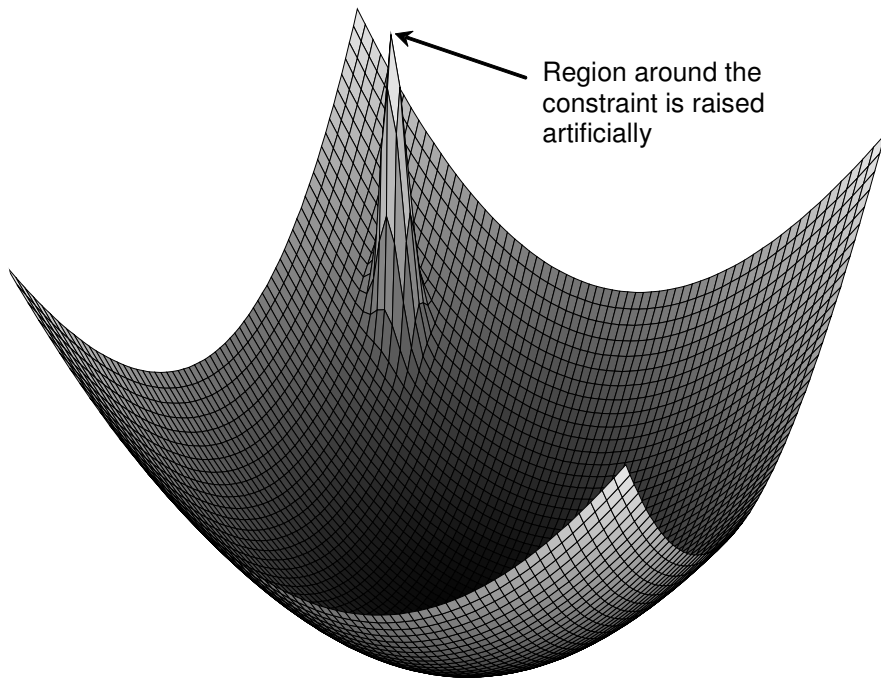


Fig. 1.3 Phase plane visualization of artificial potential function

McInnes (1994) adopted quadratic and Gaussian functions for the attractive and the repulsive parts, respectively, of the artificial potential function. Moreover, the author used Euler angles as the attitude parameterization. Radice and McInnes (2001) extended the concept for multiple target selection and obstacle avoidance again using Euler angles for the attitude representation. The methodology was further augmented in (Casasco and Radice, 2004) and (Casasco and Radice, 2005a) for the constrained attitude stabilization and tracking, respectively, in the sense that quaternions and modified Rodrigues parameters were used as the attitude parameterizations instead of the Euler angles. Radice and Casasco (2007) reported a comparison of the use of different attitude parameterizations for the constrained attitude stabilization manoeuvres. Radice and McInnes (1999) considered constrained manoeuvres with gas jets-based discrete on-off torques whereas Mengali and Quarta (2004) achieved fine pointing with the help of FEEP (Field Emission Electric Propulsion) thrusters while also considering the solar array pointing requirements. Casasco and Radice (2005b) attempted to optimize the control of constrained attitude stabilization manoeuvres by employing integrator backstepping-based inverse optimality approach whereas Tatsch, Xu and Fitz-Coy (2005) used a genetic algorithm to optimally tune the controller parameters.

1.12 Actuators for Spacecraft Attitude Control

Torques about the centre of mass of the spacecraft, as mentioned in Section 1.1, can be regarded as external or internal. The former change its total angular momentum whereas later affect only the distribution of momentum among its various moving parts. Usually the spacecraft will always be subject to naturally occurring disturbance torques which will cause a progressive build-up of its angular momentum over a period of time. This identifies the need of providing the spacecraft attitude control system with external torquers for controlling the said momentum build-up.

The most common external torquers are mass expulsion devices, such as gas jets or ion thrusters; electromagnetic coils, which provide a torque by interacting with the Earth's magnetic field and gravity-gradient torques which result from the differential gravitational forces acting on an asymmetrical spacecraft forcing its minimum moment of inertia axis to

be perpendicular to the gravitational equipotential. General internal torquers include reaction wheels, momentum wheels and gimballed momentum wheels (also called as CMGs), which are the rotating masses inside spacecraft body used to exchange angular momentum with it so that the overall momentum remains constant. Gravity-gradient or magnetic torques can be used for controlling the attitude of the satellite however the torque levels that can be achieved with these actuators are normally low and generally insufficient for fast attitude manoeuvres.

For very accurate attitude control systems and for moderately fast manoeuvres, the reaction wheels are preferred because they allow continuous and smooth control with the lowest possible parasitic disturbing torques. The level of torque that can be achieved with reaction wheels is of the order of 0.05 to 2 Nm. For three-axis control, three orthogonal reaction wheels will be the minimum requirement. A redundant fourth is normally added at an equal angle to the other three, in order to avoid a single-point failure. When the prime means of attitude control are reaction or momentum wheels then thrusters can be used for momentum dumping. In low earth orbit, gravity-gradient and magnetic torques rather than the thrusters can be employed to desaturate the wheels.

Thrusters are usually fired in pairs to minimize translational motion. These are commonly used with spin-stabilized spacecraft for attitude manoeuvring and spin rate control. For this type of spacecraft, a minimum of two reorientation thrusters and two spin rate control thrusters are required. For a three-axis stabilized system, six possible directions are available for manoeuvring the spacecraft and a minimum of six thrusters are required. The level of control torques that can be achieved with thrusters is almost unbounded leading to fast attitude manoeuvres but their inherent impulsive nature hinders attaining smooth control. Pointing accuracy with the typical on-off thrusters is limited to about 0.1 to 1.0 degrees (amplitude of limit cycles). More accurate pointing can be achieved by using either reaction wheels or thrusters capable of providing small and consistent impulses with minimum switch-on time of several milliseconds leading to a low maximum thrust (typically as low as 10^{-2} N with a minimum thrust impulse of order 10^{-4} Ns).

1.13 Control Moment Gyros as Actuators

Control moment gyro (CMG) is a momentum exchange device which is used as an actuator for spacecraft attitude control. The working principle of CMG installed on a spacecraft can be described as a rotor that spins at a constant speed and is gimballed to apply a gyroscopic torque on the spacecraft (Fig. 1.4). When the gimbal is rotated, the spin axis of the rotor points along different directions causing a change in its angular momentum orientation. The gyroscopic torque is proportional to the rate of change of the angular momentum. The classification of a CMG as a single-gimbal CMG or a double-gimbal CMG is attributed to one or two motorized gimbal mechanisms, respectively, used to control the direction of its angular momentum. CMG is energy efficient owing to the fact that a large apparent control torque can be obtained at the expense of a relatively small gimbal torque. This characteristic, known as torque amplification, motivated for the use of CMGs as attitude effectors for large spacecraft platforms such as the Mir Space Station, Skylab, the International Space Station and the Hubble telescope. However, a recent interest for agile small satellites has caused a renewed attention towards this actuator. CMGs can be used in the form of a cluster of units where the three-axis attitude control of a spacecraft needs a cluster of three or more single-gimbal CMGs. An algorithm that calculates the desired motion for each CMG of the cluster for the task of attitude control is called a steering law or logic. There are generally two ways for using clusters of CMGs in the context of attitude control (Wie, Heiberg and Bailey, 2001). In the first approach, the torque desired by an attitude controller is used to calculate the required gimbal rate for each CMG of the cluster (called the gimbal rate command) with the help of some steering law. The second approach involves the use of the steering logic for the calculation of the required gimbal angle trajectories for all the CMGs of the cluster (known as gimbal position command) that generate the commanded angular momentum trajectory. A steering logic also needs to meet various hardware constraints like the gimbal rate limits and gimbal stops but the issue of foremost concern to be addressed is the existence of singular states for the cluster of CMGs known as singularities (Wie, 2004). At such a state, the gyroscopic torques from the individual CMGs of the cluster lie on a plane whereas the required torque happens to have a component along the perpendicular to that plane (Yoon, 2004). One way to deal with this

difficulty is to use approximate singularity avoiding/transiting solutions at the cost of accuracy of control.

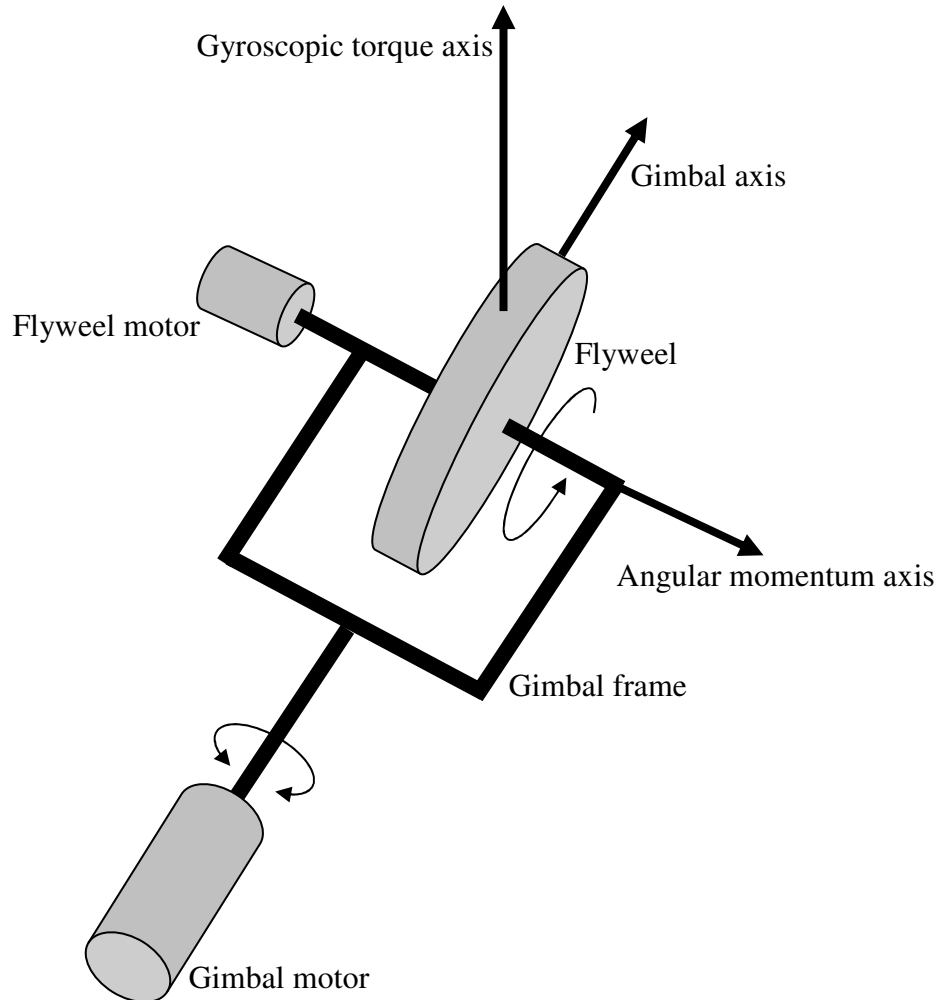


Fig. 1.4 Single Gimbal Control Moment Gyro Unit

The investigations regarding the use of CMGs for spacecraft attitude control problem can be found as far back in the literature as the work by Jacot and Liska (1966). An important work by Margulies and Aubrun (1978) laid down the foundations for the singularity analysis of clusters of single-gimbal CMGs where they employed a systematic geometrical framework for establishing the fundamental properties of such clusters. They explored the angular momentum envelopes for different configurations of CMGs to come up with the idea of null motion of redundant CMG systems where CMGs motions do not produce torque. Such a motion was proposed as a possible means of avoiding singularities. Their work opened up an active area of research leading to a variety of CMGs steering logics, to

avoid/escape singularities, which can be broadly classified between open-loop schemes and pseudoinverse-based solutions. The results by Bedrossian, Paradiso, Bergmann and Rowell (1990a, 1990b) fall into the latter category where the singularity robust inverse proposed by Nakamura and Hanafusa (1986) for robotic manipulators was used to find an approximate gimbal rate command leading to feasible solutions in the neighbourhood of singularities. However, the singularity robust inverse failed to avoid a special class of singularities known as internal elliptic-type singularities. Wie, Heiberg and Bailey (2001) utilized the time-dependent modulation functions to modify the singularity robust steering law to propose a generalized singularity robust steering logic which was successful in transiting the internal elliptic singularities. Nevertheless, the proposed solution had a deficiency of being trapped in the momentum saturation singularities, a problem that was addressed in Wie (2005). The generalized singularity robust steering logic by Wie, Heiberg and Bailey (2001) was explored by Lappas and Wie (2009) in the context of accommodating mechanical gimbal angle constraints. The approach of perturbing the desired torque near the singularities rather than changing the singularity robust law was investigated in (Oh and Vadali, 1991).

The above mentioned schemes, manipulating variations of pseudoinverse to formulate different steering laws, while avoiding/escaping singularities, introduce some error between the torque desired by the attitude controller and the output torque from the cluster of CMGs. Spacecraft applications with precision pointing and tracking requirements require, however, accurate generation of the autopilot-requested torques during a manoeuvre. The schemes involving some level of preplanning (Paradiso, 1992; Vadali, Oh and Walker, 1990; Vadali and Krishnan, 1995) are successful in addressing the issue of singularities while generating the commanded torques precisely, however, these approaches, being open-loop in nature, are of limited use for feedback control. Paradiso (1992) used the commanded angular momentum trajectories for a tree search algorithm which avoids the singularities while utilizing null motion. Vadali, Oh and Walker (1990) proposed a method of finding a set of preferred initial gimbal angles that ensure to avoid singularities for a particular class of manoeuvres. Moreover, a null motion-based scheme was also presented to place the gimbals at the preferred angles. The work was extended by

Kurokawa (1997) while ensuring simplicity and repeatability. Vadali and Krishnan (1995) proposed an algorithm involving suboptimal planning with respect to a singularity avoidance objective function. Pechev (2007) considered the problem of singularity avoidance from a control point of view and proposed to calculate the gimbal rates in feedback loop avoiding the computation of matrix inversion. The survey paper by Kurokawa (2007) provides a detailed account of various steering laws and singularity avoidance methods for single-gimbal CMGs.

The potential function method has also been used recently in order to deal with the singular-configuration issue (Avanzini and Palmas, 2007), where singularities themselves are treated as obstacles in the control parameter space rather than in the phase space and a gimbal-rate command which avoids them is formulated. Unfortunately, the simultaneous definition of obstacles in both the control and state spaces makes the shape of the potential function highly complex and this may lead to the formation of local minima for the (global) potential function, thus harming the global stability property of the approach.

The generation of gimbal position command is based on the inversion of the kinematic relation between gimbal angles and the platform commanded angular velocity which can be expressed as a function of attitude error. The basic idea originating from the conservation of angular momentum is to drive the cluster of CMGs in an arrangement that implements an angular velocity command rather than a torque command. In the reference position (zero rotation angles for all the gimbals), the total angular momentum delivered by the CMG cluster is zero. Considering the satellite platform initially also at rest makes the total angular momentum as zero. A non-zero angular momentum vector can be generated by rotating each CMG about the gimbal axis perpendicular to the direction of the spin axis of the CMG. In response, the platform will rotate to achieve an angular velocity such that the vector sum of cluster and platform angular momentum remains constant being zero. Now, the rotation angles of the gimbals of all the CMGs can be chosen in such a way that the resulting angular velocity of the platform equals the commanded angular velocity for a certain desired manoeuvre of the platform. The rotation rate of the gimbals thus results in an apparent gyroscopic torque (Wie, 1998) that can be used for steering the spacecraft for the prescribed manoeuvre. The scheme works in the same way for the case of a nonzero

total angular momentum of the platform and the CMG cluster at the start of the manoeuvre. However, such a situation causes a reduction of the maximum available angular momentum that is exchangeable between the CMG cluster and the platform. In other words, the effectiveness of the CMGs is reduced, as is the case when using any momentum exchange device under such circumstances. That is why, spacecraft usually have a mechanism (e.g. a set of thrusters or magnetorquer rods) on board to perform desaturation manoeuvres intended at dumping the undesired angular momentum accumulated because of external disturbance torques.

Avanzini (2005) used the approach of gimbal position command generation for a cluster of four single-gimbal CMGs in pyramid configuration. A small angle assumption about the reference positions of the CMGs (zero rotation angles for all the gimbals so that the total angular momentum delivered by the CMG cluster is zero) is employed in conjunction with sacrificing the redundancy in the CMG cluster to find an approximate linear solution for the gimbal angles. As for the case of the kinematic relation between gimbal angles and the spacecraft commanded angular momentum, the higher order terms for the expression involving the time-rates of the gimbal angles and the commanded angular momentum are neglected to prove the closed-loop system stability. However, the gimbal angles conforming to the small angle approximation cannot track higher values of the commanded angular momentum. The author also proposed some amendments to allow for larger gimbal angles but the system stability for such fast manoeuvres was demonstrated only through numerical simulations. Variable speed control moment gyro (VSCMG) with an extra degree of freedom of variable rotor speed has also been studied as an alternative solution to the standard CMG related problems (Schaub and Junkins, 2000; Yoon, 2004).

1.14 Research Objectives

The research reported in this thesis considers spacecraft as a rigid body and assumes that the spacecraft attitude and angular velocity measurements exist for feedback. The actuators that provide torques about three mutually perpendicular axes are assumed to be available for controlling the spacecraft. The attitude control problem of a rigid spacecraft with the

number of actuators less than the controlled degrees of freedom (Shen and Tsiotras, 1999; Tsiotras and Doumtchenko, 2000; Wan and Bernstein, 1995) is not studied in this thesis.

In this work, unlike the approaches of nonlinear proportional-integral-derivative control (Wie and Lu, 1995), Lyapunov-optimal control (Robinett et al., 1997a, 1997b), variable structure sliding mode control (Bošković, Li and Mehra, 2001), we explore the nonlinear integrator backstepping control design as a nonadaptive scheme for addressing the issue of control input saturation in the context of spacecraft attitude manoeuvres. We seek to prove stability for the cases of both attitude stabilization and tracking problems under control input saturation. We also carry out robustness analysis of the approach against external disturbance torques and uncertainties in spacecraft moments of inertia. We shall make use of an inverse tangent based tracking function (Kim and Kim, 2003) and a family of augmented Lyapunov functions (Mazenc and Iggidr, 2004) for the accomplishment of aforesaid task.

As the use of artificial potential function method for constrained large angle manoeuvres planning has not been explored in the context of satisfying the spacecraft control torque constraints (Kim et al., in press), we seek to blend nonlinear integrator backstepping scheme with the artificial potential function method to control the spacecraft large angle slew manoeuvres with autonomous ability of avoiding pointing constraints. The resulting feedback controls shall be explored for ensuring stability while avoiding control torque saturation in the presence of bounded external disturbance torque and prescribed uncertain variations in the spacecraft moments of inertia.

A CMG steering logic based upon a gimbal position command is advantageous because of its inherent singularity robustness. Existing gimbal position steering laws (Avanzini, 2005), however, do not exploit the maximum angular momentum deliverable by the CMG cluster. In this thesis, we shall address this issue which is particularly important for an agile spacecraft which is meant for undergoing rapid attitude manoeuvres.

1.15 Thesis Outlines

- Chapter 1: This chapter introduces problems of rigid spacecraft attitude stabilization and tracking control and identifies the issues that need to be addressed in the context of this problem. It surveys various schemes that have been utilized for solving this problem. It also talks of the autonomous avoidance of pointing constraints as an additional requirement imposed on the spacecraft attitude control system and the use of CMGs as an actuator for this problem. Finally, the objectives of the research presented in the thesis are set up.
- Chapter 2: First, different reference frames to be used in the following developments of the thesis are defined. Then, the kinematics and dynamics of rigid spacecraft are summarized while developing equation for the spacecraft attitude tracking error dynamics and defining the attitude tracking control objective. Next, the details of the design procedure for the proposed attitude tracking controller and the analytical bounds for the control torque components are given. The proposed controller is analysed in terms of robustness against bounded external disturbance torque and prescribed uncertainties in the spacecraft moments of inertia. The conditions ensuring stability and allowing the calculation of control torque bound in this non-nominal case are also developed. It follows with the specialization of the proposed controller for the case of attitude stabilization. Lastly, the efficacy of the proposed scheme is demonstrated by the numerical simulations for the cases of attitude stabilization and tracking both.
- Chapter 3: First section briefly describes the pointing constraints in the context of spacecraft large angle slew manoeuvres. Then, the attitude stabilization specialization of the methodology of Chapter 2 is blended with the artificial potential function method for the incorporation of capability of avoiding the pointing constraints while undergoing the said manoeuvres. Gaussian function based repulsive potential is used for the construction of an artificial potential function. Next, the proposed methodology is explored for robustness against bounded external disturbance torque and prescribed uncertainties in the spacecraft

moments of inertia. Here, the stability and control torque bound-related conditions for the non-nominal case are developed for the constrained attitude slews. Finally, the effectiveness of the proposed methodology is established by the numerical simulations.

- Chapter 4: At the start, the details of the dynamics of the rigid spacecraft equipped with a cluster of single-gimbal CMGs are provided. Next section introduces the concept of gimbal rate command-based steering law for the CMG cluster. The following section presents the idea of steering the CMG cluster using a gimbal position command. It also details a gimbal position steering logic for a pyramid-type cluster of four single gimbal CMGs. In the subsequent section, a novel gimbal position steering law is proposed which exploits the maximum angular momentum deliverable by the CMG cluster corresponding to the direction of the commanded angular velocity for the major part of the spacecraft reorientation manoeuvre. The chapter ends with the section reporting the numerical simulation results that employ the proposed algorithm of the previous section for the generation of gimbal position command. The obtained results are also compared with some benchmark results in the literature for proving the significance of the proposed gimbal position steering logic.
- Chapter 5: The conclusions of the thesis are presented here and possible directions for further research are also identified.

Chapter 2

Spacecraft Attitude Control with Bounded Torque Input

This chapter studies the nonlinear control of spacecraft attitude tracking manoeuvres while addressing the issue of control torque saturation. First of all, different reference frames to be used in the following developments are defined. Then, the kinematics and dynamics of rigid spacecraft are summarized while developing equation for the spacecraft attitude tracking error dynamics and defining the attitude tracking control objective. Next, the details of the design procedure for the proposed attitude tracking controller and the analytical bounds for the control torque components are given. The proposed controller is analysed in terms of robustness against bounded external disturbance torque and prescribed uncertainties in the spacecraft moments of inertia. The conditions ensuring stability and allowing the calculation of control torque bound in this non-nominal case are also developed. It follows with the specialization of the proposed controller for the case of attitude stabilization. Lastly, the efficacy of the proposed scheme is demonstrated by the numerical simulations for the cases of attitude stabilization and tracking both. Some of the results reported in this chapter have been published in (Ali, Radice and Kim, 2010).

2.1 Rigid Spacecraft Attitude Motion

First, we introduce various reference frames which will be used in the following developments. The spacecraft is assumed to be a rigid body and three mutually perpendicular axes fixed in the spacecraft define a body frame \mathbf{B} with origin at the centre of mass of the spacecraft. The spacecraft is assumed to be equipped with the actuators that can provide torques about the axes of the body frame \mathbf{B} . Let \mathbf{N} be an inertial frame. The orientation of the body frame \mathbf{B} with respect to the inertial frame \mathbf{N} is represented by the quaternion $\tilde{\mathbf{q}} = [\tilde{\mathbf{q}}_v^T, \tilde{q}_4]^T$ with $\tilde{\mathbf{q}}_v \in \mathfrak{R}^3$, $\tilde{q}_4 \in \mathfrak{R}$ and $\tilde{\mathbf{q}}_v^T \tilde{\mathbf{q}}_v + \tilde{q}_4^2 = 1$, where \mathfrak{R} is the real number set.

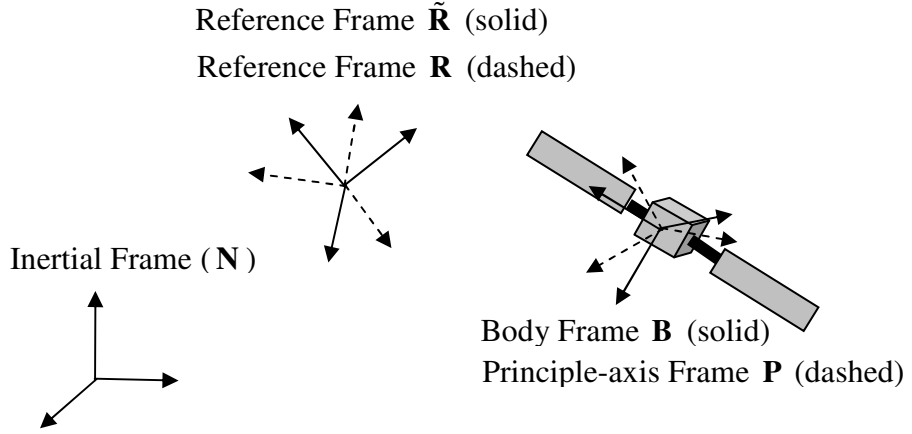


Fig. 2.1 Relations between the used frames: The reference frame \mathbf{R} is rigidly connected to the reference frame $\tilde{\mathbf{R}}$ and is misaligned with it in the same way as the principle-axis frame \mathbf{P} with the body frame \mathbf{B} .

The reference frame corresponding to the commanded motion is denoted by $\tilde{\mathbf{R}}$ and its attitude with respect to the inertial frame \mathbf{N} is specified by the quaternion $\mathbf{q}_r = [q_{rv}^T, q_{r4}]^T$.

The quaternion $\tilde{\boldsymbol{\sigma}} = [\tilde{\boldsymbol{\sigma}}_v^T, \tilde{\sigma}_4]^T$ describes the orientation of the body frame \mathbf{B} with respect to the reference frame $\tilde{\mathbf{R}}$ and is written as

$$\begin{aligned}\tilde{\boldsymbol{\sigma}}_v &= q_{r4} \tilde{\mathbf{q}}_v - \tilde{q}_4 \mathbf{q}_{rv} - \mathbf{q}_{rv} \times \tilde{\mathbf{q}}_v \\ \tilde{\sigma}_4 &= \mathbf{q}_{rv}^T \tilde{\mathbf{q}}_v + q_{r4} \tilde{q}_4\end{aligned}\tag{2.1}$$

Let \mathbf{P} represent the spacecraft principal-axis frame. We choose to define a reference frame \mathbf{R} which is rigidly connected to the reference frame $\tilde{\mathbf{R}}$ and is misaligned with it in the same way as the principal-axis frame \mathbf{P} with the body frame \mathbf{B} . The attitude tracking error is taken as $\boldsymbol{\sigma} = [\boldsymbol{\sigma}_v^T, \sigma_4]^T$ which is the quaternion representing the attitude of the principal-axis frame \mathbf{P} relative to the reference frame \mathbf{R} . If \mathbf{S} denotes the direction cosine matrix of the principal-axis frame \mathbf{P} relative to the body frame \mathbf{B} then $\boldsymbol{\sigma}_v = \mathbf{S}\tilde{\boldsymbol{\sigma}}_v$ and $\sigma_4 = \tilde{\sigma}_4$. With the mentioned choice for the definition of attitude tracking error, the coincidence of the principal-axis frame \mathbf{P} with the reference frame \mathbf{R} makes the body frame \mathbf{B} align to the reference frame $\tilde{\mathbf{R}}$. A graphical description of all the aforesaid frames is available as Fig. 2.1. The equations of rotational motion of the spacecraft are given by (Shuster, 1993)

$$\dot{\tilde{\mathbf{q}}}_v = \frac{1}{2}(\tilde{q}_4\tilde{\boldsymbol{\omega}} - \tilde{\boldsymbol{\omega}} \times \tilde{\mathbf{q}}_v), \quad \dot{\tilde{q}}_4 = -\frac{1}{2}\tilde{\boldsymbol{\omega}}^T \tilde{\mathbf{q}}_v \quad (2.2)$$

$$\mathbf{J}_B \dot{\tilde{\boldsymbol{\omega}}} + \tilde{\boldsymbol{\omega}} \times [\mathbf{J}_B \tilde{\boldsymbol{\omega}}] = \mathbf{T}_B \quad (2.3)$$

where $\tilde{\boldsymbol{\omega}} = [\tilde{\omega}_1, \tilde{\omega}_2, \tilde{\omega}_3]^T$ is the angular velocity of the spacecraft with respect to the inertial frame \mathbf{N} expressed in the body frame \mathbf{B} , $\mathbf{J}_B = \mathbf{J}_B^T$ is the body frame \mathbf{B} referenced, positive definite inertia matrix of the spacecraft, \mathbf{T}_B is the control torque vector in the body frame \mathbf{B} and the superscript, $(\cdot)^T$, is the transpose of vector or matrix. We define the three subscripts i, j and k as the element of the set Id as follows: $(i, j, k) \in \text{Id}$, where $\text{Id} = \{(1, 2, 3), (2, 3, 1), (3, 1, 2)\}$. The first part of Eq. (2.2) can be written as

$$\dot{\tilde{q}}_i = \frac{1}{2}(\tilde{q}_4\tilde{\omega}_i - \tilde{q}_k\tilde{\omega}_j + \tilde{q}_j\tilde{\omega}_k) \quad (2.4)$$

for $(i, j, k) \in \text{Id}$.

Let us have $\boldsymbol{\omega} = \mathbf{S}\tilde{\boldsymbol{\omega}}$, $\mathbf{T} = \mathbf{S}\mathbf{T}_B$ and $\mathbf{J} = \mathbf{S}\mathbf{J}_B\mathbf{S}^T$ where $\boldsymbol{\omega} = [\omega_1, \omega_2, \omega_3]^T$, $\mathbf{T} = [T_1, T_2, T_3]^T$ and $\mathbf{J} = \text{diag}(J_1, J_2, J_3)$. For the principal-axis frame \mathbf{P} , Eq. (2.3) becomes

$$\dot{\omega}_i = p_i \omega_j \omega_k + u_i \quad (2.5)$$

where $p_i = (J_j - J_k) / J_i$ and $u_i = T_i / J_i$, for $(i, j, k) \in \text{Id}$. Further, the spacecraft principal-axis frame \mathbf{P} is desired to track the attitude motion of the reference frame \mathbf{R} whose angular velocity and angular acceleration relative to the inertial frame \mathbf{N} expressed in the principal-axis frame \mathbf{P} are denoted by $\boldsymbol{\omega}_r = [\omega_1^r, \omega_2^r, \omega_3^r]^T$ and $\dot{\boldsymbol{\omega}}_r = [\dot{\omega}_1^r, \dot{\omega}_2^r, \dot{\omega}_3^r]^T$, respectively. The angular velocity tracking error is written as

$$\delta\boldsymbol{\omega} = \boldsymbol{\omega} - \boldsymbol{\omega}_r \quad (2.6)$$

whereas for the angular acceleration tracking error we have

$$\frac{{}^P d}{dt}(\delta\boldsymbol{\omega}) = \dot{\boldsymbol{\omega}} - \dot{\boldsymbol{\omega}}_r + \boldsymbol{\omega} \times \boldsymbol{\omega}_r \quad (2.7)$$

where $\frac{{}^P d}{dt}(\delta\boldsymbol{\omega}) = [\delta\dot{\omega}_1, \delta\dot{\omega}_2, \delta\dot{\omega}_3]^T$ represents the derivative of $\delta\boldsymbol{\omega}$ as seen by the principal-axis frame \mathbf{P} (Schaub and Junkins, 2003). Equations (2.5) and (2.7) can be used to write the tracking error dynamics equation as

$$\delta\dot{\omega}_i = p_i \omega_j \omega_k + u_i - \dot{\omega}_i^r + \omega_j \omega_k^r - \omega_k \omega_j^r \quad (2.8)$$

for $(i, j, k) \in \text{Id}$. Finally, the attitude tracking control objective becomes the regulation of $\lim_{t \rightarrow \infty} [\boldsymbol{\sigma}_v(t), \delta\boldsymbol{\omega}(t)] = \mathbf{0}$.

2.2 Control Design and Torque Bound

The candidate Lyapunov function for the kinematics subsystem stabilization is

$$V = \frac{1}{2} [\sigma_1^2 + \sigma_2^2 + \sigma_3^2 + (1 - \sigma_4)^2] \quad (2.9)$$

which is continuously differentiable and zero at the equilibrium point $\boldsymbol{\sigma}_v = \mathbf{0}$ and $\sigma_4 = 1$.

The time derivative of V comes out to be

$$\dot{V} = \frac{1}{2} \sum_{i=1}^3 \sigma_i \delta\omega_i \quad (2.10)$$

For stabilizing the kinematics subsystem, the pseudo control input, $\delta\omega_i^s$, is based on a nonlinear tracking function $\phi(\sigma_i)$ as follows (Kim and Kim, 2003)

$$\delta\omega_i^s = -s\phi(\sigma_i) \quad (2.11)$$

where s is a positive constant and the nonlinear tracking function $\phi(\sigma_i)$ is given by

$$\phi(\sigma_i) = \alpha \tan^{-1}(\beta\sigma_i) \quad (2.12)$$

with α and β as positive constants. This choice of the pseudo control for the kinematics subsystem achieves the objective of $\lim_{t \rightarrow \infty} \sigma_v(t) = \mathbf{0}$ as it makes the time derivative of the Lyapunov function V given by Eq. (2.9) as the negative semidefinite as follows:

$$\dot{V} = -\frac{1}{2}s \sum_{i=1}^3 \sigma_i \phi(\sigma_i) \quad (2.13)$$

Further, the convergence to $\sigma_v = \mathbf{0}$ and $\sigma_4 = 1$ is achieved asymptotically for all initial conditions $\sigma(t_0)$ whenever the initial condition $\sigma_4(t_0) \neq -1$, where t_0 is the initial time (Luo, Chu and Ling, 2005b). Next, the function V is augmented with the dynamics part of the system as follows (Mazenc and Iggidr, 2004)

$$U = V + \frac{1}{2} \sum_{i=1}^3 \left[\Omega(\delta\omega_i) - \Omega(\delta\omega_i^s) \right]^2 \quad (2.14)$$

where $\Omega(\cdot)$ is a class κ_∞ function, i.e. it is zero at zero, strictly increasing and becomes unbounded as its argument increases to infinity (Mazenc and Iggidr, 2004). The time derivative of the overall Lyapunov function U yields

$$\begin{aligned}
 \dot{U} &= \frac{1}{2} \sum_{i=1}^3 \sigma_i \delta \omega_i + \sum_{i=1}^3 \left[\Omega(\delta \omega_i) - \Omega(\delta \omega_i^s) \right] \left[\Omega'(\delta \omega_i) \delta \dot{\omega}_i - \Omega'(\delta \omega_i^s) \delta \dot{\omega}_i^s \right] \\
 &= \frac{1}{2} \sum_{i=1}^3 \sigma_i \delta \omega_i^s + \sum_{i=1}^3 \frac{1}{2} \sigma_i (\delta \omega_i - \delta \omega_i^s) + \sum_{i=1}^3 \left[-\Omega'(\delta \omega_i^s) \delta \dot{\omega}_i^s + \right. \\
 &\quad \left. \Omega'(\delta \omega_i) (p_i \omega_j \omega_k + u_i - \dot{\omega}_i^r + \omega_j \omega_k^r - \omega_k \omega_j^r) \right] \left[\Omega(\delta \omega_i) - \Omega(\delta \omega_i^s) \right] \quad (2.15) \\
 &= -\frac{1}{2} s \sum_{i=1}^3 \sigma_i \phi(\sigma_i) + \sum_{i=1}^3 \left\{ \frac{1}{2} \sigma_i + \left[-\Omega'(\delta \omega_i^s) \delta \dot{\omega}_i^s + \right. \right. \\
 &\quad \left. \left. \Omega'(\delta \omega_i) (p_i \omega_j \omega_k + u_i - \dot{\omega}_i^r + \omega_j \omega_k^r - \omega_k \omega_j^r) \right] \frac{\Omega(\delta \omega_i) - \Omega(\delta \omega_i^s)}{\delta \omega_i - \delta \omega_i^s} \right\} (\delta \omega_i - \delta \omega_i^s)
 \end{aligned}$$

where $\Omega(x)$ is chosen such that

$$\left[\Omega(\delta \omega_i) - \Omega(\delta \omega_i^s) \right] / (\delta \omega_i - \delta \omega_i^s) \neq 0$$

where $\Omega'(x)$ denotes the derivative of $\Omega(x)$ with respect to x . A negligibly small numerator on the left hand side of above equation may cause numerical problems so it should be large enough to avoid such practical implementation issues. In order to make the time derivative of U equal to the following:

$$\dot{U} = -\frac{1}{2} s \sum_{i=1}^3 \sigma_i \phi(\sigma_i) - g \sum_{i=1}^3 (\delta \omega_i - \delta \omega_i^s)^2 \quad (2.16)$$

the backstepping controller comes out to be

$$u_i = \frac{1}{\Omega'(\delta \omega_i)} \left\{ -\frac{\delta \omega_i - \delta \omega_i^s}{\Omega(\delta \omega_i) - \Omega(\delta \omega_i^s)} \left[\frac{1}{2} \sigma_i + g(\delta \omega_i - \delta \omega_i^s) \right] + \Omega'(\delta \omega_i^s) \delta \dot{\omega}_i^s \right\} - \quad (2.17)$$

$$p_i \omega_j \omega_k + \dot{\omega}_i^r - \omega_j \omega_k^r + \omega_k \omega_j^r$$

for $(i, j, k) \in \text{Id}$, where g is a positive constant. Now, for the closed loop system, the attitude tracking control objective $\lim_{t \rightarrow \infty} [\sigma_v(t), \delta \omega(t)] = \mathbf{0}$ is achieved ‘almost’ globally and asymptotically as Eq. (2.16) is negative semidefinite. The standard terminology of ‘almost’ global stability for this problem means stability over an open and dense set in the set of the special group of rotation matrices that describe spacecraft orientation in three dimensions $SO(3)$ (Tsiotras, 1998; Seo and Akella, 2007). This is because of the well-known fact that $SO(3)$ is not a contractible space and, hence, the quaternion-based

controllers do not offer globally continuous stabilizing formulations (Wen and Kreutz-Delgado, 1991; Bhat and Bernstein, 2000).

Note that by equating Eqs. (2.15) and (2.16) we can find the time derivative of $U - V$ as given below which is subject to the condition that the control input is given by Eq. (2.17):

$$\frac{d}{dt} \left(\frac{1}{2} \left[\Omega(\delta\omega_i) - \Omega(\delta\omega_i^s) \right]^2 \right) = -g(\delta\omega_i - \delta\omega_i^s)^2 - \frac{1}{2} \sigma_i (\delta\omega_i - \delta\omega_i^s) \quad (2.18)$$

for $i = 1, 2, 3$.

We choose a simple form of class κ_∞ function as $\Omega(\delta\omega_i) = \eta \delta\omega_i$ with $\eta > 0$, which satisfies the condition $\left[\Omega(\delta\omega_i) - \Omega(\delta\omega_i^s) \right] / (\delta\omega_i - \delta\omega_i^s) = \eta \neq 0$, for $i = 1, 2, 3$. Then, the control input is rewritten as follows:

$$u_i = -\frac{1}{\eta^2} \left[\frac{1}{2} \sigma_i + g(\delta\omega_i - \delta\omega_i^s) \right] - \frac{1}{2} s \phi'(\sigma_i) (\sigma_4 \delta\omega_i - \sigma_k \delta\omega_j + \sigma_j \delta\omega_k) - p_i \omega_j \omega_k + \dot{\omega}_i^r - \omega_j \omega_k^r + \omega_k \omega_j^r \quad (2.19)$$

for $(i, j, k) \in \text{Id}$, where $\phi'(\sigma_i)$ is the derivative of $\phi(\sigma_i)$ with respect to σ_i . The control law given by the above expression can be decomposed into the terms involving the proportional and derivative actions (Seo and Akella, 2007). The proportional action term gain comes out to be a constant whereas that for the derivative action term happens to be a nonlinear function of the attitude tracking error. That is why, it is said to belong to nonlinear proportional-derivative type. Defining $e = [e_1, e_2, e_3]^T$ where $e_i \equiv \delta\omega_i - \delta\omega_i^s$, the above equation can be written as

$$u_i = -\frac{1}{\eta^2} \left[\frac{1}{2} \sigma_i + g e_i \right] - \frac{1}{2} s \phi'(\sigma_i) (\sigma_4 e_i - \sigma_k e_j + \sigma_j e_k + \sigma_4 \delta\omega_i^s - \sigma_k \delta\omega_j^s + \sigma_j \delta\omega_k^s) - p_i (e_j + \delta\omega_j^s + \omega_j^r) (e_k + \delta\omega_k^s + \omega_k^r) + \dot{\omega}_i^r - (e_j + \delta\omega_j^s) \omega_k^r + (e_k + \delta\omega_k^s) \omega_j^r \quad (2.20)$$

As $|\sigma_i| \leq 1$, $|\delta\omega_i^s| \leq s\alpha \tan^{-1}(\beta)$, $|\phi'(\sigma_i)| \leq \alpha\beta$, $|\omega_i^r| \leq \xi$ and $|\dot{\omega}_i^r| \leq \gamma$ for $i = 1, 2, 3$, the control torque bound is derived using the triangle inequalities as follows:

$$\begin{aligned}
 |u_i| &\leq \frac{1}{\eta^2} \left(\frac{1}{2} |\sigma_i| + g |e_i| \right) + \frac{1}{2} s |\phi'(\sigma_i)| \left| \sigma_4 e_i - \sigma_k e_j + \sigma_j e_k + \sigma_4 \delta \omega_i^s - \sigma_k \delta \omega_j^s + \sigma_j \delta \omega_k^s \right| + \\
 &\quad \left| p_i (e_j + \delta \omega_j^s + \omega_j^r) (e_k + \delta \omega_k^s + \omega_k^r) \right| + \left| \dot{\omega}_i^r \right| + \left| (e_j + \delta \omega_j^s) \omega_k^r \right| + \left| (e_k + \delta \omega_k^s) \omega_j^r \right| \\
 &\leq \frac{1}{\eta^2} \left(\frac{1}{2} + g |e_i| \right) + \frac{1}{2} s \alpha \beta \left(\left| \sigma_4 e_i \right| + \left| \sigma_k e_j \right| + \left| \sigma_j e_k \right| + \left| \sigma_4 \delta \omega_i^s \right| + \left| \sigma_k \delta \omega_j^s \right| + \left| \sigma_j \delta \omega_k^s \right| \right) + \\
 &\quad \left| p_i \right| \left| e_j e_k + e_j \delta \omega_k^s + e_j \omega_k^r + \delta \omega_j^s e_k + \delta \omega_j^s \delta \omega_k^s + \delta \omega_j^s \omega_k^r + \omega_j^r e_k + \omega_j^r \delta \omega_k^s + \omega_j^r \omega_k^r \right| + \left| \dot{\omega}_i^r \right| + \\
 &\quad \left| e_j + \delta \omega_j^s \right| \left| \omega_k^r \right| + \left| e_k + \delta \omega_k^s \right| \left| \omega_j^r \right| \\
 &\leq \frac{1}{\eta^2} \left(\frac{1}{2} + g |e_i| \right) + \frac{1}{2} s \alpha \beta \left(|e_i| + |e_j| + |e_k| + 3s \alpha \tan^{-1}(\beta) \right) + \\
 &\quad \left| p_i \right| \left\{ |e_j| |e_k| + \left(\xi + s \alpha \tan^{-1}(\beta) \right) \left(|e_j| + |e_k| + s \alpha \tan^{-1}(\beta) \right) + \xi s \alpha \tan^{-1}(\beta) + \xi^2 \right\} + \\
 &\quad \gamma + \left(|e_j| + |e_k| + 2s \alpha \tan^{-1}(\beta) \right) \xi
 \end{aligned} \tag{2.21}$$

for $(i, j, k) \in \text{Id}$. Rearranging the terms, the above inequality becomes

$$|u_i| \leq k_{1i} + k_2 |e_i| + k_{3i} \left(|e_j| + |e_k| \right) + |p_i| |e_j| |e_k| \tag{2.22}$$

for $(i, j, k) \in \text{Id}$, where the constants k_{1i} , k_2 and k_{3i} are

$$\begin{aligned}
 k_{1i} &= \frac{1}{2\eta^2} + \left(\frac{3}{2} s \alpha \beta + 2\xi \right) s \alpha \tan^{-1}(\beta) + |p_i| \left(\xi + s \alpha \tan^{-1}(\beta) \right)^2 + \gamma \\
 k_2 &= \frac{g}{\eta^2} + \frac{1}{2} s \alpha \beta \\
 k_{3i} &= s \alpha \left(\frac{1}{2} \beta + |p_i| \tan^{-1}(\beta) \right) + \left(|p_i| + 1 \right) \xi
 \end{aligned} \tag{2.23}$$

However, the angular rate error $e_i(t)$, for $i = 1, 2, 3$, is unknown in Eq. (2.22). Hence, Eq. (2.22) does not give any useful information about the control torque bound. To obtain the bound for the angular rate error, recall Eq. (2.18) with $\Omega(\delta \omega_i) = \eta \delta \omega_i$ for $i = 1, 2, 3$. Then,

$$\eta^2 \frac{d}{dt} \left(\frac{1}{2} e_i^2 \right) = -g e_i^2 - \frac{1}{2} \sigma_i e_i \tag{2.24}$$

for $i = 1, 2, 3$. Eq. (2.24) implies that if $|e_i| > |\sigma_i| / (2g)$, then $|e_i|$ is guaranteed to be decreasing to a certain value that is bounded by $1 / (2g)$. Therefore, $|e_i|$ is bounded by the following inequality:

$$|e_i(t)| \leq \max \left[|e_i(t_0)|, \frac{1}{2g} \right] \quad (2.25)$$

for all t in $[t_0, \infty)$ for $i=1,2,3$, where t_0 is the initial time and $\max(,)$ is the function whose value is the maximum of two arguments .

Finally, Eq. (2.22) is used to calculate the bounds of the controls u_i and the control torque is bounded by

$$|T_i| \leq J_i \left[k_{1i} + k_2 |e_i(t)| + k_{3i} (|e_j(t)| + |e_k(t)|) + |p_i| |e_j(t)| |e_k(t)| \right] \quad (2.26)$$

for $(i, j, k) \in \text{Id}$ where $|e_i(t)|$ for $i=1,2,3$ follows the inequality (2.25). Hence, the minimum value of the bound for $|T_i|$ identifiable by Eq. (2.26) comes out to be

$$J_i \left[k_{1i} + \frac{1}{2g} \left(k_2 + 2k_{3i} + \frac{1}{2g} |p_i| \right) \right] \quad (2.27)$$

The control torque components bounds given by Eq. (2.26) can be used to calculate the bound for Euclidean-norm $\|T\|$. Moreover, the direction cosine matrix \mathbf{S} mentioned in the previous section can be used to calculate T_B from T however this transformation does not affect the bound for the Euclidean-norm of control torque.

2.3 Robustness Analysis

The attitude control design of satellites is coupled to main issues like disturbances from space environment, perturbation from spacecraft's moments of inertia variations and control input constraints (Wu, Cao and Li, 2009). Gravity gradient torque, aerodynamic torque and Earth magnetic field torque are among the major disturbances for low-Earth orbit (LEO) satellites being below 1000 km altitude. Moments of inertia variations are caused by the movement of payload and appendages such as telescope, camera, solar array panels etc. and attitude control systems of microsattellites with mass less than 100 kg and moment of inertia of around 20 kg m² are quite sensitive to the aforesaid disturbance

torques and moments of inertia variations (Wu, Cao and Li, 2009). So, the spacecraft attitude control design, while dealing with the issue of control input saturation, should also take into account the existence of external disturbances and parameters like moments of inertia uncertainties (Kim and Kim, 2003; Wu, Cao and Li, 2009). In this section, the control law given by Eq. (2.17) is explored for robustness against the said uncertainties in the nominal moments of inertia J_i , $i=1,2,3$ and external disturbance torque.

Incorporating in the time derivative of the Lyapunov function U the non-nominal moments of inertia J_i^a and the external disturbance torque components T_i^d where $i=1,2,3$ we get

$$\begin{aligned} \dot{U} &= \frac{1}{2} \sum_{i=1}^3 \sigma_i \delta \omega_i + \sum_{i=1}^3 \left[\Omega(\delta \omega_i) - \Omega(\delta \omega_i^s) \right] \left[\Omega'(\delta \omega_i) \delta \dot{\omega}_i - \Omega'(\delta \omega_i^s) \delta \dot{\omega}_i^s \right] \\ &= -\frac{1}{2} s \sum_{i=1}^3 \sigma_i \phi(\sigma_i) + \sum_{i=1}^3 \left\{ \frac{1}{2} \sigma_i + \left[\Omega'(\delta \omega_i) \left(p_i^a \omega_j \omega_k + \frac{J_i}{J_i^a} u_i - \dot{\omega}_i^r + \omega_j \omega_k^r - \omega_k \omega_j^r + \frac{T_i^d}{J_i^a} \right) - \right. \right. \\ &\quad \left. \left. \Omega'(\delta \omega_i^s) \delta \dot{\omega}_i^s \right] \frac{\Omega(\delta \omega_i) - \Omega(\delta \omega_i^s)}{\delta \omega_i - \delta \omega_i^s} \right\} (\delta \omega_i - \delta \omega_i^s) \end{aligned} \quad (2.28)$$

where $\mathbf{J}_a = \text{diag}(J_1^a, J_2^a, J_3^a)$ is the principal-axis frame \mathbf{P} referenced non-nominal inertia matrix of the spacecraft and $\mathbf{T}_d = [T_1^d, T_2^d, T_3^d]^T$ the external disturbance torque vector expressed in the principal-axis frame \mathbf{P} . Substituting the control law u_i given by Eq. (2.17) in the above equation we get

$$\begin{aligned} \dot{U} &= -\frac{1}{2} s \sum_{i=1}^3 \sigma_i \phi(\sigma_i) + \sum_{i=1}^3 \left\{ \left(\Omega'(\delta \omega_i) \left[\left(p_i^a - p_i J_i / J_i^a \right) \omega_j \omega_k + T_i^d / J_i^a \right] + \right. \right. \\ &\quad \left. \left. \left(J_i / J_i^a - 1 \right) \left[\Omega'(\delta \omega_i) \left(\dot{\omega}_i^r - \omega_j \omega_k^r + \omega_k \omega_j^r \right) + \Omega'(\delta \omega_i^s) \delta \dot{\omega}_i^s \right] \right) \frac{\Omega(\delta \omega_i) - \Omega(\delta \omega_i^s)}{\delta \omega_i - \delta \omega_i^s} + \right. \\ &\quad \left. \left(1 - J_i / J_i^a \right) \frac{1}{2} \sigma_i - \left(J_i / J_i^a \right) g(\delta \omega_i - \delta \omega_i^s) \right\} (\delta \omega_i - \delta \omega_i^s) \end{aligned} \quad (2.29)$$

For $\Omega(x) = \eta x$, the above equation becomes

$$\begin{aligned}
 \dot{U} = & -\frac{1}{2}s \sum_{i=1}^3 \sigma_i \phi(\sigma_i) + \sum_{i=1}^3 \left\{ \eta^2 \left[\left(p_i^a - p_i J_i / J_i^a \right) \omega_j \omega_k + T_i^d / J_i^a + \right. \right. \\
 & \left. \left. \left(J_i / J_i^a - 1 \right) \left(\dot{\omega}_i^r - \omega_j \omega_k^r + \omega_k \omega_j^r + \delta \dot{\omega}_i^s \right) \right] + \left(1 - J_i / J_i^a \right) \frac{1}{2} \sigma_i - \right. \\
 & \left. \left. \left(J_i / J_i^a \right) g \left(\delta \omega_i - \delta \omega_i^s \right) \right\} \left(\delta \omega_i - \delta \omega_i^s \right)
 \end{aligned} \tag{2.30}$$

The condition for the above expression to be negative comes out to be

$$\begin{aligned}
 \left(J_i / J_i^a \right) g \left| \delta \omega_i - \delta \omega_i^s \right| > & \left[\left(1 - J_i / J_i^a \right) \frac{1}{2} \sigma_i + \eta^2 \left[\left(p_i^a - p_i J_i / J_i^a \right) \omega_j \omega_k + \right. \right. \\
 & \left. \left. T_i^d / J_i^a + \left(J_i / J_i^a - 1 \right) \left(\dot{\omega}_i^r - \omega_j \omega_k^r + \omega_k \omega_j^r + \delta \dot{\omega}_i^s \right) \right] \right]
 \end{aligned} \tag{2.31}$$

or

$$\begin{aligned}
 g \left| \delta \omega_i - \delta \omega_i^s \right| > & \left[\left(J_i^a / J_i - 1 \right) \frac{1}{2} \sigma_i + \eta^2 \left[\left(p_i^a J_i^a / J_i - p_i \right) \omega_j \omega_k + \right. \right. \\
 & \left. \left. T_i^d / J_i + \left(1 - J_i^a / J_i \right) \left(\dot{\omega}_i^r - \omega_j \omega_k^r + \omega_k \omega_j^r + \delta \dot{\omega}_i^s \right) \right] \right]
 \end{aligned} \tag{2.32}$$

for $i=1,2,3$.

Regarding the variations of the moments of inertia, the non-nominal values J_i^a can be written as the sum of nominal values J_i and perturbations ΔJ_i as (Wu, Cao and Li, 2009)

$$J_i^a = J_i + \Delta J_i \tag{2.33}$$

for $i=1,2,3$ where if the uncertain perturbations in the moments of inertia ΔJ_i are considered to be 100λ percent with respect to their nominal values then the variations envelopes of ΔJ_i are given by $\Delta J_i \in [-\lambda J_i, \lambda J_i]$ and uncertain non-nominal moments of inertia J_i^a come out to be $J_i^a \in [J_i(1-\lambda), J_i(1+\lambda)]$ for $i=1,2,3$. For example, if we allow 20 percent variation of moments of inertia with respect to their nominal values then the uncertain non-nominal moments of inertia J_i^a can assume any values across the variations envelopes $J_i^a \in [0.8J_i, 1.2J_i]$ for $i=1,2,3$. So, we can write

$$\left|J_i^a/J_i - 1\right| \leq \lambda \quad (2.34)$$

for $i=1,2,3$ and

$$\left|p_i^a J_i^a/J_i - p_i\right| \leq \lambda(J_j + J_k)/J_i \quad (2.35)$$

for $(i, j, k) \in \text{Id}$.

For the bound of the right hand side term of the condition given by inequality (2.32) we can write

$$\begin{aligned} & \left| \left(J_i^a/J_i - 1 \right) \frac{1}{2} \sigma_i + \eta^2 \left[\left(p_i^a J_i^a/J_i - p_i \right) \omega_j \omega_k + T_i^d/J_i + \right. \right. \\ & \quad \left. \left. \left(1 - J_i^a/J_i \right) \left(\dot{\omega}_i^r - \omega_j \omega_k^r + \omega_k \omega_j^r + \delta \dot{\omega}_i^s \right) \right] \right| \\ & \leq \frac{1}{2} \lambda + \eta^2 \left[\left[\lambda (J_j + J_k)/J_i \right] \left| (e_j + \delta \omega_j^s + \omega_j^r)(e_k + \delta \omega_k^s + \omega_k^r) \right| + \left| T_i^d \right|/J_i + \right. \\ & \quad \left. \lambda \left| \dot{\omega}_i^r - \omega_j \omega_k^r + \omega_k \omega_j^r + \delta \dot{\omega}_i^s \right| \right] \\ & \leq \frac{1}{2} \lambda + \\ & \quad \eta^2 \left[\left[\lambda (J_j + J_k)/J_i \right] \left\{ |e_j| |e_k| + \left(\xi + s\alpha \tan^{-1}(\beta) \right) \left(|e_j| + |e_k| + s\alpha \tan^{-1}(\beta) + \xi \right) \right\} + D_i/J_i + \right. \\ & \quad \left. \lambda \left\{ \gamma + \xi \left(|e_j| + |e_k| + 2s\alpha \tan^{-1}(\beta) \right) + \frac{1}{2} s\alpha \beta \left(|e_i| + |e_j| + |e_k| + 3s\alpha \tan^{-1}(\beta) \right) \right\} \right] \end{aligned} \quad (2.36)$$

where $\left|T_i^d\right| \leq D_i$ for $i=1,2,3$. So, a conservative version of the condition given by inequality (2.31) can be found as

$$g|e_i(t)| > \frac{1}{2} \lambda + \Theta_i(\mathbf{e}(t)) \quad (2.37)$$

where

$$\begin{aligned}
 \Theta_i(\mathbf{e}(t)) = & \eta^2 \left[D_i/J_i + [\lambda(J_j + J_k)/J_i] \left\{ |e_j(t)| |e_k(t)| + \right. \right. \\
 & \left. \left. (\xi + s\alpha \tan^{-1}(\beta)) (|e_j(t)| + |e_k(t)| + s\alpha \tan^{-1}(\beta) + \xi) \right\} + \right. \\
 & \left. \lambda \left\{ \gamma + \xi (|e_j(t)| + |e_k(t)| + 2s\alpha \tan^{-1}(\beta)) + \right. \right. \\
 & \left. \left. \frac{1}{2} s\alpha \beta (|e_i(t)| + |e_j(t)| + |e_k(t)| + 3s\alpha \tan^{-1}(\beta)) \right\} \right]
 \end{aligned} \tag{2.38}$$

for $(i, j, k) \in \text{Id}$. Further, in this case the Eq. (2.24) takes the form

$$\begin{aligned}
 \eta^2 \frac{d}{dt} \left(\frac{1}{2} e_i^2 \right) = & \left\{ - \left(J_i/J_i^a \right) g e_i - J_i/J_i^a \frac{1}{2} \sigma_i + \eta^2 \left[\left(p_i^a - p_i J_i/J_i^a \right) \omega_j \omega_k + T_i^d/J_i^a + \right. \right. \\
 & \left. \left. \left(J_i/J_i^a - 1 \right) \left(\dot{\omega}_i^r - \omega_j \omega_k^r + \omega_k \omega_j^r + \delta \dot{\omega}_i^s \right) \right] \right\} e_i
 \end{aligned} \tag{2.39}$$

for $(i, j, k) \in \text{Id}$. The above equation implies that the condition

$$g |e_i(t)| > \frac{1}{2} + \Theta_i(\mathbf{e}(t_0)) \tag{2.40}$$

ensures $|e_i(t)|$ to decrease to a certain value that is bounded by $(1/2 + \Theta_i(\mathbf{e}(t_0)))/g$ where $\Theta_i(\mathbf{e}(t_0))$ is calculated using Eq. (2.38). Hence, $|e_i|$ is bounded as

$$|e_i(t)| \leq \max \left[|e_i(t_0)|, \frac{1 + 2\Theta_i(\mathbf{e}(t_0))}{2g} \right] \tag{2.41}$$

for $i=1,2,3$. Lastly, the bound for the control torque components is given by Eq. (2.26) where $|e_i(t)|$ for $i=1,2,3$ follows the inequality (2.41) and the minimum value of the bound for $|T_i|$ identifiable by Eq. (2.26) comes out to be

$$J_i \left[k_{1i} + \frac{1 + 2\Theta_i(\mathbf{e}(t_0))}{2g} \left(k_2 + 2k_{3i} + \frac{1 + 2\Theta_i(\mathbf{e}(t_0))}{2g} |p_i| \right) \right] \tag{2.42}$$

2.4 Attitude Stabilization Specialization

Developments of the previous two sections can be specialized to the case of attitude stabilization for which the reference frame $\tilde{\mathbf{R}}$ becomes coincident with the inertial frame \mathbf{N} (whereas the reference frame \mathbf{R} coincides with an inertial frame $\tilde{\mathbf{N}}$). The case of set point regulation, where the desired target frame is different from the inertial frame, can also be treated similarly. For this case, the pseudo controls are given by

$$\omega_i^s = -s\phi(q_i) \quad (2.43)$$

where $\phi(q_i) = \alpha \tan^{-1}(\beta q_i)$ and the unit quaternion $\mathbf{q} = [\mathbf{q}_v^T, q_4]^T$ with $\mathbf{q}_v = [q_1, q_2, q_3]^T$ is defined as $\mathbf{q}_v = \mathbf{S}\tilde{\mathbf{q}}_v$ and $q_4 = \tilde{q}_4$ representing the attitude of the principal-axis frame \mathbf{P} with respect to the inertial frame $\tilde{\mathbf{N}}$. The control law given by Eq. (2.17) with general class κ_∞ function $\Omega(\cdot)$ takes the form

$$u_i = \frac{1}{\Omega'(\omega_i)} \left\{ -\frac{\omega_i - \omega_i^s}{\Omega(\omega_i) - \Omega(\omega_i^s)} \left[\frac{1}{2} q_i + g(\omega_i - \omega_i^s) \right] + \Omega'(\omega_i^s) \dot{\omega}_i^s \right\} - p_i \omega_j \omega_k \quad (2.44)$$

whereas the one given by Eq. (2.19) for $\Omega(\omega_i) = \eta \omega_i$ with $\eta > 0$ is written as

$$u_i = -\frac{1}{\eta^2} \left[\frac{1}{2} q_i + g(\omega_i - \omega_i^s) \right] - \frac{1}{2} s \phi'(q_i) (q_4 \omega_i - q_k \omega_j + q_j \omega_k) - p_i \omega_j \omega_k \quad (2.45)$$

The bounds of the controls are given by Eq. (2.22) where $e_i \equiv \omega_i - \omega_i^s$ and the constants k_{1i} , k_2 and k_{3i} become

$$\begin{aligned} k_{1i} &= \frac{1}{2\eta^2} + \left(\frac{3}{2}\beta + |p_i| \tan^{-1}(\beta) \right) s^2 \alpha^2 \tan^{-1}(\beta) \\ k_2 &= \frac{g}{\eta^2} + \frac{1}{2} s \alpha \beta \\ k_{3i} &= s \alpha \left(\frac{1}{2} \beta + |p_i| \tan^{-1}(\beta) \right) \end{aligned} \quad (2.46)$$

Inequality (2.25) defines the bounds of $|e_i|$ to be used in Eq. (2.22) for calculating the bounds of the controls u_i for the nominal case. The bounds for $|e_i|$ to be employed in Eq. (2.22) for the bounds of the controls u_i under the action of uncertainties in moments of inertia and external disturbances are given by Eq. (2.41) and the condition for ensuring stability in this case is given by Eq. (2.37) where

$$\begin{aligned} \Theta_i(\mathbf{e}(t)) = & \eta^2 \left[D_i/J_i + [\lambda(J_j + J_k)/J_i] \left\{ |e_j(t)| |e_k(t)| + \right. \right. \\ & \left. \left. s\alpha \tan^{-1}(\beta) \left(|e_j(t)| + |e_k(t)| + s\alpha \tan^{-1}(\beta) \right) \right\} + \right. \\ & \left. \frac{1}{2} s\alpha\beta\lambda \left(|e_i(t)| + |e_j(t)| + |e_k(t)| + 3s\alpha \tan^{-1}(\beta) \right) \right] \end{aligned} \quad (2.47)$$

2.5 Numerical Simulation

Numerical simulation examples for the cases of both attitude stabilization and tracking are considered here for demonstrating the efficacy of proposed scheme.

2.5.1 Stabilization Case

If the reference frame $\tilde{\mathbf{R}}$ coincides with the inertial frame \mathbf{N} i.e. $\boldsymbol{\omega}_r(t) = \mathbf{0}$, $\mathbf{q}_r(t) = [0 \ 0 \ 0 \ 1]^T$, $\boldsymbol{\xi} = 0$ and $\gamma = 0$ then the problem is reduced to attitude stabilization. The effectiveness of the proposed backstepping controller for the case of attitude stabilization is evaluated through the numerical simulation of a rest-to-rest slew manoeuvre. The simulation scenario considered by Krstić and Tsiotras (1999) and Kim and Kim (2003) is used for this purpose in the following. The numerical data for the scenario is given in Table 2.1 where t_0 represents the starting time. For the sake of comparison, the values of the gains s , α , β and g are adopted from (Kim and Kim, 2003). For the given values, the control torque bounds are obtained using Eq. (2.26) as follows:

$$\begin{aligned}
|T_1| &\leq \frac{103}{\eta^2} + 201 \\
|T_2| &\leq \frac{120}{\eta^2} + 316 \quad [\text{N m}] \\
|T_3| &\leq \frac{222}{\eta^2} + 382
\end{aligned} \tag{2.48}$$

Table 2.1 Stabilization Example Nominal Case by Trial and Error

Parameter	Value	Units
J_1	10	kg.m ²
J_2	15	kg.m ²
J_3	20	kg.m ²
$\mathbf{q}(t_0)$	[0.4646 0.1928 0.8047 0.3153] ^T	
$\boldsymbol{\omega}(t_0)$	[0 0 0] ^T	rad.s ⁻¹
s	1	
g	10	
α	0.75	
β	8	
η	3.5196	
$\ \mathbf{T}_{\text{analytical}}\ $	556	N.m
$\max(\ \mathbf{T}\)$	21.6	N.m
t_{settling}	5.18	s

Hence, the Euclidean norm bound is given by

$$\|\mathbf{T}\|_2 \leq 535 \sqrt{\frac{1.0}{\eta^4} + \frac{0.26}{\eta^2} + 1} \quad [\text{N m}] \tag{2.49}$$

For comparison with the results of (Kim and Kim, 2003), the gain η is tuned so that for the considered rest-to-test manoeuvre the value for $\max(\|\mathbf{T}\|)$ becomes 21.6 Nm where $\max(\|\mathbf{T}\|)$ denotes the peak Euclidean norm of the actual control torque from the simulation. By trial and error, η is tuned to the value given in Table 2.1. For the chosen η , the bound given by Eq. (2.49) becomes about 556 Nm whereas the settling time t_{settling}

comes out to be nearly 5.18 seconds. The simulation results are given by Fig. 2.2. Here, t_{settling} is defined as the time such that the norm of the states vector $[\mathbf{q}_v^T, \boldsymbol{\omega}^T]^T$ is bounded by 1% error from the steady state, which is zero in this case, for all $t \geq t_{\text{settling}}$. Better performance in the settling time is mainly because of the incorporation of the nonlinear tracking function $\phi(q_i)$ whereas the reduction of the peak control torque has been achieved through the introduction of the constant control gain η .

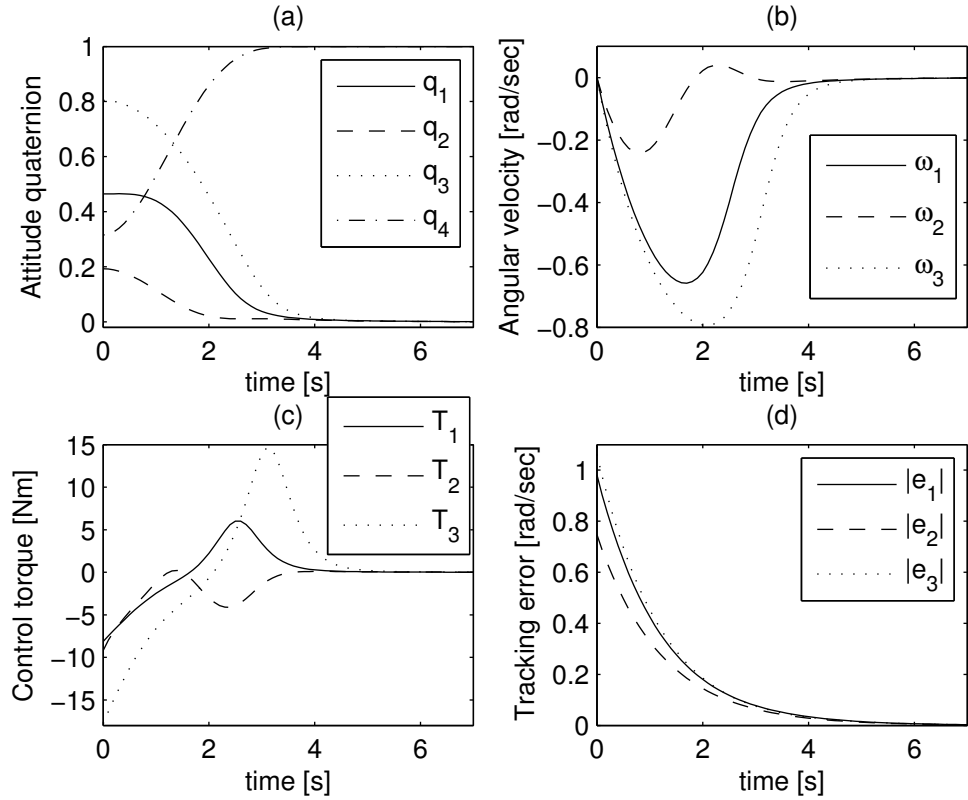


Fig. 2.2 Simulation results for the stabilization case example with the control gains tuned by trial and error

The proposed controller offers adequate performance despite the fact that it has a much simpler form than the one in (Kim and Kim, 2003), which uses additional switching parameters to obtain the robustness with respect to moments of inertia uncertainty. Moreover, as summarized in Table 2.3, it shows better performance when compared to other existing methods (Krstić and Tsotras, 1999; Wie and Barba, 1985; Joshi, Kelkar and Wen, 1995).

The bound given by Eq. (2.49) is very conservative being about 25 times larger than the actual maximum torque. This is caused by the short desired settling time as the corresponding control parameters become large to achieve that specification. Moreover, in this case, only one parameter, η , has been tuned. If all the five parameters in the bound, i.e. s , α , β , g and η , are simultaneously used for lowering the bound, this will be less conservative. To demonstrate this, the following optimization problem is solved using sequential quadratic programming (SQP):

$$\min_{\alpha>0.1, \beta>0.1, s>0.1, g>0.1, \eta>0.1} \left\| \mathbf{T}_{\text{analytical}} \right\|$$

subject to $t_{\text{settling}} \leq 5$ seconds, $\max(\|\mathbf{T}\|) \leq 21.6$ Nm and the closed loop differential equations, where $\mathbf{T}_{\text{analytical}}$ is the analytical upper bound given by Eq. (2.26). The lower bounds of all the gains are set to 0.1 as values of these parameters smaller than this would hardly achieve the given settling time specification of the closed loop response. Starting from the values of the gains given in Table 2.1, the above optimization problem is solved using SQP. The converged values of the parameters s , α , β , g and η are given in Table 2.2. Fig. 2.3 provides the simulation results for this case. The resulting $\left\| \mathbf{T}_{\text{analytical}} \right\|$ is about 174 Nm whereas the corresponding $\max(\|\mathbf{T}\|)$ is 21.6 Nm. The conservativeness of the upper bound is significantly reduced, i.e., from 25 times to just over 8 times bigger than the actual maximum torque. Moreover, the optimized bound guarantees that the actual control torque never exceeds the bound with the condition that $|e_i(t_0)|$ is less than or equal to the value for the current scenario.

Table 2.2 Stabilization Example Nominal Case with Minimized Analytical Bound for Control Torque Norm

Parameter	Value	Units
s	0.3356	
g	1.1644	
α	0.9835	
β	10.8985	

η	1.0131	
$\ T_{\text{analytical}}\ $	174	N.m
$\max(\ T\)$	21.6	N.m
t_{settling}	5	s

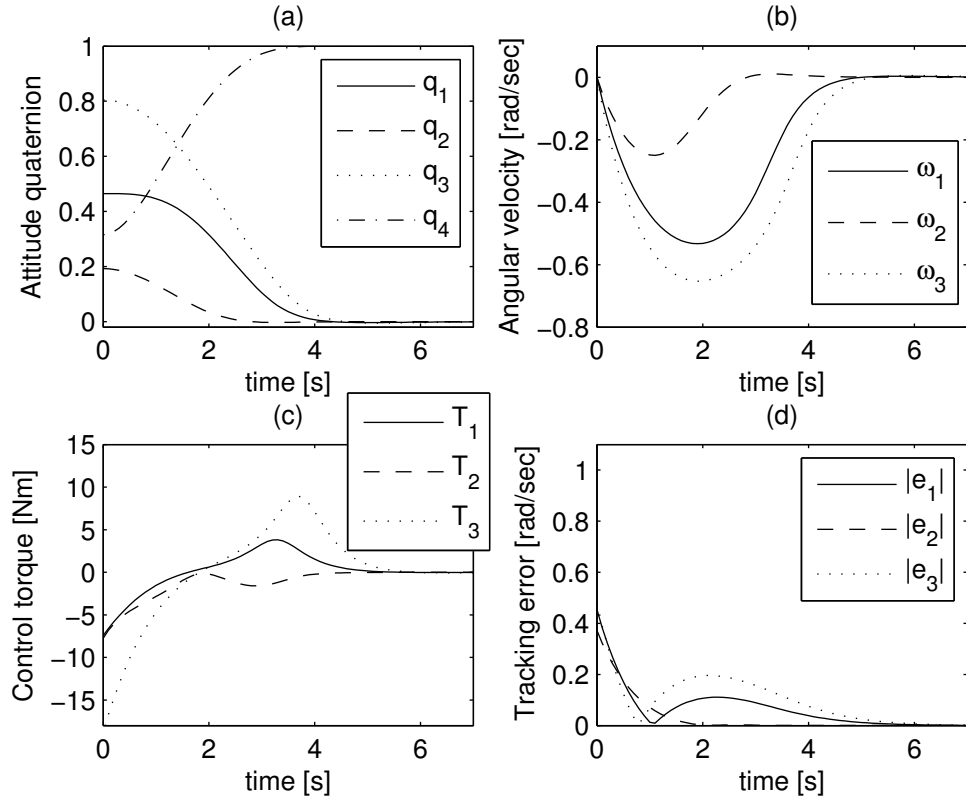


Fig. 2.3 Simulation results for the stabilization case example with the control gains tuned to minimize the analytical bound for control torque norm

It is noteworthy to compare the obtained value of the analytical torque bound even with the simulation values of the peak control torque mentioned in Table 2.3 where it is almost twice the one for (Wie and Barba, 1985) and is less than the ones by (Krstić and Tsiotras, 1999; Joshi, Kelkar and Wen, 1995; Kim and Kim, 2003). Here, we compare the linear version of the backstepping controller by (Kim and Kim, 2003). Moreover, in this study, we have exploited the integrator backstepping design methodology for developing an analytical bound for the control torque with the control law given by Eq. (2.19) being similar in shape to the one already existing in the literature (Seo and Akella, 2007). The methodology can be turned to further advantage by exploiting it to avoid the cancelation of ‘good’ nonlinearities, if any, in the system (Krstić, Kanellakopoulos and Kokotovic, 1995).

It may be helpful to decrease both the peak control torque from the simulation and its analytical bound. As we used a simple local optimization algorithm, the bound may also be improved further with some global optimization techniques.

In the above numerical example, the body axes \mathbf{B} and the principal axes \mathbf{P} of the spacecraft are taken as coincident. Otherwise, one can always find the inertia matrix about the principal axes \mathbf{P} and proceed as mentioned above. Later, the results can be transformed back to the body axes \mathbf{B} employing the transformation matrix \mathbf{S} however it does not change the findings regarding the bound for the Euclidean norm of the control torque.

Table 2.3 Stabilization Example Nominal Case Simulation Results Comparison: All values taken from (Kim and Kim, 2003) except the ones for the proposed controller

Controller	Peak control torque $\max(\ \mathbf{T}\)$ (N.m)	Angular velocity norm $\ \boldsymbol{\omega}\ $ (rad.s ⁻¹) at 5 s	Quaternion norm $\ \mathbf{q}_v\ $ at 5 s
Linear backstepping controller (Kim and Kim, 2003)	178.4	0.1151	0.1093
Controller in (Wie and Barba, 1985)	85.0	0.1170	0.1039
Controller in (Joshi, Kelkar and Wen, 1995)	311.8	0.1402	0.1957
Controller in (Krstić and Tsiotras, 1999)	196.2	0.1327	0.2304
Controller in (Kim and Kim, 2003)	21.6	5.75e-4	9.64e-5
Proposed Controller	21.6	10.2e-3	5.6e-3

The nominal values of the spacecraft moments of inertia considered for the numerical simulations are typical of a microsatellite with mass around 100 kg. The variation in the moments of inertia of a microsatellite caused by some instrument or payload movement is an important consideration for the attitude controller design and robustness against such uncertainties needs to be ensured (Wu, Cao and Li, 2009). Now, we consider the ongoing

numerical example with 20 percent uncertain variation in the moments of inertia with respect to their nominal values.

For this perturbation we have $\lambda = 0.2$. At the same time we also consider the presence of external disturbance with bounds $D_i = 0.1732$ Nm for $i = 1, 2, 3$. This external torque disturbance is substantially larger than what a spacecraft in orbit would usually be subjected to because of solar or atmospheric drag (Schaub and Junkins, 2003). Next, we solve the aforementioned optimization problem subject to $t_{\text{settling}} \leq 9.0125$ seconds, $(1/2 + \Theta_i(\mathbf{e}(t_0))) / g \leq 0.05$ for $i = 1, 2, 3$ and the closed-loop dynamics. The values of the gains mentioned in Table 2.1 are used as the starting guess. The optimized values of the gains s , α , β , g and η are given in Table 2.4 which also mentions the resulting $\|\mathbf{T}_{\text{analytical}}\|$ and $\max(\|\mathbf{T}\|)$ being about 176 Nm and 109 Nm, respectively. Simulation results are given as Fig. 2.4.

Table 2.4 Stabilization Example Nominal Case with Minimized Analytical Bound for Control Torque Norm while Robustness Ensured

Parameter	Value	Units
s	0.0763	
g	971.6201	
α	2.6396	
β	13.4999	
η	8.1861	
$\ \mathbf{T}_{\text{analytical}}\ $	176.28	N.m
$\max(\ \mathbf{T}\)$	109.41	N.m
t_{settling}	9.0125	s
λ	0.2	
D_i for $i = 1, 2, 3$	0.1732	N.m
$(1/2 + \Theta_1(\mathbf{e}(t_0))) / g$	0.0499	
$(1/2 + \Theta_2(\mathbf{e}(t_0))) / g$	0.0434	
$(1/2 + \Theta_3(\mathbf{e}(t_0))) / g$	0.0390	

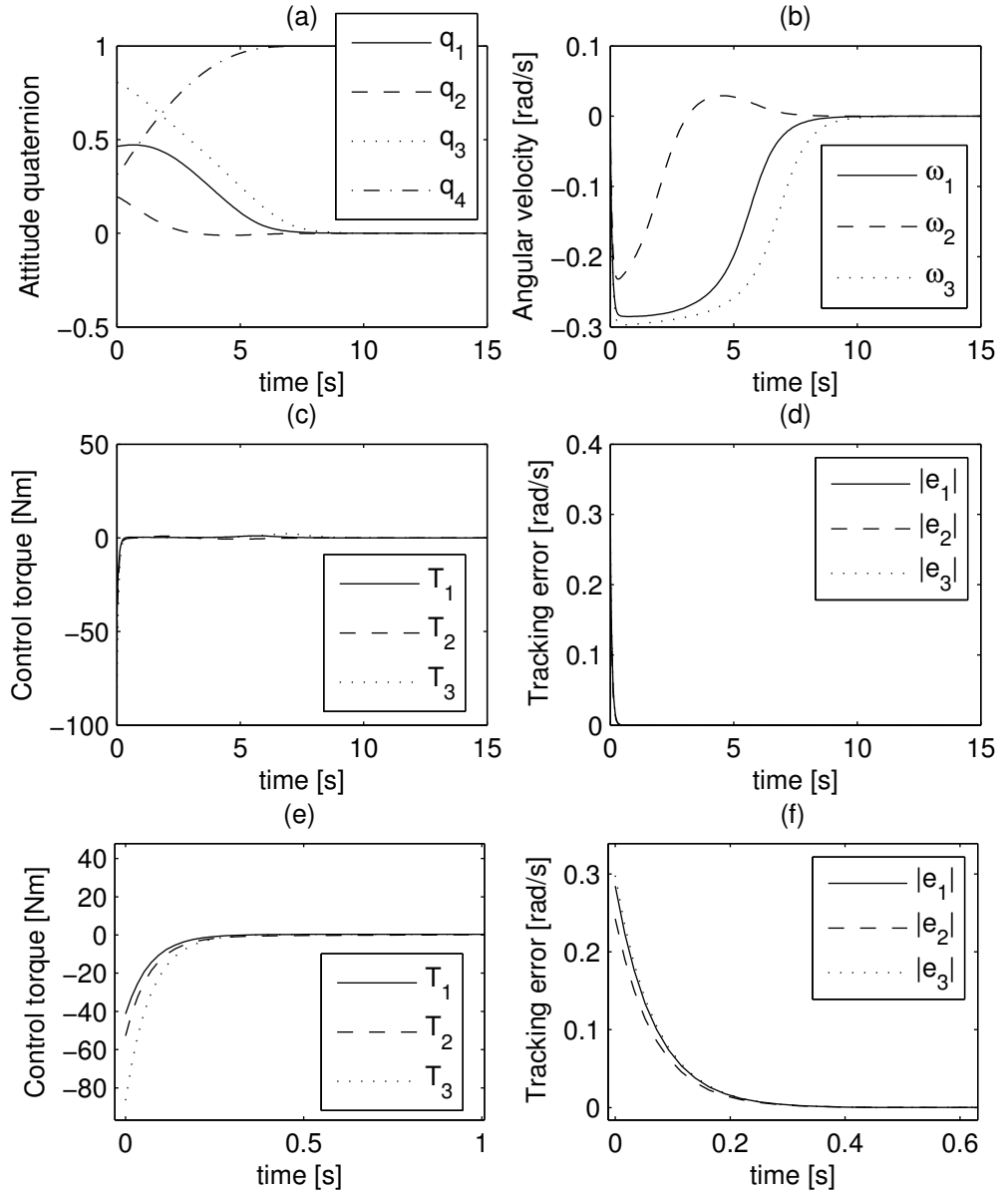


Fig. 2.4 Simulation results for the stabilization case example with the control gains tuned to ensure robustness against bounded external disturbance and uncertain moments of inertia

The analytical upper bound is approximately 1.6 times the actual maximum torque. Here, $|e_1(t)|$, $|e_2(t)|$ and $|e_3(t)|$ are guaranteed to decrease to values bounded by 0.0499, 0.0434 and 0.0390, respectively, as mentioned in Table 2.4 and the stability ensuring condition given by Eq. (2.37), while considering the upper bound of the right hand side which is given by its value at time t_0 , becomes

$$\begin{aligned}
 |e_1(t)| &> 0.0499 - 0.00041168 \cong 0.0495 \\
 |e_2(t)| &> 0.0434 - 0.00041168 \cong 0.0430 \\
 |e_3(t)| &> 0.0390 - 0.00041168 \cong 0.0386
 \end{aligned} \tag{2.50}$$

where $(1-\lambda)/(2g) \cong 0.00041168$. The above stability related conditions allow for some angular velocity and attitude convergence errors. The condition $0.05 < |e_i(t)| \leq |\omega_i| + |\alpha \tan^{-1}(\beta q_i)|$ implies that if the attitude error $|q_i|$ is zero then the angular velocity error $|\omega_i|$ can be up to 0.05 rad.s^{-1} otherwise the maximum possible attitude error $|q_i|$ comes out to be 0.0188 . So, the overall attitude error is bounded by $2 \sin^{-1}[(q_1^2 + q_2^2 + q_3^2)^{1/2}] = 2 \sin^{-1}(0.0188\sqrt{3}) \cong 3.73 \text{ deg}$ and the overall angular velocity error $(\omega_1^2 + \omega_2^2 + \omega_3^2)^{1/2}$ is bounded by 0.087 rad.s^{-1} . Using bounds for $|e_i(t)|$ with $i = 1, 2, 3$ given by Eq. (2.50), the overall attitude and angular velocity errors become 3.27 deg and 0.076 rad.s^{-1} , respectively.

After tuning the gains s , α , β , g and η for minimizing the analytical bound for control torque norm $\|\mathbf{T}_{\text{analytical}}\|$ while ensuring robustness against 20 percent variations in the moments of inertia and external disturbance torque with the absolute values of the components bounded above by 0.1732 Nm , the manoeuvre is actually subject to non-nominal moments of inertia in conjunction with the external disturbance torque. Here, Fig. 2.5 reports the simulation results for the case of constant external disturbance torque (mentioned in Table 2.5) whereas Fig. 2.6 provides the same while considering the disturbance as time varying (stated in Table 2.6). The non-nominal moments of inertia considered for both the cases are mentioned in Table 2.5. The peak control torque and the settling time performance parameters for both the cases are almost the same as for the nominal case given in Table 2.4.

Table 2.5 Stabilization Example Non-nominal Case with Constant External Disturbance Torque

Parameter	Value	Units
J_1^a	8	kg.m ²
J_2^a	16.5	kg.m ²
J_3^a	24	kg.m ²
$\max(\ T\)$	109.41	N.m
t_{settling}	8.978	s
T_d	$[0.1728 \ 0.2592 \ -0.3456]^T$	N.m
steady state value	0.000759	

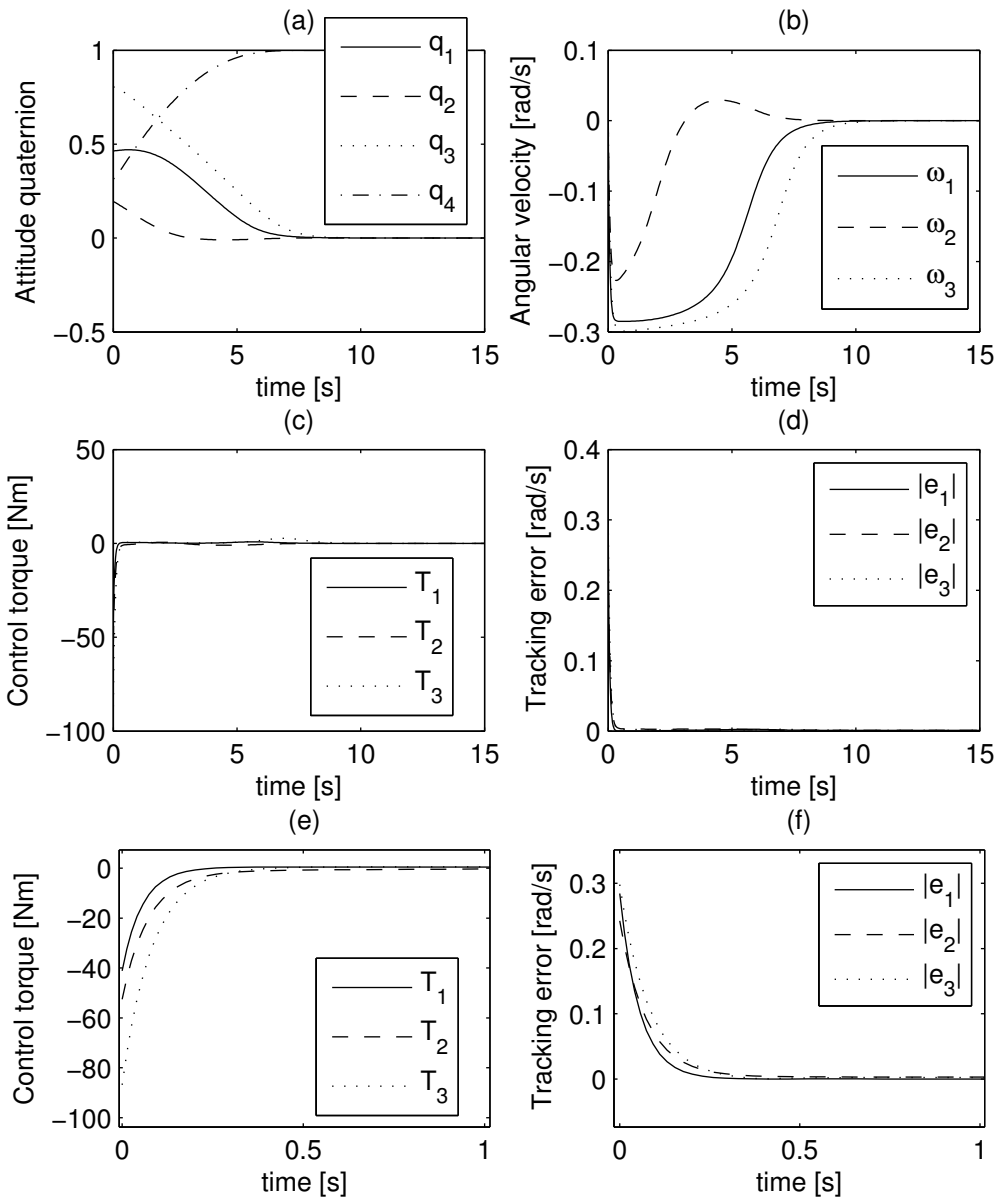


Fig. 2.5 Simulation results for the stabilization case example under the action of constant bounded external disturbance and non-nominal moments of inertia

Table 2.6 Stabilization Example Non-nominal Case with Time Varying External Disturbance Torque

Parameter	Value	Units
$\max(\ \mathbf{T}\)$	109.41	N.m
t_{settling}	9.087	s
\mathbf{T}_d	$\begin{bmatrix} 0.1728 \sin(\pi t) \\ 0.2592 \sin\left(\frac{3\pi}{2}t + \frac{\pi}{2}\right) \\ 0.3456 \sin\left(2\pi t + \frac{3\pi}{2}\right) \end{bmatrix}$	N.m
steady state value	fluctuating between 0.0007 and 0.0017	

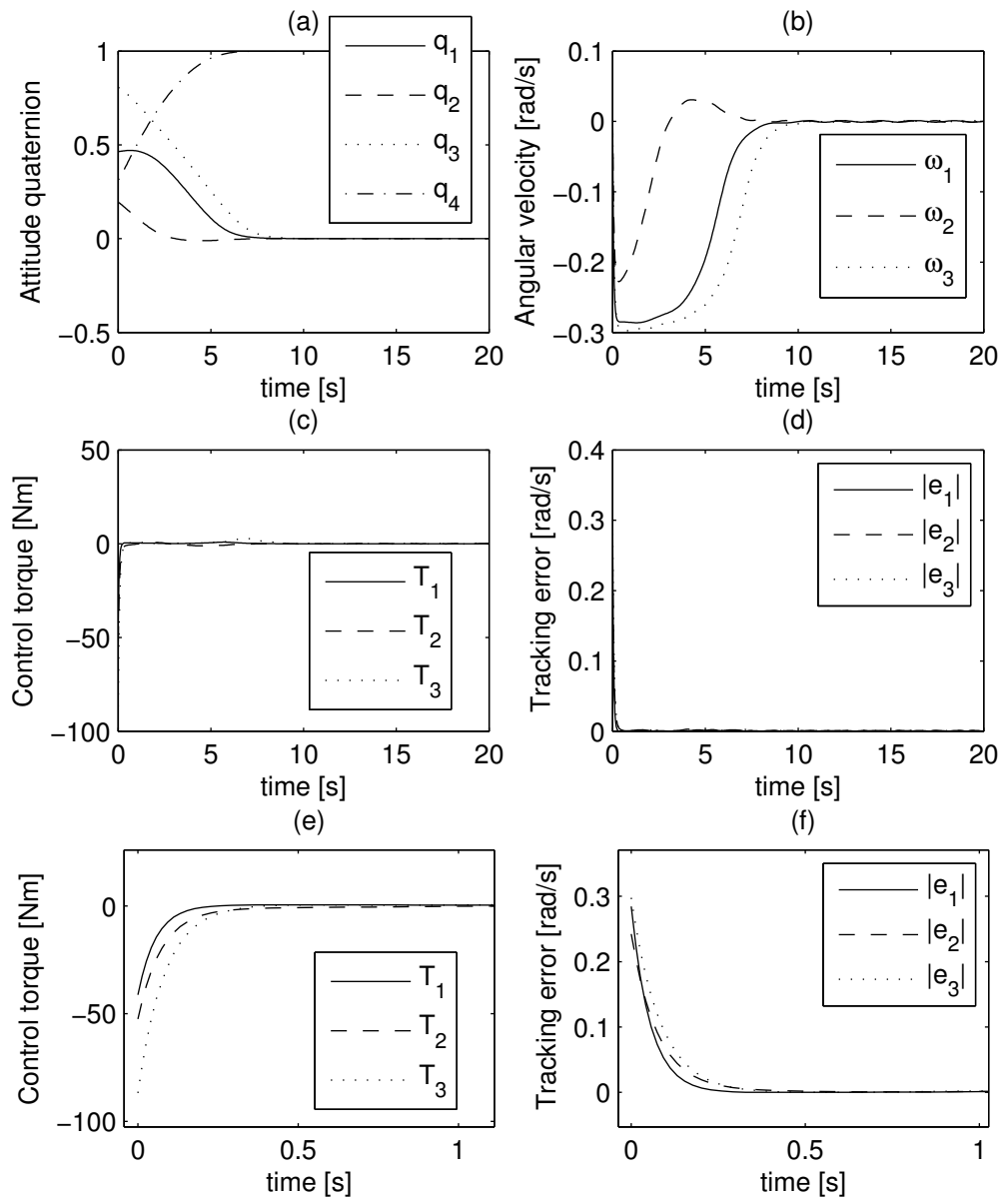


Fig. 2.6 Simulation results for the stabilization case example under the action of time varying bounded external disturbance and non-nominal moments of inertia

2.5.2 Tracking Case

In this subsection, we carry out the numerical simulation of the tracking attitude manoeuvre in order to demonstrate the proposed control law. The diagonal inertia matrix of the spacecraft has the same values as used for the stabilization example. The open-loop reference manoeuvre is a smoothed near-minimum-time manoeuvre starting at rest but having a certain angular velocity at the end of the manoeuvre as desirable for landmark tracking (Schaub, Robinett and Junkins, 1996; Robinett et al., 1997a, 1997b). It takes the spacecraft from the 3-1-3 Euler angles $(-20, 15$ and 4 deg) or the unit attitude quaternion $\mathbf{q}_r(t_0) = [0.1277 \quad -0.0271 \quad -0.1380 \quad 0.9818]^T$ to the angles $(40, 35$ and 40 deg) or $\mathbf{q}_r(t_f) = [0.3007 \quad 0 \quad 0.6130 \quad 0.7306]^T$ with a final body angular velocity $\boldsymbol{\omega}_r(t_f) = [0 \quad 1 \quad 0]^T$ deg/s (see Fig. 2.7). More complete details regarding the reference manoeuvre are available in (Schaub, Robinett and Junkins, 1996). For the chosen manoeuvre, the upper bounds for the absolute values of the reference angular velocity and angular acceleration components are $\xi = 1.7316$ deg/s and $\gamma = 0.0469$ deg/s², respectively, and the final manoeuvre time is $t_f = 112$ seconds. The initial attitude error in 3-1-3 Euler angles is taken as $(10, -20, 10$ deg) resulting in the spacecraft initial attitude quaternion $\mathbf{q}(t_0) = [-0.0427 \quad 0.0091 \quad 0.0349 \quad 0.9984]^T$ and the initial angular velocity error is chosen to be $(-2.5, 1.0$ and 2.5 deg/s) leading to the initial spacecraft angular velocity $\boldsymbol{\omega}(t_0) = [-2.5 \quad 1.0 \quad 2.5]^T$ deg/s.

The abovementioned tracking manoeuvre is simulated using the proposed backstepping control law given by Eq. (2.19) with the control gains s , α , β , g and η chosen by trial and error. With the choice of the control gains mentioned in Table 2.7, the analytical upper bound for the control torque norm $\|\mathbf{T}_{\text{analytical}}\|$, given by Eq. (2.26), is 7.1075 times bigger than the peak Euclidean norm of the actual control torque from the simulation $\max(\|\mathbf{T}\|)$. The simulation results are provided as Fig. 2.8. Here, the settling time t_{settling} is defined to

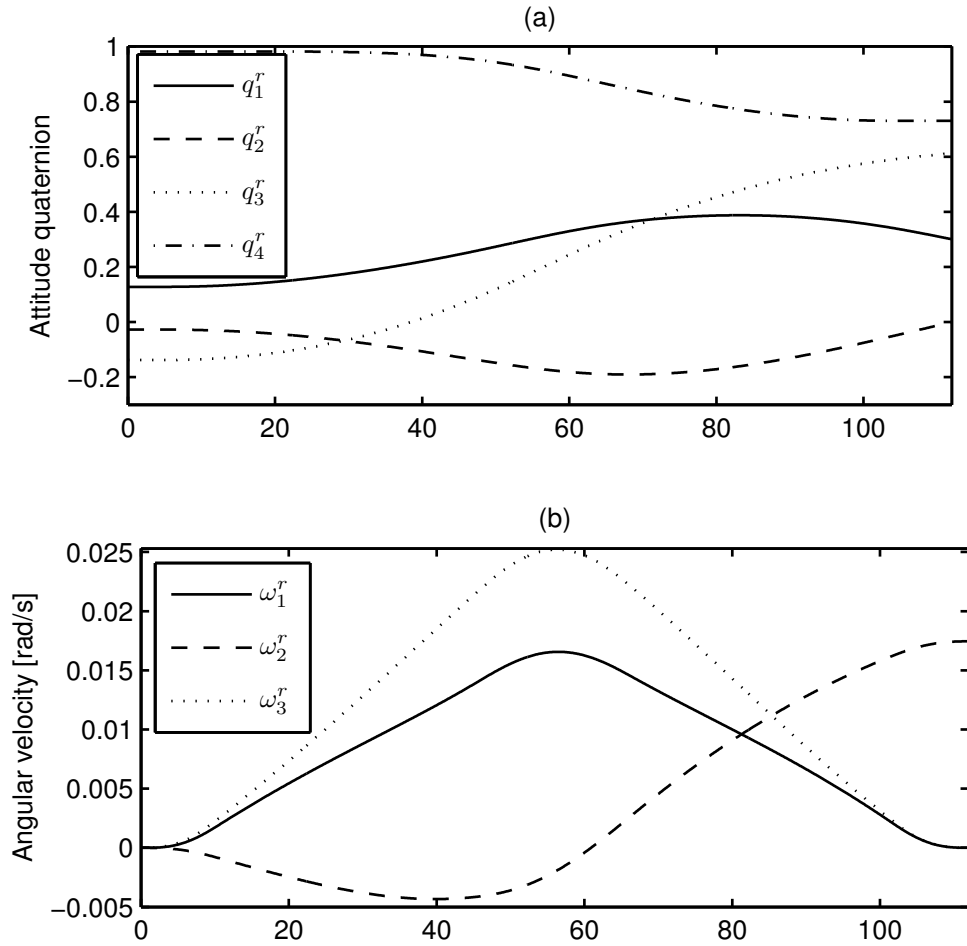


Fig. 2.7 Reference manoeuvre for the tracking case example

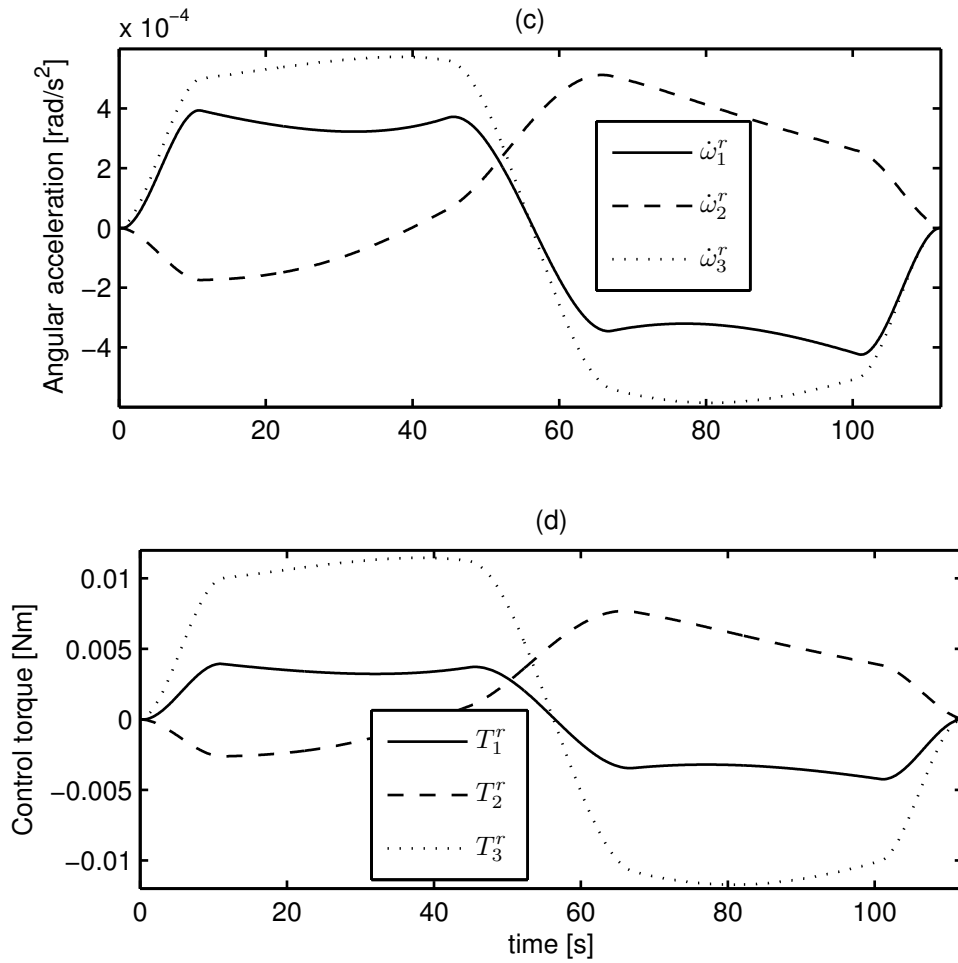


Fig. 2.7 Reference manoeuvre for the tracking case example

be the time at and after which the norm of the error states vector $[\boldsymbol{\sigma}_v^T, \delta\boldsymbol{\omega}^T]^T$ is bounded by 1% error from the steady state being zero.

As for the stabilization case example, the same optimization problem is solved subject to $t_{\text{settling}} \leq 13$ seconds and the closed-loop dynamics. The values of the control gains given in Table 2.7 are chosen as the starting guess. As a result of optimization, the values of the gains converged to the ones presented in Table 2.8.

Figure 2.9(a–d) shows the simulation results for these converged values of the gains employed in the controller given by Eq. (2.19). The conservativeness of the upper bound $\|\mathbf{T}_{\text{analytical}}\|$ is reduced from 7.1075 to 4.029 times bigger than the actual maximum Euclidean norm $\max(\|\mathbf{T}\|)$ while significantly improving the settling time from 24.7576 to 13 seconds. Again, the optimized bound guarantees that the actual control torque never exceeds the bound with the condition that $|e_i(t_0)|$ is less than or equal to the value for the current scenario.

Table 2.7 Tracking Example Nominal Case by Trial and Error

Parameter	Value	Units
s	0.001	
g	2	
α	0.75	
β	8	
η	1	
$\ T_{\text{analytical}}\ $	28.3	N.m
$\max(\ T\)$	3.982	N.m
t_{settling}	24.76	s

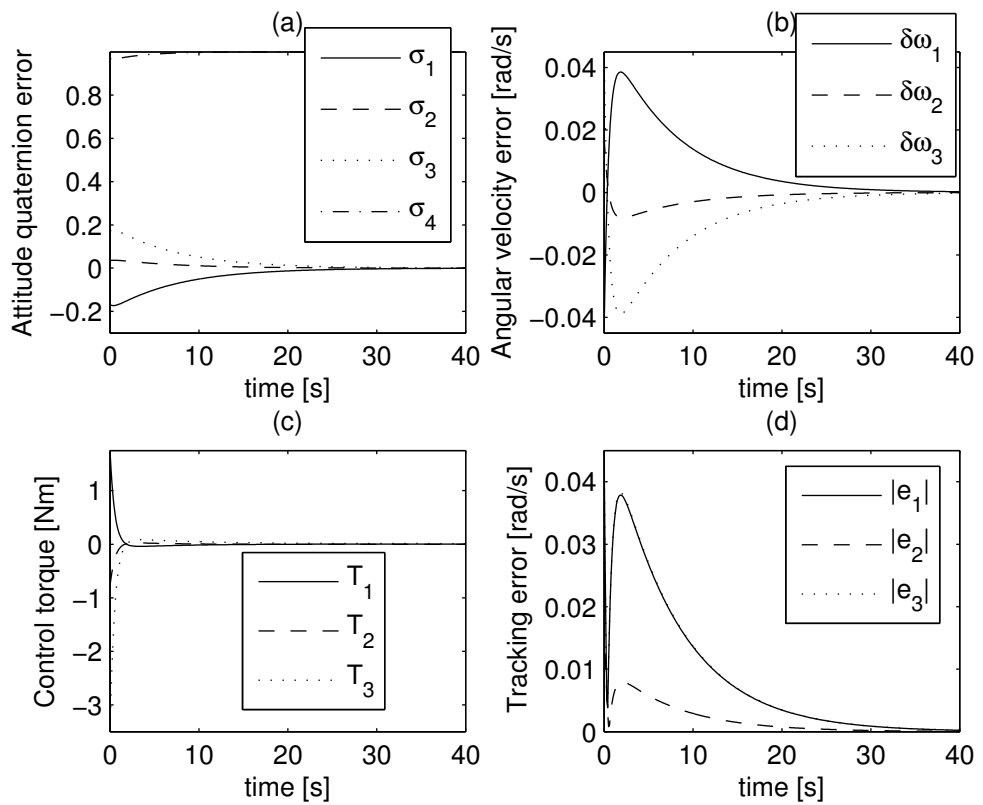


Fig. 2.8 Simulation results for the tracking case example with the control gains tuned by trial and error

Table 2.8 Tracking Example Nominal Case with Minimized Analytical Bound for Control Torque Norm

Parameter	Value	Units
s	0.1673	
g	12.1032	
α	0.2277	
β	20.9253	
η	4	
$\ T_{\text{analytical}}\ $	7.2799	N.m
$\max(\ T\)$	1.8069	N.m
t_{settling}	13	s

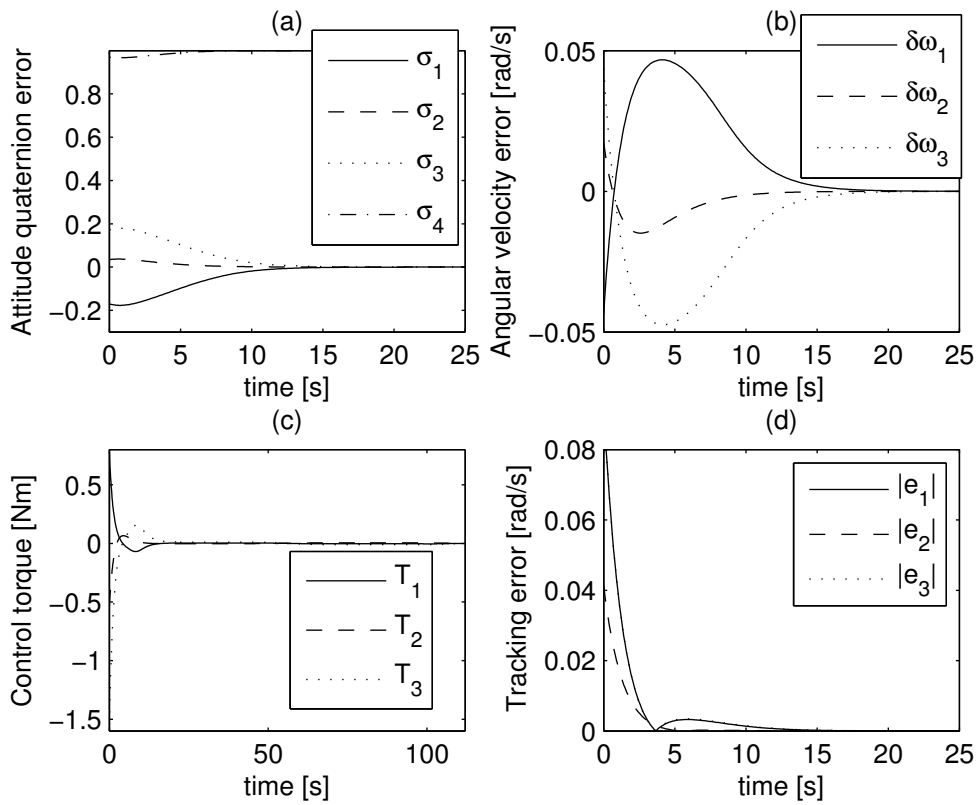


Fig. 2.9 Simulation results for the tracking case example with the control gains optimized for the minimum analytical bound of control torque norm

Now, we consider the ongoing tracking case numerical example in conjunction with 20 percent uncertainty in the moments of inertia with respect to their nominal values. Such perturbation in the moments of inertia is quantified as $\lambda = 0.2$. As for the case of attitude stabilization example in the previous subsection, we consider the presence of external disturbance torque with upper bounds for its components as $D_i = 0.1732$ Nm for $i = 1, 2, 3$. As before, we solve the aforementioned optimization problem subject to $t_{\text{settling}} \leq 19.027$ seconds, $(1/2 + \Theta_i(e(t_0))) / g \leq 0.01$ for $i = 1, 2, 3$ and the closed-loop dynamics. The values of the gains mentioned in Table 2.7 are used as the starting guess. The optimized values of the gains s , α , β , g and η are given in Table 2.9 which also presents the resulting $\|T_{\text{analytical}}\|$ and $\max(\|T\|)$ being about 16 Nm and 13.8 Nm, respectively. The analytical upper bound is approximately 1.6 times the actual maximum torque. Here, $|e_1(t)|$, $|e_2(t)|$ and $|e_3(t)|$ are guaranteed to decrease to values bounded by 0.01, 0.0089 and 0.0073, respectively, as mentioned in Table 2.9 and the stability ensuring condition given by Eq. (2.37), while considering the upper bound of the right hand side which is given by its value at time t_0 , becomes

$$\begin{aligned} |e_1(t)| &> 0.01 - 0.00047942 \cong 0.0095 \\ |e_2(t)| &> 0.0089 - 0.00047942 \cong 0.0084 \\ |e_3(t)| &> 0.0073 - 0.00047942 \cong 0.0068 \end{aligned} \quad (2.51)$$

where $(1 - \lambda) / (2g) \cong 0.00047942$. The above stability related conditions allow for some angular velocity and attitude tracking errors. The condition $0.01 < |e_i(t)| \leq |\delta\omega_i| + |\alpha \tan^{-1}(\beta\sigma_i)|$ implies that if the attitude error $|\sigma_i|$ is zero then the angular velocity error $|\delta\omega_i|$ can be up to 0.01 rad.s⁻¹ and otherwise the maximum possible attitude error $|\sigma_i|$ comes out to be 0.0195. So, the overall attitude error is bounded by $2 \sin^{-1}[(\sigma_1^2 + \sigma_2^2 + \sigma_3^2)^{1/2}] = 2 \sin^{-1}(0.0195\sqrt{3}) \cong 3.87$ deg and the overall angular velocity error $(\delta\omega_1^2 + \delta\omega_2^2 + \delta\omega_3^2)^{1/2}$ is bounded by 0.0173 rad.s⁻¹. Using bounds for $|e_i(t)|$

with $i = 1, 2, 3$ given by Eq. (2.51), the overall attitude and angular velocity errors become 3.13 deg and $0.0144 \text{ rad.s}^{-1}$, respectively.

Fig. 2.10 provides the results of nominal attitude tracking manoeuvre employing the gains s , α , β , g and η tuned for minimizing the analytical bound for control torque norm $\|\mathbf{T}_{\text{analytical}}\|$ while ensuring robustness against 20 percent variations in the moments of inertia and external disturbance torque with the absolute values of the components bounded above by 0.1732 Nm. Then, the tracking manoeuvre is undergone under the action of same non-nominal moments of inertia and the external disturbance torques as for the case of attitude stabilization numerical example. The simulation results for the case of constant external disturbance torque are given as Fig. 2.11 and the manoeuvre details while considering the disturbance as time varying are presented as Fig. 2.12. The peak control torque and the settling time performance parameters for both the kinds of external disturbance are almost the same as for the nominal case given by Table 2.9.

Table 2.9 Tracking Example Nominal Case with Minimized Analytical Bound for Control Torque Norm while Robustness Ensured

Parameter	Value	Units
s	0.0279	
g	834.3461	
α	0.6923	
β	29.2698	
η	10	
$\ \mathbf{T}_{\text{analytical}}\ $	16.061	N.m
$\max(\ \mathbf{T}\)$	13.7568	N.m
t_{settling}	19.0267	s
λ	0.2	
D_i	0.0216	
$(1/2 + \Theta_1(\mathbf{e}(t_0)))/g$	0.01	
$(1/2 + \Theta_2(\mathbf{e}(t_0)))/g$	0.0089	
$(1/2 + \Theta_3(\mathbf{e}(t_0)))/g$	0.0073	

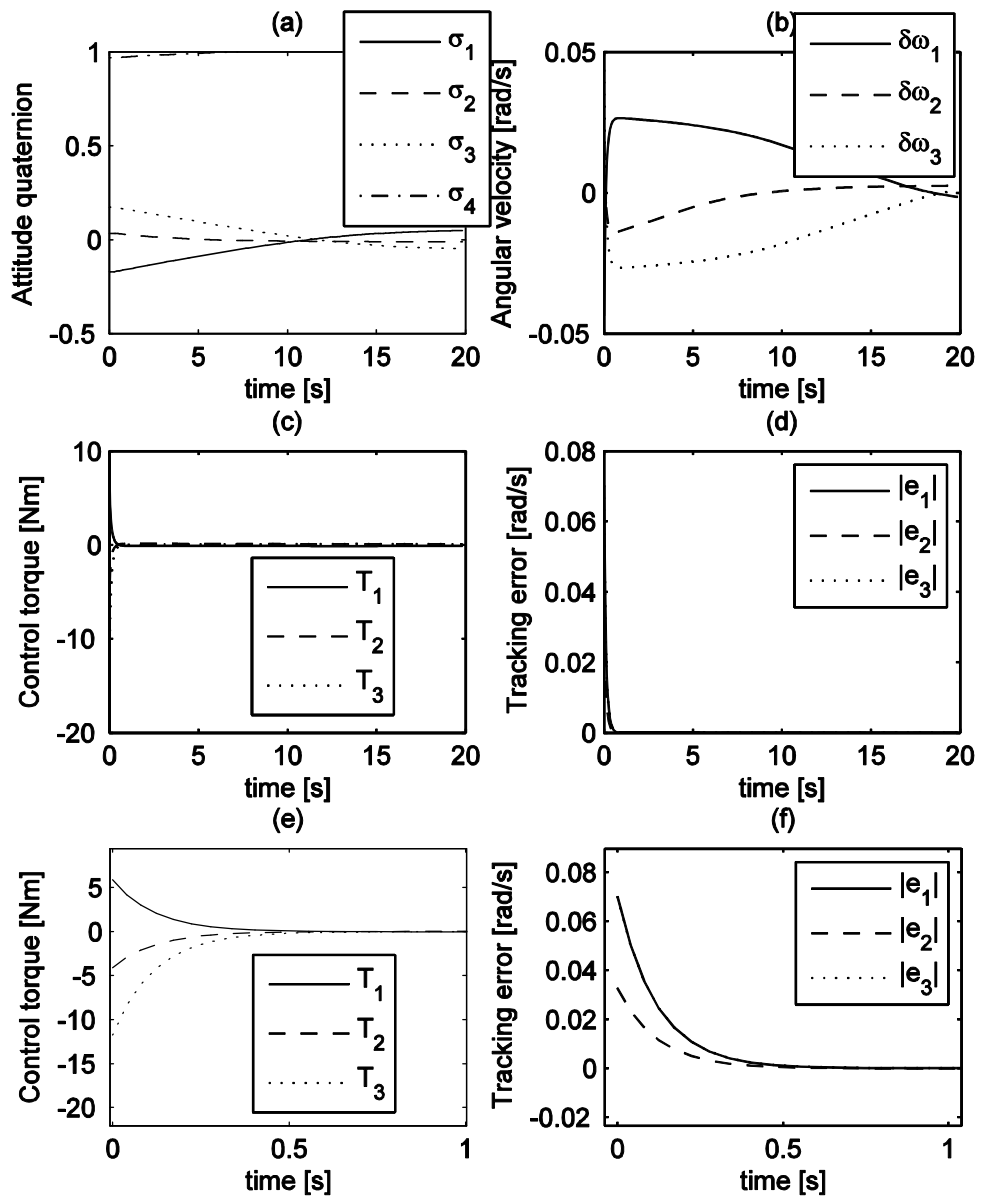


Fig. 2.10 Simulation results for the tracking case example with the control gains tuned to ensure robustness against bounded external disturbance and uncertain moments of inertia

Table 2.10 Tracking Example Non-nominal Case with Constant External Disturbance Torque

Parameter	Value	Units
$\max(\ T\)$	13.7568	N.m
t_{settling}	17.19	s
steady state value	0.006	

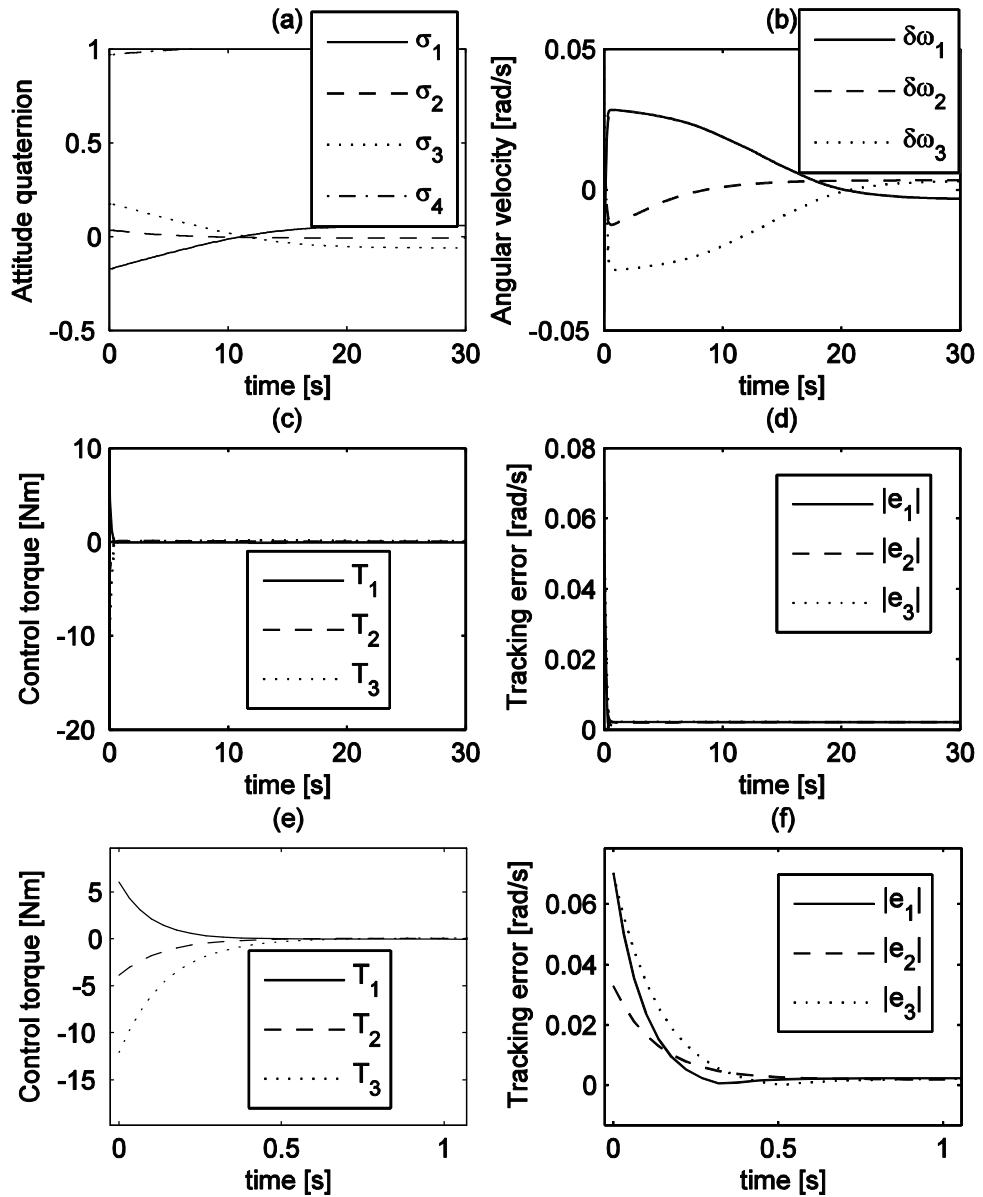


Fig. 2.11 Simulation results for the tracking case example under the action of constant bounded external disturbance and non-nominal moments of inertia

Table 2.11 Tracking Example Non-nominal Case with Time Varying External Disturbance Torque

Parameter	Value	Units
$\max(\ T\)$	13.7568	N.m
t_{settling}	19.145	s
steady state value	fluctuating between 0.002 and 0.003	

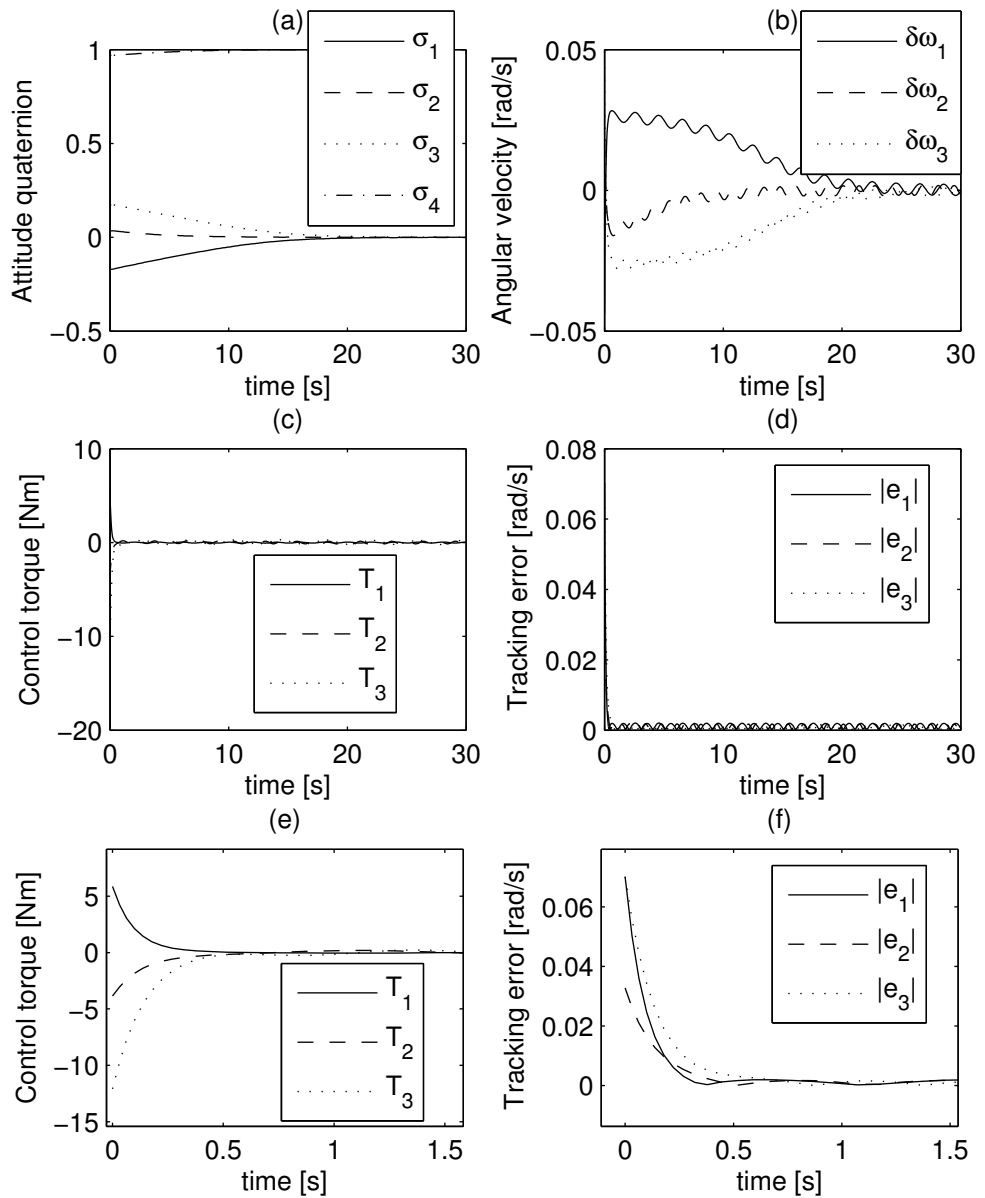


Fig. 2.12 Simulation results for the tracking case example under the action of time varying bounded external disturbance and non-nominal moments of inertia

Chapter 3

Spacecraft Constrained Slew Manoeuvres with Bounded Control Torque

In previous chapter, we have studied an inverse tangent-based nonlinear tracking function for the spacecraft attitude stabilization and tracking control problems. In this chapter we explore another nonlinear tracking function which accommodates the avoidance of pointing constraints for the spacecraft while undergoing large angle slew manoeuvres. First section briefly describes the pointing constraints in the context of spacecraft large angle slew manoeuvres. Then, the attitude stabilization specialization of the methodology of Chapter 2 is blended with the artificial potential function method for the incorporation of capability of avoiding the pointing constraints while undergoing the said manoeuvres. Gaussian function based repulsive potential is used for the construction of an artificial potential function. Next, the proposed methodology is explored for robustness against bounded external disturbance torque and prescribed uncertainties in the spacecraft moments of inertia. Here, the stability and control torque bound-related conditions for the non-nominal case are developed for the constrained attitude slews. Finally, the

effectiveness of the proposed methodology is established by the numerical simulations. Some of the results reported in this chapter have been published in (Ali and Radice, 2008).

3.1 Pointing Constraint Avoidance

The attitude stabilization specialization of the methodology of the previous chapter will be extended here to include potential shaping for avoiding undesired attitudes. The proposed solution can be used for spacecraft large angle slew manoeuvres without directing the spacecraft payload along the undesired directions. The undesired directions, also called pointing constraints, can be represented by the unit quaternions which describe the inadmissible attitudes relative to the inertial frame \mathbf{N} (McInnes, 1994). The Lyapunov function of the previous chapter employed for the kinematics subsystem stabilization is modified by artificially superimposing on it regions of high potential around the undesired orientations. The resulting function is called artificial potential function. If the inadmissible attitude to be avoided by the body frame \mathbf{B} is represented relative to the inertial frame \mathbf{N} by the quaternion $\tilde{\mathbf{q}}_c = [\tilde{\mathbf{q}}_{cv}^T, \tilde{q}_{c4}]^T$ where $\tilde{\mathbf{q}}_{cv} = [\tilde{q}_{c1}, \tilde{q}_{c2}, \tilde{q}_{c3}]^T$ then, for the principal-axis frame \mathbf{P} , it can be transformed to one that is represented with respect to the inertial frame $\tilde{\mathbf{N}}$ (as defined in Section 2.4 of Chapter 2) by the quaternion $\mathbf{q}_c = [\mathbf{q}_{cv}^T, q_{c4}]^T$ with $\mathbf{q}_{cv} = [q_{c1}, q_{c2}, q_{c3}]^T$ where $\mathbf{q}_{cv} = \mathbf{S}\tilde{\mathbf{q}}_{cv}$ and $q_{c4} = \tilde{q}_{c4}$. The orientation of the principal-axis frame \mathbf{P} with respect to the transformed inadmissible attitude is given by the quaternion $\mathbf{b} = [\mathbf{b}_v^T, b_4]^T$, $\mathbf{b}_v = [b_1, b_2, b_3]^T$ as

$$\mathbf{b}_v = q_{c4}\mathbf{q}_v - q_4\mathbf{q}_{cv} - \mathbf{q}_{cv} \times \mathbf{q}_v \quad (3.1)$$

$$b_4 = \mathbf{q}_{cv}^T \mathbf{q}_v + q_{c4}q_4 \quad (3.2)$$

The separation of the spacecraft payload axis from the inadmissible direction is denoted by the angle $\Delta\theta$ that is written as

$$\Delta\theta = 2 \sin^{-1} \left[(\mathbf{b}_v^T \mathbf{b})^{1/2} \right] \quad (3.3)$$

Moreover, the constraint on the admissible attitudes is assumed to be fixed with respect to the inertial space and the time rate of change of $\mathbf{b} = [\mathbf{b}_v^T, b_4]^T$ can be written as

$$\dot{\mathbf{b}}_v = \frac{1}{2}(b_4\boldsymbol{\omega} - \boldsymbol{\omega} \times \mathbf{b}_v) \quad (3.4)$$

$$\dot{b}_4 = -\frac{1}{2}\boldsymbol{\omega}^T \mathbf{b}_v \quad (3.5)$$

3.2 Control Design and Torque Bound

The artificial potential function for the kinematics subsystem stabilization is chosen to be the sum of attractive and repulsive potentials V and V_r , respectively, as

$$W = V + V_r \quad (3.6)$$

where the attractive part is given as

$$V = \frac{1}{2}[q_1^2 + q_2^2 + q_3^2 + (1 - q_4)^2] \quad (3.7)$$

and the repulsive part V_r , which the avoidance of the undesired attitude $\mathbf{q}_c = [q_{c4}^T, q_{c4}]^T$ is attributed to, is chosen here to be a Gaussian function as follows

$$V_r = A \exp\left(-\frac{1}{2}B[b_1^2 + b_2^2 + b_3^2 + (1 - b_4)^2]\right) \quad (3.8)$$

where the components of the unit quaternion \mathbf{b} are given by Eqs. (3.1) and (3.2) and A and B are the positive constants shaping the repulsive potential topology. The choice of the Gaussian functions for artificially raising the potential for the regions around the undesired attitudes has the advantages of being free of singularities, resulting in bounded controls and decaying rapidly away from the inadmissible attitudes (McInnes, 1994). However, the Gaussian functions displace the minimum of the attractive potential by a small amount and such superpositions of the attractive and repulsive potentials may lead to the introduction of local minima which may cause the spacecraft to converge towards the attitudes other than the desired one (McInnes, 1994). For simpler superpositions as considered here,

however, the local minima happen to be unstable saddle points (McInnes, 1994). The artificial potential function W is continuously differentiable and zero at the equilibrium point $\mathbf{q}_v = \mathbf{0}$ and $q_4 = 1$. The time derivative of the potential function W given by Eq. (3.6) comes out to be

$$\dot{W} = \frac{1}{2} \sum_{i=1}^3 (q_i - BV_r b_i) \omega_i \quad (3.9)$$

For stabilizing the kinematics subsystem, the pseudo control input, ω_i^s , is based on a nonlinear tracking function $\tilde{\boldsymbol{\phi}}(\mathbf{q}) = [\tilde{\phi}_1(\mathbf{q}), \tilde{\phi}_2(\mathbf{q}), \tilde{\phi}_3(\mathbf{q})]^T$ as follows

$$\omega_i^s = -s \tilde{\phi}_i(\mathbf{q}) \quad (3.10)$$

where s is a positive constant and the nonlinear tracking function $\tilde{\phi}_i(\mathbf{q})$ is given by

$$\tilde{\phi}_i(\mathbf{q}) = q_i - BV_r b_i \quad (3.11)$$

With the mentioned choice for the pseudo control, the time derivative of the artificial potential function \dot{W} given by Eq. (3.9) becomes

$$\dot{W} = -\frac{1}{2} s \sum_{i=1}^3 (q_i - BV_r b_i)^2 \quad (3.12)$$

which is negative semi-definite with respect to the chosen equilibrium point. Next, the function W is augmented with the dynamics part of the system as follows (Mazenc and Iggidr, 2004)

$$U = W + \frac{1}{2} \sum_{i=1}^3 [\Omega(\omega_i) - \Omega(\omega_i^s)]^2 \quad (3.13)$$

where $\Omega(\cdot)$ is a class κ_∞ function that is defined to be zero at zero, strictly increasing and becomes unbounded as its argument does so (Mazenc and Iggidr, 2004). The derivative of the overall potential function U with respect to time comes out to be

$$\begin{aligned}
 \dot{U} &= \frac{1}{2} \sum_{i=1}^3 (q_i - BV_r b_i) \omega_i + \sum_{i=1}^3 \left[\Omega(\omega_i) - \Omega(\omega_i^s) \right] \left[\Omega'(\omega_i) \dot{\omega}_i - \Omega'(\omega_i^s) \dot{\omega}_i^s \right] \\
 &= \frac{1}{2} \sum_{i=1}^3 (q_i - BV_r b_i) \omega_i^s + \sum_{i=1}^3 \frac{1}{2} (q_i - BV_r b_i) (\omega_i - \omega_i^s) + \sum_{i=1}^3 \left[\Omega'(\omega_i) (p_i \omega_j \omega_k + u_i) - \right. \\
 &\quad \left. \Omega'(\omega_i^s) \dot{\omega}_i^s \right] \left[\Omega(\omega_i) - \Omega(\omega_i^s) \right] \quad (3.14) \\
 &= -\frac{1}{2} s \sum_{i=1}^3 (q_i - BV_r b_i)^2 + \sum_{i=1}^3 \left\{ \frac{1}{2} (q_i - BV_r b_i) + \left[\Omega'(\omega_i) (p_i \omega_j \omega_k + u_i) - \right. \right. \\
 &\quad \left. \left. \Omega'(\omega_i^s) \dot{\omega}_i^s \right] \frac{\Omega(\omega_i) - \Omega(\omega_i^s)}{\omega_i - \omega_i^s} \right\} (\omega_i - \omega_i^s)
 \end{aligned}$$

where $\Omega(x)$ is selected so that $[\Omega(\omega_i) - \Omega(\omega_i^s)] / (\omega_i - \omega_i^s) \neq 0$ and $\Omega'(x)$ denotes the derivative of $\Omega(x)$ with respect to x . In order to make the time derivative of U equal to the following

$$\dot{U} = -\frac{1}{2} s \sum_{i=1}^3 (q_i - BV_r b_i)^2 - g \sum_{i=1}^3 (\omega_i - \omega_i^s)^2 \quad (3.15)$$

the backstepping controller comes out to be

$$u_i = \frac{1}{\Omega'(\omega_i)} \left\{ -\frac{\omega_i - \omega_i^s}{\Omega(\omega_i) - \Omega(\omega_i^s)} \left[\frac{1}{2} (q_i - BV_r b_i) + g (\omega_i - \omega_i^s) \right] + \Omega'(\omega_i^s) \dot{\omega}_i^s \right\} - p_i \omega_j \omega_k \quad (3.16)$$

for $(i, j, k) \in \text{Id}$, where g is a positive constant. Now, for the closed loop system, the attitude stabilization control objective $\lim_{t \rightarrow \infty} [\mathbf{q}_v(t), \boldsymbol{\omega}(t)] = \mathbf{0}$ is obtained ‘almost’ globally asymptotically as mentioned in Chapter 2 provided that $q_i(t) \neq BV_r(t) b_i(t) \quad \forall t \in [t_0, \infty)$ as Eq. (3.15) is negative semi-definite. Note that by equating Eqs. (3.14) and (3.15) we can find the time derivative of $U - W$ as given below which is subject to the condition that the control input is given by Eq. (3.16):

$$\frac{d}{dt} \left(\frac{1}{2} \left[\Omega(\omega_i) - \Omega(\omega_i^s) \right]^2 \right) = -g (\omega_i - \omega_i^s)^2 - \frac{1}{2} (q_i - BV_r b_i) (\omega_i - \omega_i^s) \quad (3.17)$$

for $i = 1, 2, 3$.

Again, we choose a simple form of class κ_∞ function as $\Omega(\omega_i) = \eta\omega_i$ with $\eta > 0$, which satisfies the condition $[\Omega(\omega_i) - \Omega(\omega_i^s)] / (\omega_i - \omega_i^s) = \eta \neq 0$, for $i = 1, 2, 3$. Then, the control input is rewritten as follows:

$$u_i = -\frac{1}{\eta^2} \left[\frac{1}{2}(q_i - BV_r b_i) + g(\omega_i - \omega_i^s) \right] - \frac{1}{2} s \left(\left[q_4 - (b_4 - Bb_i^2)BV_r \right] \omega_i + \right. \\ \left. \left[-q_k - (-b_k - Bb_i b_j)BV_r \right] \omega_j + \left[q_j - (b_j - Bb_i b_k)BV_r \right] \omega_k \right) - p_i \omega_j \omega_k \quad (3.18)$$

for $(i, j, k) \in \text{Id}$. Defining $e = [e_1, e_2, e_3]^T$ where $e_i \equiv \omega_i - \omega_i^s$ for $i = 1, 2, 3$, the above equation can be written as

$$u_i = -\frac{1}{\eta^2} \left[\frac{1}{2}(q_i - BV_r b_i) + g e_i \right] - \frac{1}{2} s \left(\left[q_4 - (b_4 - Bb_i^2)BV_r \right] (e_i + \omega_i^s) + \right. \\ \left. \left[-q_k - (-b_k - Bb_i b_j)BV_r \right] (e_j + \omega_j^s) + \left[q_j - (b_j - Bb_i b_k)BV_r \right] (e_k + \omega_k^s) \right) - \\ p_i (e_j + \omega_j^s)(e_k + \omega_k^s) \quad (3.19)$$

As $|q_i| \leq 1$, $|b_i| \leq 1$, $V_r \leq \bar{V}_r$ and $|\omega_i^s| \leq s(1 + B\bar{V}_r)$ for $i = 1, 2, 3$, the control torque bound is derived using the triangle inequalities as follows:

$$|u_i| \leq \frac{1}{\eta^2} \left(\frac{1}{2}|q_i - BV_r b_i| + g|e_i| \right) + \frac{1}{2} s \left(\left| q_4 - (b_4 - Bb_i^2)BV_r \right| |e_i + \omega_i^s| + \right. \\ \left. \left| -q_k - (-b_k - Bb_i b_j)BV_r \right| |e_j + \omega_j^s| + \left| q_j - (b_j - Bb_i b_k)BV_r \right| |e_k + \omega_k^s| \right) + \\ \left| p_i (e_j + \omega_j^s)(e_k + \omega_k^s) \right| \\ \leq \frac{1}{\eta^2} \left[\frac{1}{2}(1 + B\bar{V}_r) + g|e_i| \right] + \frac{1}{2} s \left(\left[1 + (1 + B)B\bar{V}_r \right] [|e_i| + s(1 + B\bar{V}_r)] + \right. \\ \left. \left[1 + (1 + B)B\bar{V}_r \right] [|e_j| + s(1 + B\bar{V}_r)] + \left[1 + (1 + B)B\bar{V}_r \right] [|e_k| + s(1 + B\bar{V}_r)] \right) + \\ \left| p_i \right| |e_j e_k + e_j \omega_k^s + \omega_j^s e_k + \omega_j^s \omega_k^s| \\ \leq \frac{1}{\eta^2} \left[\frac{1}{2}(1 + B\bar{V}_r) + g|e_i| \right] + \frac{1}{2} s \left[1 + (1 + B)B\bar{V}_r \right] \left[|e_i| + |e_j| + |e_k| + 3s(1 + B\bar{V}_r) \right] + \\ \left| p_i \right| \left\{ |e_j| |e_k| + s(1 + B\bar{V}_r) \left[|e_j| + |e_k| + s(1 + B\bar{V}_r) \right] \right\} \quad (3.20)$$

for $(i, j, k) \in \text{Id}$. Here, \bar{V}_r is the lower bound of V_r corresponding to the minimum value of the separation angle $\Delta\theta$ acquired during a constrained slew manoeuvre. Rearranging the terms, the above inequality becomes

$$|u_i| \leq k_{1i} + k_2 |e_i| + k_{3i} (|e_j| + |e_k|) + |p_i| |e_j| |e_k| \quad (3.21)$$

for $(i, j, k) \in \text{Id}$, where the constants k_{1i} , k_2 and k_{3i} are

$$\begin{aligned} k_{1i} &= \frac{1}{2\eta^2} (1 + B\bar{V}_r) + \frac{3}{2}s^2 [1 + (1+B)B\bar{V}_r] (1 + B\bar{V}_r) + |p_i| [s(1 + B\bar{V}_r)]^2 \\ k_2 &= \frac{g}{\eta^2} + \frac{1}{2}s [1 + (1+B)B\bar{V}_r] \\ k_{3i} &= s \left(\frac{1}{2} [1 + (1+B)B\bar{V}_r] + |p_i| (1 + B\bar{V}_r) \right) \end{aligned} \quad (3.22)$$

However, the angular velocity error $e_i(t)$, for $i=1,2,3$, is unknown in Eq. (3.21). Hence, Eq. (3.21) does not provide any useful information about the control torque bound. To obtain the bound for the angular velocity error, recall Eq. (3.17) with $\Omega(\omega_i) = \eta\omega_i$ for $i=1,2,3$. Then,

$$\eta^2 \frac{d}{dt} \left(\frac{1}{2} e_i^2 \right) = -g e_i^2 - \frac{1}{2} (q_i - BV_r b_i) e_i \quad (3.23)$$

for $i=1,2,3$. Eq. (3.23) implies that if $|e_i| > |q_i - BV_r b_i| / (2g)$, then $|e_i|$ is guaranteed to be decreasing to a certain value that is bounded by $(1 + B\bar{V}_r) / (2g)$. Therefore, $|e_i|$ is bounded by the following inequality:

$$|e_i(t)| \leq \max \left[|e_i(t_0)|, (1 + B\bar{V}_r) / (2g) \right] \quad (3.24)$$

for all t in $[t_0, \infty)$ for $i=1,2,3$, where t_0 is the initial time and $\max(\cdot, \cdot)$ is the function whose value is the maximum of two arguments.

Finally, Eq. (3.21) is used to calculate the bounds of the controls u_i and the control torque is bounded by

$$|T_i| \leq J_i \left[k_{1i} + k_2 |e_i(t)| + k_{3i} (|e_j(t)| + |e_k(t)|) + |p_i| |e_j(t)| |e_k(t)| \right] \quad (3.25)$$

for $(i, j, k) \in \text{Id}$ where $|e_i(t)|$ for $i=1,2,3$ follows from the inequality (3.24). Also, the minimum value of the bound for $|T_i|$ which can be identified by Eq. (3.25) comes out to be

$$J_i \left[k_{1i} + \frac{1 + B\bar{V}_r}{2g} \left(k_2 + 2k_{3i} + \frac{1 + B\bar{V}_r}{2g} |p_i| \right) \right]$$

The control torque components bounds provided by Eq. (3.25) can be used to calculate the bound for Euclidean-norm $\|\mathbf{T}\|$. Moreover, the direction cosine matrix \mathbf{S} mentioned in the previous chapter can be used to calculate T_b from \mathbf{T} however this transformation does not affect the bound for the Euclidean-norm of control torque.

3.3 Robustness Analysis

As considered in Chapter 2 for the case of unconstrained spacecraft attitude manoeuvres, this section explores the spacecraft constrained slew manoeuvres control for robustness against the uncertainties in the spacecraft nominal moments of inertia and the existence of external disturbances (Kim and Kim, 2003; Wu, Cao and Li, 2009). In order to evaluate the control law given by Eq. (3.16) for said robustness, the non-nominal moments of inertia J_i^a and the external disturbance torque components T_i^d where $i=1,2,3$ are incorporated in the time derivative of the Lyapunov function U to get

$$\begin{aligned} \dot{U} &= \frac{1}{2} \sum_{i=1}^3 (q_i - BV_r b_i) \omega_i + \sum_{i=1}^3 \left[\Omega(\omega_i) - \Omega(\omega_i^s) \right] \left[\Omega'(\omega_i) \dot{\omega}_i - \Omega'(\omega_i^s) \dot{\omega}_i^s \right] \\ &= -\frac{1}{2} s \sum_{i=1}^3 (q_i - BV_r b_i)^2 + \sum_{i=1}^3 \left\{ \frac{1}{2} (q_i - BV_r b_i) + \left[\Omega'(\omega_i) (p_i^a \omega_j \omega_k + \frac{J_i}{J_i^a} u_i + \frac{T_i^d}{J_i^a}) - \right. \right. \\ &\quad \left. \left. \Omega'(\omega_i^s) \dot{\omega}_i^s \right] \frac{\Omega(\omega_i) - \Omega(\omega_i^s)}{\omega_i - \omega_i^s} \right\} (\omega_i - \omega_i^s) \end{aligned} \quad (3.26)$$

Substituting the control law u_i given by Eq. (3.16) in the above equation we get

$$\begin{aligned}
 \dot{U} = & -\frac{1}{2}s \sum_{i=1}^3 (q_i - BV_r b_i)^2 + \sum_{i=1}^3 \left\{ \left(\Omega'(\omega_i) \left[(p_i^a - p_i J_i / J_i^a) \omega_j \omega_k + T_i^d / J_i^a \right] + \right. \right. \\
 & \left. \left. (J_i / J_i^a - 1) \Omega'(\omega_i^s) \dot{\omega}_i^s \right) \frac{\Omega(\omega_i) - \Omega(\omega_i^s)}{\omega_i - \omega_i^s} + \right. \\
 & \left. (1 - J_i / J_i^a) \frac{1}{2} (q_i - BV_r b_i) - (J_i / J_i^a) g(\omega_i - \omega_i^s) \right\} (\omega_i - \omega_i^s)
 \end{aligned} \tag{3.27}$$

For $\Omega(x) = \eta x$, the above equation becomes

$$\begin{aligned}
 \dot{U} = & -\frac{1}{2}s \sum_{i=1}^3 (q_i - BV_r b_i)^2 + \sum_{i=1}^3 \left\{ \eta^2 \left[(p_i^a - p_i J_i / J_i^a) \omega_j \omega_k + T_i^d / J_i^a + \right. \right. \\
 & \left. \left. (J_i / J_i^a - 1) \dot{\omega}_i^s \right] + (1 - J_i / J_i^a) \frac{1}{2} (q_i - BV_r b_i) - \right. \\
 & \left. (J_i / J_i^a) g(\omega_i - \omega_i^s) \right\} (\omega_i - \omega_i^s)
 \end{aligned} \tag{3.28}$$

The condition for the above expression to be negative comes out to be

$$\begin{aligned}
 (J_i / J_i^a) g |\omega_i - \omega_i^s| > \left| (1 - J_i / J_i^a) \frac{1}{2} (q_i - BV_r b_i) + \eta^2 \left[(p_i^a - p_i J_i / J_i^a) \omega_j \omega_k + \right. \right. \\
 \left. \left. T_i^d / J_i^a + (J_i / J_i^a - 1) \dot{\omega}_i^s \right] \right|
 \end{aligned} \tag{3.29}$$

or

$$\begin{aligned}
 g |\omega_i - \omega_i^s| > \left| (J_i^a / J_i - 1) \frac{1}{2} (q_i - BV_r b_i) + \eta^2 \left[(p_i^a J_i^a / J_i - p_i) \omega_j \omega_k + \right. \right. \\
 \left. \left. T_i^d / J_i + (1 - J_i^a / J_i) \dot{\omega}_i^s \right] \right|
 \end{aligned} \tag{3.30}$$

for $i=1,2,3$. For the bound of the right hand side term of the above inequality we can write

$$\begin{aligned}
 & \left| \left(J_i^a / J_i - 1 \right) \frac{1}{2} (q_i - B V_r b_i) + \eta^2 \left[\left(p_i^a J_i^a / J_i - p_i \right) \omega_j \omega_k + T_i^d / J_i + \right. \right. \\
 & \quad \left. \left. \left(1 - J_i^a / J_i \right) \dot{\omega}_i^s \right] \right| \\
 & \leq \frac{1}{2} \lambda (1 + B \bar{V}_r) + \eta^2 \left[\lambda (J_j + J_k) / J_i \left| (e_j + \omega_j^s)(e_k + \omega_k^s) \right| + \left| T_i^d \right| / J_i + \right. \\
 & \quad \left. \lambda \left| \dot{\omega}_i^s \right| \right] \tag{3.31} \\
 & \leq \frac{1}{2} \lambda (1 + B \bar{V}_r) + \\
 & \quad \eta^2 \left[\lambda (J_j + J_k) / J_i \left\{ |e_j| |e_k| + s(1 + B \bar{V}_r) (|e_j| + |e_k| + s(1 + B \bar{V}_r)) \right\} + D_i / J_i + \right. \\
 & \quad \left. \frac{1}{2} \lambda s \{ 1 + (1 + B) B \bar{V}_r \} \left\{ |e_i| + |e_j| + |e_k| + 3s(1 + B \bar{V}_r) \right\} \right]
 \end{aligned}$$

where $|J_i^a / J_i - 1| \leq \lambda$, $|p_i^a J_i^a / J_i - p_i| \leq \lambda (J_j + J_k) / J_i$ and $|T_i^d| \leq D_i$ for $i=1,2,3$. So, a conservative version of the condition given by inequality (3.30) can be found as

$$g|e_i(t)| > \frac{1}{2} \lambda (1 + B \bar{V}_r) + \Theta_i(e(t)) \tag{3.32}$$

where

$$\begin{aligned}
 \Theta_i(e(t)) = & \eta^2 \left[D_i / J_i + \lambda (J_j + J_k) / J_i \left\{ |e_j(t)| |e_k(t)| + \right. \right. \\
 & \left. \left. s(1 + B \bar{V}_r) (|e_j(t)| + |e_k(t)| + s(1 + B \bar{V}_r)) \right\} + \right. \\
 & \left. \frac{1}{2} \lambda s \{ 1 + (1 + B) B \bar{V}_r \} \left\{ |e_i(t)| + |e_j(t)| + |e_k(t)| + 3s(1 + B \bar{V}_r) \right\} \right] \tag{3.33}
 \end{aligned}$$

for $(i, j, k) \in \text{Id}$. Further, in this case Eq. (3.23) takes the form

$$\begin{aligned}
 \eta^2 \frac{d}{dt} \left(\frac{1}{2} e_i^2 \right) = & \left\{ - \left(J_i / J_i^a \right) [g e_i + \frac{1}{2} (q_i - B V_r b_i)] + \eta^2 \left[\left(p_i^a - p_i J_i / J_i^a \right) \omega_j \omega_k + \right. \right. \\
 & \left. \left. T_i^d / J_i^a + \left(J_i / J_i^a - 1 \right) \dot{\omega}_i^s \right] \right\} e_i \tag{3.34}
 \end{aligned}$$

for $i=1,2,3$. The above equation implies that the condition

$$g|e_i(t)| > \frac{1}{2}(1 + B\bar{V}_r) + \Theta_i(\mathbf{e}(t_0)) \quad (3.35)$$

ensures $|e_i(t)|$ to decrease to a certain value that is bounded by $(1/2(1 + B\bar{V}_r) + \Theta_i(\mathbf{e}(t_0)))/g$ where $\Theta_i(\mathbf{e}(t_0))$ is calculated using Eq. (3.33). Therefore, $|e_i|$ is bounded by the following inequality:

$$|e_i(t)| \leq \max \left[|e_i(t_0)|, (1 + B\bar{V}_r + 2\Theta_i(\mathbf{e}(t_0)))/(2g) \right] \quad (3.36)$$

for $i=1,2,3$ with $t \in [t_0, \infty)$. Again, the bound for the control torque components is given by Eq. (3.25) but now $|e_i(t)|$ for $i=1,2,3$ follows from the inequality (3.36) rather than the inequality (3.24). Also, the minimum value of the bound for $|T_i|$ which can be identified by Eq. (3.25) comes out to be

$$J_i \left[k_{1i} + \frac{1 + B\bar{V}_r + 2\Theta_i(\mathbf{e}(t_0))}{2g} \left(k_2 + 2k_{3i} + \frac{1 + B\bar{V}_r + 2\Theta_i(\mathbf{e}(t_0))}{2g} |p_i| \right) \right] \quad (3.37)$$

3.4 Numerical Simulation

In this section, we carry out the numerical simulation of a constrained slew manoeuvre in order to demonstrate the proposed backstepping based developments of the previous two sections. The simulation scenario considered by Krstić and Tsiotras (1999) and Kim and Kim (2003) is again used for this purpose in conjunction with a forbidden or obstacle attitude given by the unit quaternion $\mathbf{q}_c = [0.2 \ 0.1 \ 0.3 \ 0.9274]^T$. The prescribed minimum separation of the spacecraft attitude from the inadmissible one is chosen to be $\Delta\theta = 10$ deg. The initial conditions and the nominal values of moments of inertia for the scenario are the same as given in Table 2.1. For the sake of comparison, the values of the gains s , g and η are also adopted from Table 2.1. Without the avoidance of obstacle attitude incorporated with the help of repulsive potential, the minimum separation angle $\min(\Delta\theta)$ comes out to be about 4 deg violating the prescribed minimum value.

Incorporating the obstacle avoidance capability, the gains A and B are tuned by trial and error as mentioned in Table 3.1 so that the prescribed obstacle separation specification is achieved. The simulation results for the chosen values of the gains are provided as Fig. 3.1. For these values of the gains, the analytical bound for the control torque norm comes out to be unreasonably high. This is caused by a high value of the gain B as square and cube of this gain are involved in the calculation of analytical bound for control torque norm, an issue being typical of the Gaussian function based repulsive potential for the spacecraft slew manoeuvre problem with unit quaternion used as attitude parameterization. The short settling time is another reason for the high control torque bound as the gains become large to achieve that specification.

Table 3.1 Constrained Slew Manoeuvre Nominal Case by Trial and Error

Parameter	Value	Units
s	1	
g	10	
η	3.5196	
A	0.033	
B	150	
$\min(\Delta\theta)$	10	deg
$\ \mathbf{T}_{\text{analytical}}\ $	1.66e7	N.m
$\max(\ \mathbf{T}\)$	14.41	N.m
t_{settling}	11.67	s

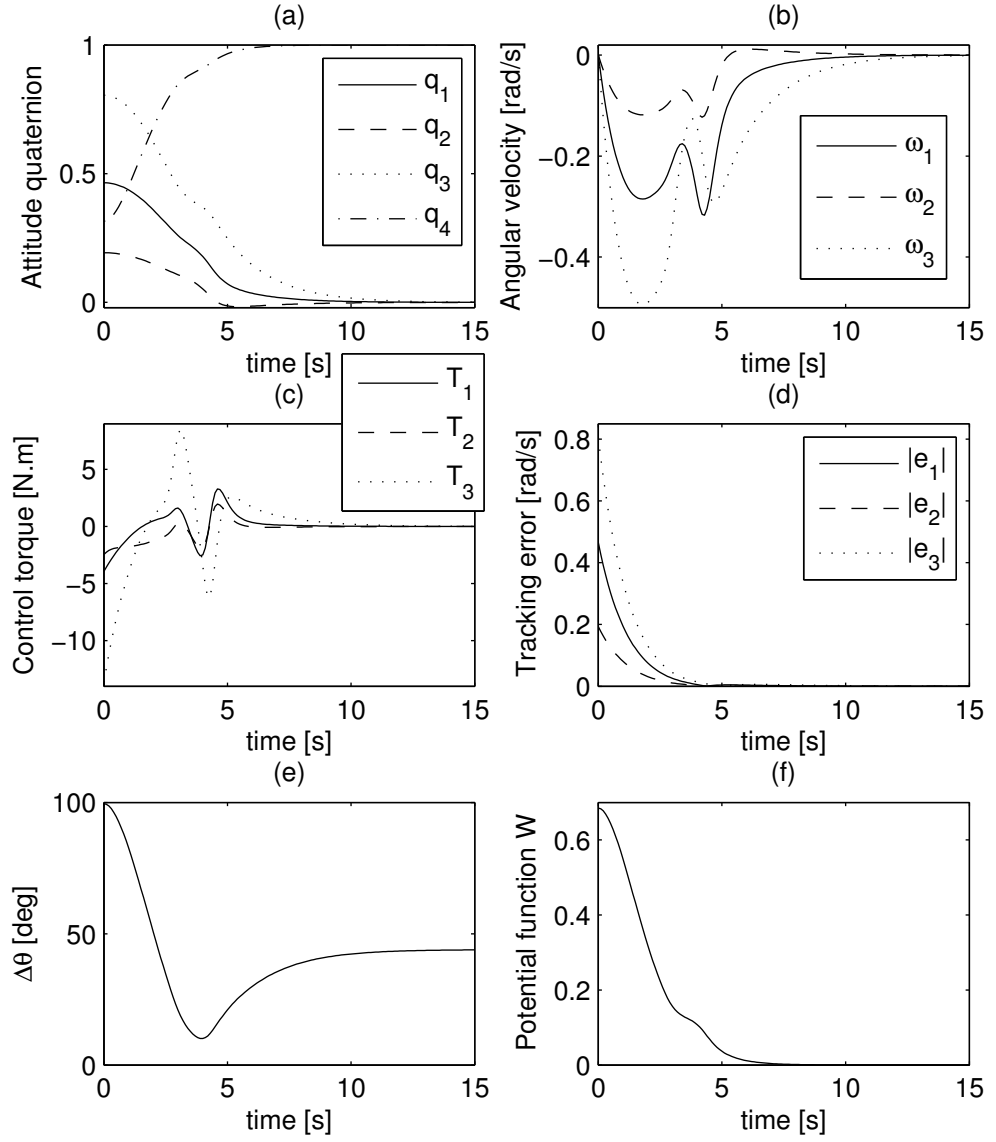


Fig. 3.1 Simulation results for the constrained slew manoeuvre example with the control gains tuned by trial and error

A larger value of the settling time may result in the smaller values for the gains s , g and η to the extent that the high value of B is also compensated for and the bound $\|T_{\text{analytical}}\|$ becomes acceptably small. In anticipation of this fact, all the five parameters in the bound, i.e. s , A , B , g , and η are simultaneously tuned for lowering the bound by setting up the following optimization problem which is solved using sequential quadratic programming (SQP):

$$\min_{s>0.01, A>0.01, B>100.0, g>0.1, \eta>0.5} \|T_{\text{analytical}}\|$$

The problem is subject to $t_{\text{settling}} \leq 47$ seconds, $\Delta\theta \geq 10$ deg and the closed loop differential equations, where $\mathbf{T}_{\text{analytical}}$ is the analytical upper bound given by Eq. (3.25). The lower bounds of all the gains are selected as mentioned because values of these parameters, smaller than this, would hardly achieve the given specifications of the closed loop response. Starting from the values of the gains given in Table 3.1 as the initial guess the above optimization problem is solved using SQP. The converged values of the parameters s , A , B , g and η are given in Table 3.2. The resulting $\|\mathbf{T}_{\text{analytical}}\|$ is about 175 Nm whereas the corresponding $\max(\|\mathbf{T}\|)$ is 4.36 Nm. So, a sacrifice of the settling time performance from around 12 to 47 seconds has resulted in a reasonable value for $\|\mathbf{T}_{\text{analytical}}\|$ despite the high value of the gain B , being 100. Fig. 3.2 shows the simulation results for the converged values of the gains employed in the controller given by Eq. (3.18). Again, the optimized bound guarantees that the actual control torque never exceeds the bound with the condition that $|e_i(t_0)|$ is less than or equal to the value for the current scenario. As we used a simple local optimization algorithm, the bound may also be improved further with some global optimization techniques.

Table 3.2 Constrained Slew Manoeuvre Nominal Case with Minimized Analytical Bound for Control Torque Norm

Parameter	Value	Units
s	0.01	
g	2.5515	
η	1.4305	
A	0.04652	
B	100	
$\min(\Delta\theta)$	10	deg
$\ \mathbf{T}_{\text{analytical}}\ $	175.28	N.m
$\max(\ \mathbf{T}\)$	4.3657	N.m
t_{settling}	47	s

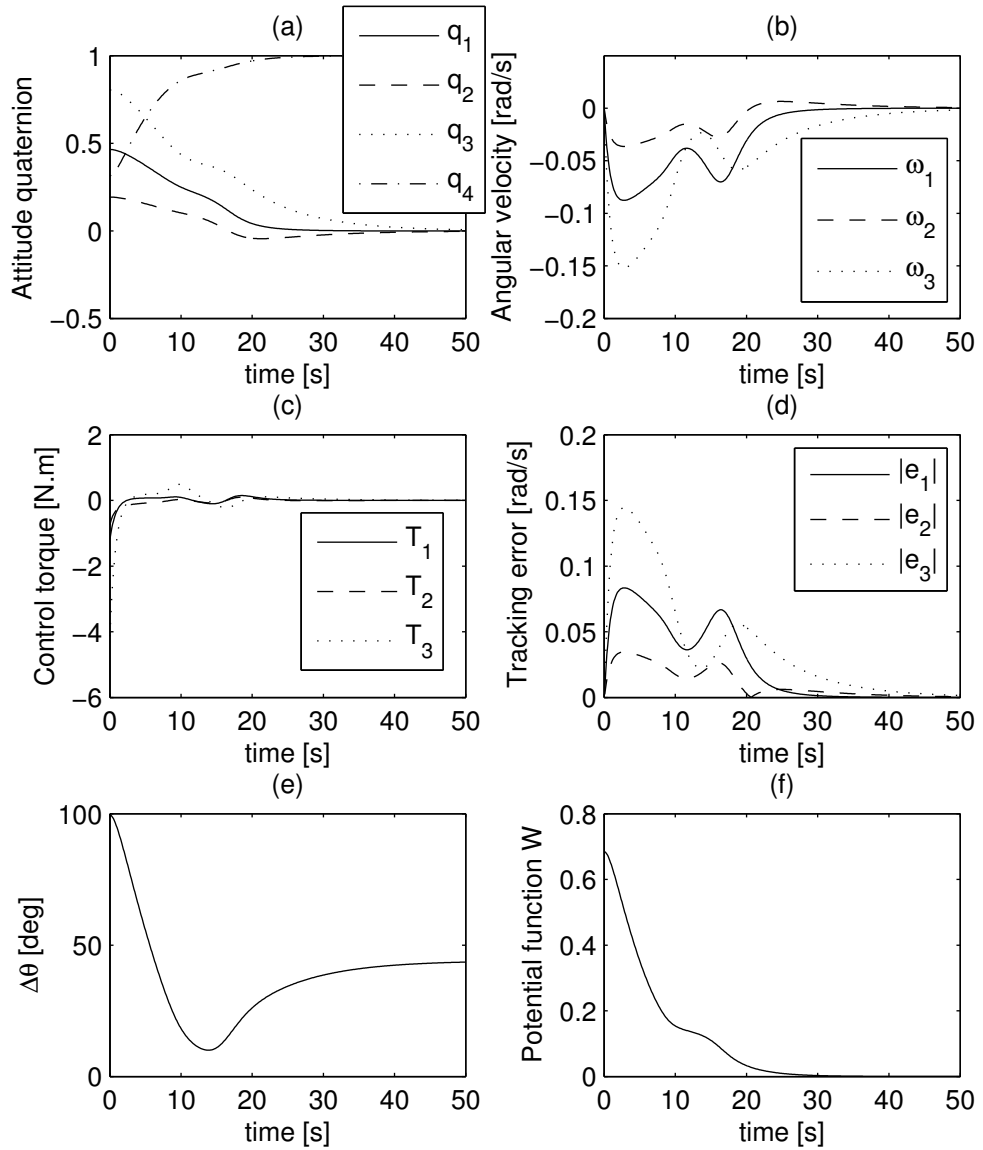


Fig. 3.2 Simulation results for the constrained slew manoeuvre example with the control gains optimized for the minimum analytical bound of control torque norm

As for the case of unconstrained attitude manoeuvre examples in Chapter 2, we augment the ongoing numerical example of constrained slew manoeuvre considering uncertain variations in the spacecraft nominal moments of inertia and the presence of external disturbance torque. As before, we consider the numerical example with 20 percent uncertain variation in the moments of inertia with respect to their nominal values and for this perturbation we have to set $\lambda = 0.2$. Similarly, external disturbance torque is assumed to be present with bounds $D_i = 0.1732$ Nm for $i=1,2,3$. Next, we solve the optimization problem:

$$\min_{s>0.01, A>0.01, B>50, g>5.0, \eta>0.5} \left\| \mathbf{T}_{\text{analytical}} \right\|$$

subject to $t_{\text{settling}} \leq 180$ seconds, $\left((1 + B\bar{V}_r)/2 + \Theta_i(\mathbf{e}(t_0)) \right) / g \leq 0.0027$ for $i = 1, 2, 3$ and the closed-loop dynamics. The values of the gains mentioned in Table 3.2 are used as the starting guess. The optimized values of the gains s , A , B , g and η are given in Table 3.3 which also presents the resulting $\left\| \mathbf{T}_{\text{analytical}} \right\|$ and $\max(\|\mathbf{T}\|)$ being about 499.98 Nm and 428.32 Nm, respectively. The analytical upper bound is approximately 1.17 times the actual maximum torque. Here, $|e_1(t)|$, $|e_2(t)|$ and $|e_3(t)|$ are guaranteed to decrease to values bounded by 0.0027, 0.00267 and 0.00265, respectively, as mentioned in Table 3.3 and the stability ensuring condition given by Eq. (3.32), while considering the upper bound of the right hand side which is given by its value at time t_0 , becomes

$$\begin{aligned} |e_1(t)| &> 0.0027 - 0.0013 = 0.0014 \\ |e_2(t)| &> 0.00267 - 0.0013 = 0.00137 \\ |e_3(t)| &> 0.00265 - 0.0013 = 0.00135 \end{aligned} \quad (3.38)$$

where $(1 - \lambda)(1 + B\bar{V}_r)/(2g) \cong 0.0013$. The above stability related conditions allow for some angular velocity and attitude convergence errors. The condition $0.0014 < |e_i(t)| \leq |\omega_i| + |s(q_i - BV_r b_i)|$ implies that if the attitude error $|q_i|$ is zero then the angular velocity error $|\omega_i|$ can be up to $0.0014 \text{ rad.s}^{-1}$ otherwise the maximum possible attitude error $|q_i|$ comes out to be 0.0262. So, the overall attitude error is bounded by $2 \sin^{-1} \left[(q_1^2 + q_2^2 + q_3^2)^{1/2} \right] = 2 \sin^{-1} (0.0262\sqrt{3}) \cong 5.2 \text{ deg}$ and the overall angular velocity error $(\omega_1^2 + \omega_2^2 + \omega_3^2)^{1/2}$ is bounded by $0.0024 \text{ rad.s}^{-1}$. Using bounds for $|e_i(t)|$ with $i = 1, 2, 3$ given by Eq. (2.50), the overall attitude and angular velocity errors become 5.11 deg and $0.00238 \text{ rad.s}^{-1}$, respectively.

Table 3.3 Constrained Slew Manoeuvre Nominal Case with Minimized Analytical Bound for Control Torque Norm while Robustness Ensured

Parameter	Value	Units
s	0.053321	
g	1000.1	
η	1.4616	
A	0.046043	
B	62.133	
$\min(\Delta\theta)$	10	deg
$\ \mathbf{T}_{\text{analytical}}\ $	499.98	N.m
$\max(\ \mathbf{T}\)$	428.32	N.m
t_{settling}	180	s
λ	0.2	
D_i for $i = 1, 2, 3$	0.1732	N.m
$\left(\frac{(1 + B\bar{V}_r)}{2} + \Theta_i(\mathbf{e}(t_0))\right)/g$	0.0027	
$\left(\frac{(1 + B\bar{V}_r)}{2} + \Theta_i(\mathbf{e}(t_0))\right)/g$	0.00267	
$\left(\frac{(1 + B\bar{V}_r)}{2} + \Theta_i(\mathbf{e}(t_0))\right)/g$	0.00265	

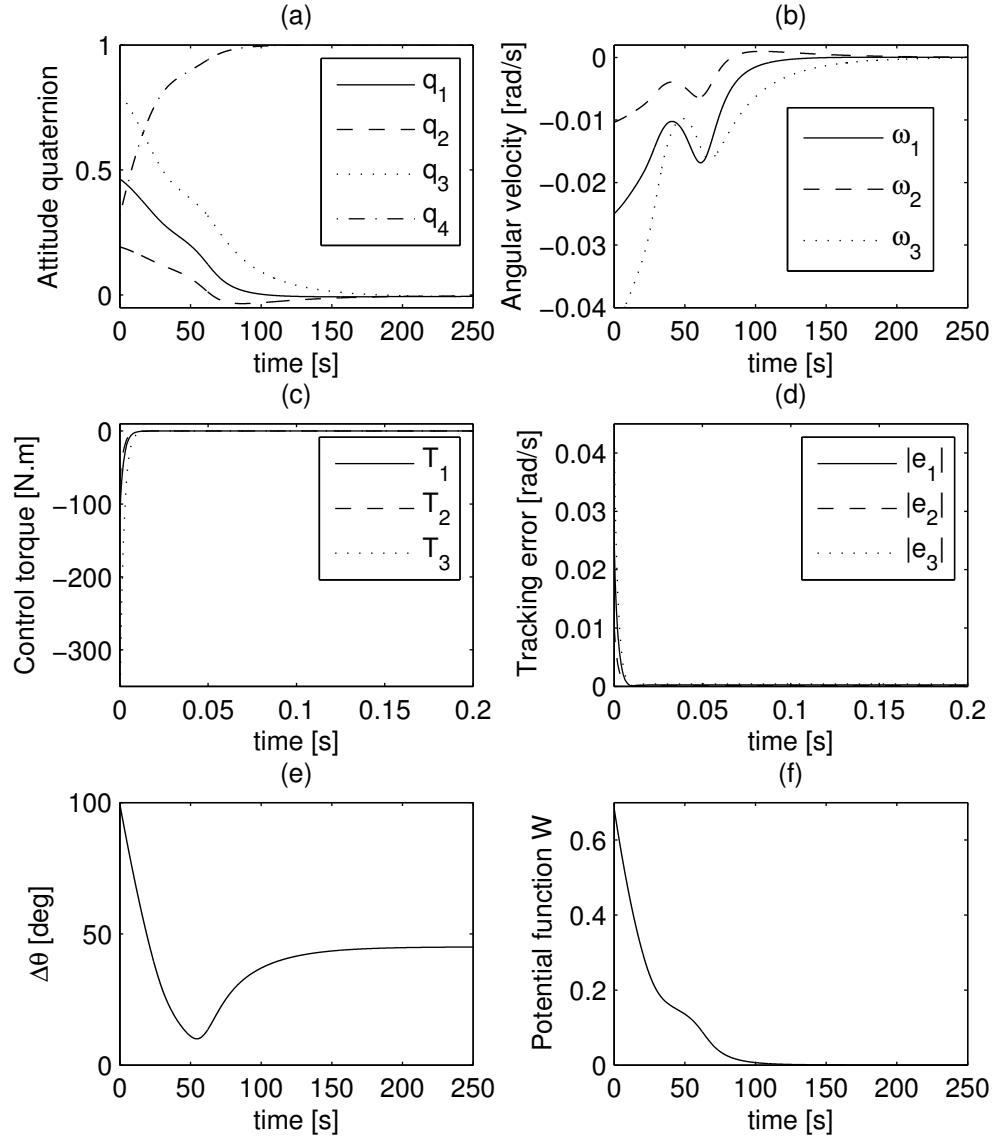


Fig. 3.3 Simulation results for the constrained slew manoeuvre example with the control gains optimized for the minimum analytical bound for control torque norm while ensuring robustness against bounded external disturbance and uncertain moments of inertia

After tuning the gains s , α , β , g and η for minimizing the analytical bound for control torque norm $\|T_{\text{analytical}}\|$ while ensuring robustness against 20 percent variations in the moments of inertia and external disturbance torque with the absolute values of the components bounded above by 0.1732 Nm, the manoeuvre is actually subject to same non-nominal moments of inertia in conjunction with the time varying external disturbance torque as considered for the spacecraft attitude manoeuvres numerical examples of Chapter 2 and the simulation results are reported in Fig. 3.4 and Table 3.4. The peak control torque, the settling time and the minimum constraint separation angle performance parameters in this case are almost the same as those for the nominal case given in Table

3.3. A higher control torque rate at the start is a common element among the manoeuvres, reported here as well as in Chapter 2, for which the control gains have been tuned for minimizing the analytical bound of the control torque norm. This observation is specially pronounced for the manoeuvres reported in Figs. 3.3 and 3.4. It identifies the need of also addressing the control torque rate saturation.

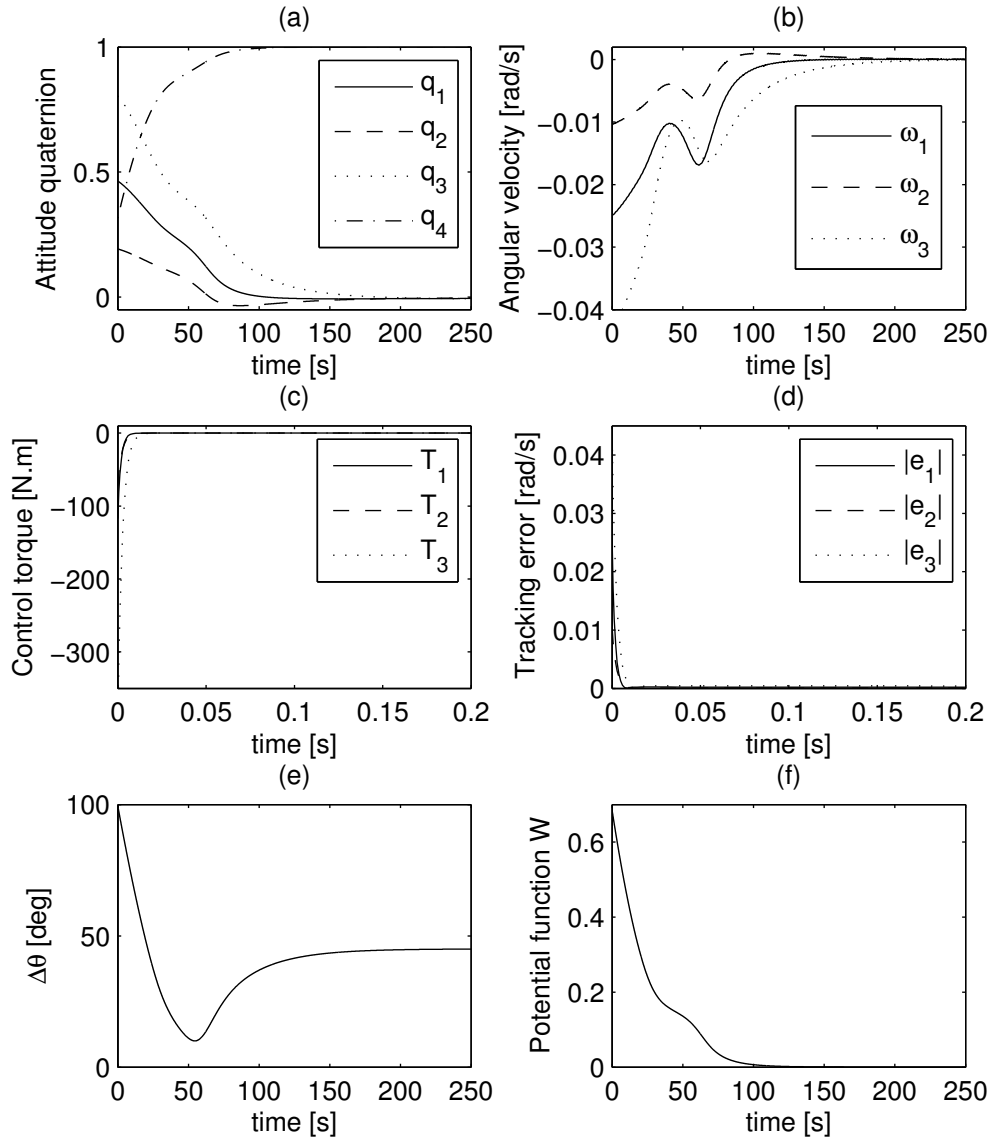


Fig. 3.4 Simulation results for the constrained slew manoeuvre example under the action of time varying bounded external disturbance and non-nominal moments of inertia

Table 3.4 Constrained Slew Manoeuvre Non-nominal Case with Time Varying External Disturbance Torque

Parameter	Value	Units
$\max(\ \mathbf{T}\)$	428.32	N.m
t_{settling}	180.1	s
$\min(\Delta\theta)$	9.9998	deg

Chapter 4

Spacecraft Rapid Slew Manoeuvres Using Control Moment Gyros

In the previous two chapters upper bounds for the control torque components are formulated analytically as a function of the initial attitude and angular velocity errors and the typical gains involved in the integrator backstepping based nonlinear control design procedure. Compensating the control torque saturation in this way prohibits the exploitation of the full availability of the control input space due to excessive detuning (Mulder, Tiwari and Kothare, 2009). In this chapter, we intend to explore the idea of undergoing rapid large angle reorientation manoeuvres by tracking the commanded angular momentum with the help of a cluster of four single gimbal CMGs in a pyramid configuration. The proposed formulation not only avoids the saturation of the angular momentum input from the CMG cluster but also exploits its maximum value along the direction of the commanded angular momentum for the major part of the manoeuvre. First section summarises the dynamics of the rigid spacecraft equipped with the said CMG cluster. Next section introduces the concept of gimbal rate command-based steering law for the CMG cluster. In the following section, the idea of steering the CMG cluster using a gimbal position command is presented. It also details a gimbal position steering logic for a

pyramid-type cluster of four single gimbal CMGs. Subsequently, a novel gimbal position steering law is proposed which exploits the maximum angular momentum deliverable by the CMG cluster corresponding to the direction of the commanded angular velocity for the major part of the spacecraft reorientation manoeuvre. The chapter ends with the section reporting the numerical simulation results that employ the proposed algorithm of the previous section for the generation of gimbal position command. The obtained results are also compared with some benchmark results in the literature for proving the significance of the proposed gimbal position steering logic. Some of the results reported in this chapter have been published in (Avanzini, Radice and Ali, 2009).

4.1 Attitude Motion of Rigid Spacecraft Equipped with CMGs

If the rigid spacecraft is equipped with a cluster of CMGs then the rotational equation of motion given by Eq. (2.3) can be written as (Wie, 1998)

$$\left(\mathbf{J}_B \dot{\tilde{\boldsymbol{\omega}}} + \tilde{\boldsymbol{h}}\right) + \tilde{\boldsymbol{\omega}} \times (\mathbf{J}_B \tilde{\boldsymbol{\omega}} + \tilde{\boldsymbol{h}}) = \tilde{\boldsymbol{T}}_d \quad (4.1)$$

where \mathbf{J}_B is the body frame \mathbf{B} referenced positive definite matrix denoting the inertia matrix of the spacecraft including the CMGs, $\tilde{\boldsymbol{T}}_d$ is the external torque vector expressed in the body frame \mathbf{B} . Here, we assume that the cluster comprises

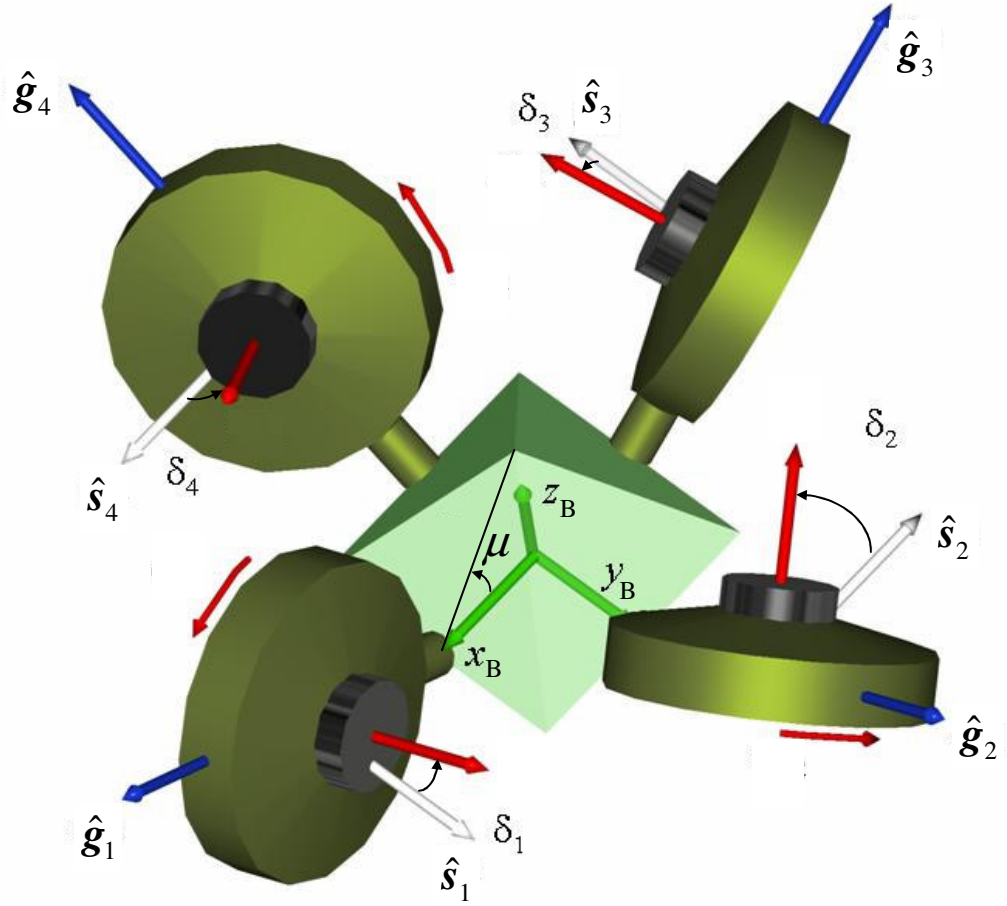


Fig. 4.1 Pyramid mounting for a cluster of four single-gimbal CMGs

four single gimbal CMGs. The total angular momentum stored in the cluster of CMGs, $\mathbf{h} = [h_1, h_2, h_3]^T$, is expressed in vector form as a function of the gimbal angles δ_i with $i = 1, 2, 3, 4$ as

$$\mathbf{h} = \sum_{i=1}^4 \mathbf{h}_i(\delta_i) = h_{CMG} \sum_{i=1}^4 \hat{\mathbf{s}}_i(\delta_i) \quad (4.2)$$

where \mathbf{h}_i and $\hat{\mathbf{s}}_i$ are the angular momentum vector and unit vector along the spin axis, respectively, of the i th CMG. All the wheels are assumed to be equal, spinning at the same angular speed and having the same constant angular momentum magnitude h_{CMG} . Neglecting the external torque vector $\tilde{\mathbf{T}}_d$ and introducing the internal (apparent) control torque vector \mathbf{T}_B generated by the CMG cluster, Eq. (4.1) takes the form of Eq. (2.3) where the control torque \mathbf{T}_B is given by

$$\mathbf{T}_B = -(\dot{\mathbf{h}} + \tilde{\boldsymbol{\omega}} \times \mathbf{h}) \quad (4.3)$$

The time derivative of the angular momentum delivered by the cluster of CMGs can be expressed as (Wie, 1998)

$$\dot{\mathbf{h}} = \mathbf{M} \dot{\boldsymbol{\delta}} \quad (4.4)$$

where $\mathbf{M} = \mathbf{M}(\boldsymbol{\delta})$ is the 3×4 jacobian matrix $\frac{\partial \mathbf{h}}{\partial \boldsymbol{\delta}}$, $\boldsymbol{\delta} = [\delta_1, \delta_2, \delta_3, \delta_4]^T$ is the gimbal angle vector and its time rate is denoted by $\dot{\boldsymbol{\delta}} = [\dot{\delta}_1, \dot{\delta}_2, \dot{\delta}_3, \dot{\delta}_4]^T$. The cluster of four CMGs is assumed to be the conventional pyramid mount as shown in Fig. 4.1. For such a mount, the total CMG angular momentum vector \mathbf{h} given by Eq. (4.2) can be written in the body frame \mathbf{B} as

$$\mathbf{h}(\boldsymbol{\delta}) = h_{CMG} \left(\begin{bmatrix} -\cos \mu \sin \delta_1 \\ \cos \delta_1 \\ \sin \mu \sin \delta_1 \end{bmatrix} + \begin{bmatrix} -\cos \delta_2 \\ -\cos \mu \sin \delta_2 \\ \sin \mu \sin \delta_2 \end{bmatrix} + \begin{bmatrix} \cos \mu \sin \delta_3 \\ -\cos \delta_3 \\ \sin \mu \sin \delta_3 \end{bmatrix} + \begin{bmatrix} \cos \delta_4 \\ \cos \mu \sin \delta_4 \\ \sin \mu \sin \delta_4 \end{bmatrix} \right) \quad (4.5)$$

where μ is the pyramid skew angle. Also, the matrix \mathbf{M} is written as

$$\mathbf{M} = \begin{bmatrix} -\cos \mu \cos \delta_1 & \sin \delta_2 & \cos \mu \cos \delta_3 & -\sin \delta_4 \\ -\sin \delta_1 & -\cos \mu \cos \delta_2 & \sin \delta_3 & \cos \mu \cos \delta_4 \\ \sin \mu \cos \delta_1 & \sin \mu \cos \delta_2 & \sin \mu \cos \delta_3 & \sin \mu \cos \delta_4 \end{bmatrix} \quad (4.6)$$

4.2 Gimbal Rate Steering Logic

For the design of this kind of CMG steering logic, the commanded $\dot{\mathbf{h}}$ is defined as

$$\dot{\mathbf{h}}_s = -\mathbf{T}_B - \tilde{\boldsymbol{\omega}} \times \mathbf{h} \quad (4.7)$$

where $\mathbf{T}_B = \mathbf{S}^T \mathbf{T}$ with $\mathbf{T} = [J_1 u_1, J_2 u_2, J_3 u_3]^T$ and u_i for $i = 1, 2, 3$ are given by Eqs. (2.19)

and (3.18). Then, the gimbal rate command $\dot{\boldsymbol{\delta}}_s$ is obtained by inverting Eq. (4.4) as

$$\dot{\boldsymbol{\delta}}_s = \mathbf{M}^\dagger \dot{\mathbf{h}}_s \quad (4.8)$$

where the inverse matrix \mathbf{M}^\dagger is computed by means of various variations of pseudo-inverse of the rectangular matrix \mathbf{M} . For example, if the Moore–Penrose pseudo-inverse is used, then

$$\mathbf{M}^\dagger = \mathbf{M}^T (\mathbf{M}\mathbf{M}^T)^{-1} \quad (4.9)$$

The drawback of this approach is related to the presence of cluster singular states (Wie, 1998, 2004), where it is not possible to provide a gimbal rate command producing a torque in an arbitrary direction. In mathematical terms, a singular state is detected whenever $\text{rank}(\mathbf{M}) < 3$, that is, the matrix $\mathbf{M}\mathbf{M}^T$ becomes singular. It should be noted that, in the neighbourhood of singular states, when $\det(\mathbf{M}\mathbf{M}^T)$ is close to zero, the gimbal rate command diverges towards infinity, so that hardware constraints, such as gimbal rate limits and gimbal stops, may be violated, thus triggering possible instabilities in the closed-loop system. Details on the issue of cluster singularities (Bedrossian et al., 1990b; Margulies and Aubrun, 1978; Wie, 1998, 2004) and strategies for either avoiding them (Ford and Hall, 2001; Oh and Vadali, 1991) or improving the robustness of the gimbal steering logic against their inception (Heiberg, Bailey and Wie, 1997; Wie, Heiberg and Bailey, 2001, 2002) have been widely discussed in the literature.

4.3 Gimbal Position Steering Logic

The spacecraft main body angular momentum $\mathbf{J}_B \tilde{\boldsymbol{\omega}}$ can be added to the angular momentum of the CMGs cluster \mathbf{h} to find the total angular momentum vector \mathbf{H} as

$$\mathbf{H} = \mathbf{J}_B \tilde{\boldsymbol{\omega}} + \mathbf{h} \quad (4.10)$$

When external torque $\tilde{\mathbf{T}}_d$ is neglected, the total angular momentum of the spacecraft \mathbf{H} is constant in the inertial space. By assuming that, for $\boldsymbol{\delta} = \mathbf{0}$, the satellite is at rest ($\tilde{\boldsymbol{\omega}} = \mathbf{0}$), the resulting value of the total angular momentum is $\mathbf{H} = \mathbf{0}$. Under this further assumption, an angular velocity command $\tilde{\boldsymbol{\omega}}_s$ can be tracked by means of a gimbal position command $\boldsymbol{\delta}_s = [\delta_{s1}, \delta_{s2}, \delta_{s3}, \delta_{s4}]^T$ being a solution of the equation

$$\mathbf{h}(\boldsymbol{\delta}_s) = \mathbf{h}_s \quad (4.11)$$

where $\mathbf{h}(\boldsymbol{\delta}_s)$ follows from Eq. (4.5) and \mathbf{h}_s is given as

$$\mathbf{h}_s = -\mathbf{J}_B \tilde{\boldsymbol{\omega}}_s \quad (4.12)$$

As a consequence, rather than inverting Eq. (4.4) to find the gimbal rate command $\dot{\boldsymbol{\delta}}_s$ which can generate the commanded $\dot{\mathbf{h}}_s$ given by Eq. (4.7), a solution $\boldsymbol{\delta}_s$ for Eq. (4.11) is sought so that the resulting angular velocity $\tilde{\boldsymbol{\omega}} = \tilde{\boldsymbol{\omega}}_s$ drives the spacecraft towards the desired attitude provided that $\tilde{\boldsymbol{\omega}}_s$ is defined in a way similar to Eq. (2.43) or (3.10). A simple possible definition can be

$$\tilde{\boldsymbol{\omega}}_s = -s\tilde{\mathbf{q}}_v \quad (4.13)$$

where s is the positive gain. In the long run, even the small disturbance torques typical of space environment result in a sizable variation of the total angular momentum. This can be easily taken into account in the control law by taking \mathbf{h}_s as

$$\mathbf{h}_s = \mathbf{H} - \mathbf{J}_B \tilde{\boldsymbol{\omega}}_s \quad (4.14)$$

where the total angular momentum \mathbf{H} can be measured from the knowledge of current spacecraft states (angular velocity components and gimbal rotation angles). A non-zero value of \mathbf{H} does not change the structure of the controller but it is detrimental for the effectiveness of any momentum exchange device, because when $\|\mathbf{H}\|$ grows, the available control power, defined by the maximum angular momentum that platform and spinning wheels can exchange, is reduced. For this reason, a set of thrusters is installed on board of spacecraft, in order to perform desaturation manoeuvres, aimed at dumping parasite angular momentum accumulated during a station-keeping phase because of an external disturbance torque. The issue of long-term stabilization during station-keeping phases in the presence of external disturbance torque and cluster desaturation is out of the scope of the present work, which deals with short-term manoeuvres during which environmental

disturbance torques have no effect and \mathbf{H} can be considered constant to any practical purpose.

A closed-form solution of the redundant system given by Eq. (4.11) is not available and Avanzini (2005) has presented two approximate solutions using the definition of symmetric Γ and anti-symmetric Π components of the overall gimbal rotation angles for the odd and even numbered pairs of gimbals as

$$\begin{aligned}
 \Gamma_o &= \frac{\delta_{s1} + \delta_{s3}}{2} \\
 \Pi_o &= \frac{\delta_{s1} - \delta_{s3}}{2} \\
 \Gamma_e &= \frac{\delta_{s2} + \delta_{s4}}{2} \\
 \Pi_e &= \frac{\delta_{s2} - \delta_{s4}}{2}
 \end{aligned} \tag{4.15}$$

Equation (4.11) can be written in terms of the symmetric and anti-symmetric parts as

$$\begin{aligned}
 h_{s1} &= -2h_{CMG} (\cos \mu \cos \Gamma_o \sin \Pi_o - \sin \Gamma_e \sin \Pi_e) \\
 h_{s2} &= -2h_{CMG} (\cos \mu \cos \Gamma_e \sin \Pi_e + \sin \Gamma_o \sin \Pi_o) \\
 h_{s3} &= 2h_{CMG} \sin \mu (\sin \Gamma_o \cos \Pi_o + \sin \Gamma_e \cos \Pi_e)
 \end{aligned} \tag{4.16}$$

The first formulation given by Avanzini (2005) is based on the small angle assumption which transforms Eq. (4.16) into a linear system as

$$\begin{aligned}
 h_{s1} &= -2h_{CMG} (\cos \mu) \Pi_o \\
 h_{s2} &= -2h_{CMG} (\cos \mu) \Pi_e \\
 h_{s3} &= 2h_{CMG} (\sin \mu) (\Gamma_o + \Gamma_e)
 \end{aligned} \tag{4.17}$$

which is solved under a further assumption that $\Gamma_o = \Gamma_e$. Since small gimbal angles result in small values of the angular velocity, the approach allows only for slow reorientations. In the second formulation, an approximate solution of the whole nonlinear system given by Eq. (4.16) is derived still assuming that $\Gamma_o = \Gamma_e$ which allows for wide gimbal rotations, thus speeding up the manoeuvre. In this case, the solution is written in terms of the transformed variables $\Gamma_o = \Gamma_e = \Gamma$, Π_o , and Π_e as

$$\begin{aligned}
\sin \Gamma &= \frac{h_{s3}}{2h_{CMG} \sin \mu (\cos \Pi_o + \cos \Pi_e)} \cong \frac{h_{s3}}{4h_{CMG} \sin \mu} \\
\sin \Pi_o &= -\frac{h_{s1} \cos \mu \cos \Gamma + h_{s2} \sin \Gamma}{2h_{CMG} (\cos^2 \mu \cos^2 \Gamma + \sin^2 \Gamma)} \\
\sin \Pi_e &= -\frac{-h_{s1} \sin \Gamma + h_{s2} \cos \mu \cos \Gamma}{2h_{CMG} (\cos^2 \mu \cos^2 \Gamma + \sin^2 \Gamma)}
\end{aligned} \tag{4.18}$$

Further details on this command law are given in Avanzini (2005), where a possible strategy for keeping the absolute value of the right-hand sides of Eqs. (4.18) below unity is also discussed. The time required for the benchmark manoeuvres tested becomes significantly shorter, when the nonlinear version of the gimbal position command is implemented. Nonetheless, the performance of the closed-loop algorithm is still suboptimal, and the resulting manoeuvre time significantly longer than that demonstrated by the singularity robust pseudo-inverse (Wie, Bailey and Heiberg, 2001), because the gimbal position command law described by Eq. (4.18) does not exploit the maximum angular momentum that the CMG cluster can deliver.

4.4 Gimbal Position Steering Logic for Maximum Angular Momentum

A new gimbal position command generation algorithm is proposed in this section, where the largest part of the reorientation is performed by exploiting the maximum available angular momentum vector component in the direction of the desired angular momentum \mathbf{h}_s . Let $\hat{\mathbf{h}}_s = \mathbf{h}_s / \|\mathbf{h}_s\|$ be the unit vector parallel to \mathbf{h}_s , the maximum angular momentum component that the cluster can deliver along $\hat{\mathbf{h}}_s$ is obtained if each CMG is rotated in such a way that the projection of the CMG spin axis $\hat{\mathbf{s}}_i$ along $\hat{\mathbf{h}}_s$ is maximum with $\hat{\mathbf{s}}_i \cdot \hat{\mathbf{h}}_s > 0$. This is true if one chooses $\hat{\mathbf{s}}_i$ as

$$\hat{\mathbf{s}}_i = \frac{(\hat{\mathbf{g}}_i \times \hat{\mathbf{h}}_s) \times \hat{\mathbf{g}}_i}{\|\hat{\mathbf{g}}_i \times \hat{\mathbf{h}}_s\|} \tag{4.19}$$

where $\hat{\mathbf{g}}_i$ is the unit vector along the gimbal axis of the i th CMG. In such a situation, the direction $\hat{\mathbf{h}}_s$ has been made singular. If we define the unit vector $\hat{\mathbf{t}}_i$ as

$$\hat{\mathbf{t}}_i = \hat{\mathbf{g}}_i \times \hat{\mathbf{s}}_i \quad (4.20)$$

then making the unit vector $\hat{\mathbf{h}}_s$ as singular means

$$\hat{\mathbf{h}}_s \cdot \hat{\mathbf{t}}_i = 0 \quad (4.21)$$

for $i = 1, 2, 3, 4$. In such a situation, there are two possibilities (Fig. 4.1):

$$\hat{\mathbf{h}}_s \cdot \hat{\mathbf{s}}_i > 0 \text{ or } \hat{\mathbf{h}}_s \cdot \hat{\mathbf{s}}_i < 0 \quad (4.22)$$

For a pyramid-type cluster of four CMGs, there are a total of sixteen possible combinations for making a given direction $\hat{\mathbf{h}}_s$ as singular. Equation (4.19) deals with the combination of $\hat{\mathbf{h}}_s \cdot \hat{\mathbf{s}}_i > 0$ for $i = 1, 2, 3, 4$ which geometrically means that each $\hat{\mathbf{s}}_i$ has a maximal projection onto the singular direction $\hat{\mathbf{h}}_s$. It makes the component of the total angular momentum of the CMG cluster along the direction $\hat{\mathbf{h}}_s$ as maximal. The locus of normalized total angular momentum of the pyramid-type CMG cluster (Fig. 4.1) for all $\hat{\mathbf{h}}_s \in \mathfrak{R}^3$ with $\hat{\mathbf{h}}_s \neq \pm \hat{\mathbf{g}}_i$ and $\hat{\mathbf{h}}_s \cdot \hat{\mathbf{s}}_i > 0$ for $i = 1, 2, 3, 4$ is given as Fig. 4.3 whereas **Fig. 4.4** shows such a singular surface for the case of $\hat{\mathbf{h}}_s \cdot \hat{\mathbf{s}}_1 < 0$ and $\hat{\mathbf{h}}_s \cdot \hat{\mathbf{s}}_i > 0$ for $i = 2, 3, 4$. The normalized angular momentum envelope for the said CMG cluster is presented as Fig. 4.5 being a smooth connection of the four singular surfaces of type as shown in **Fig. 4.4** with the one given by Fig. 4.3. A look of the complex inner construction of the angular momentum envelope is available as Fig. 4.6.

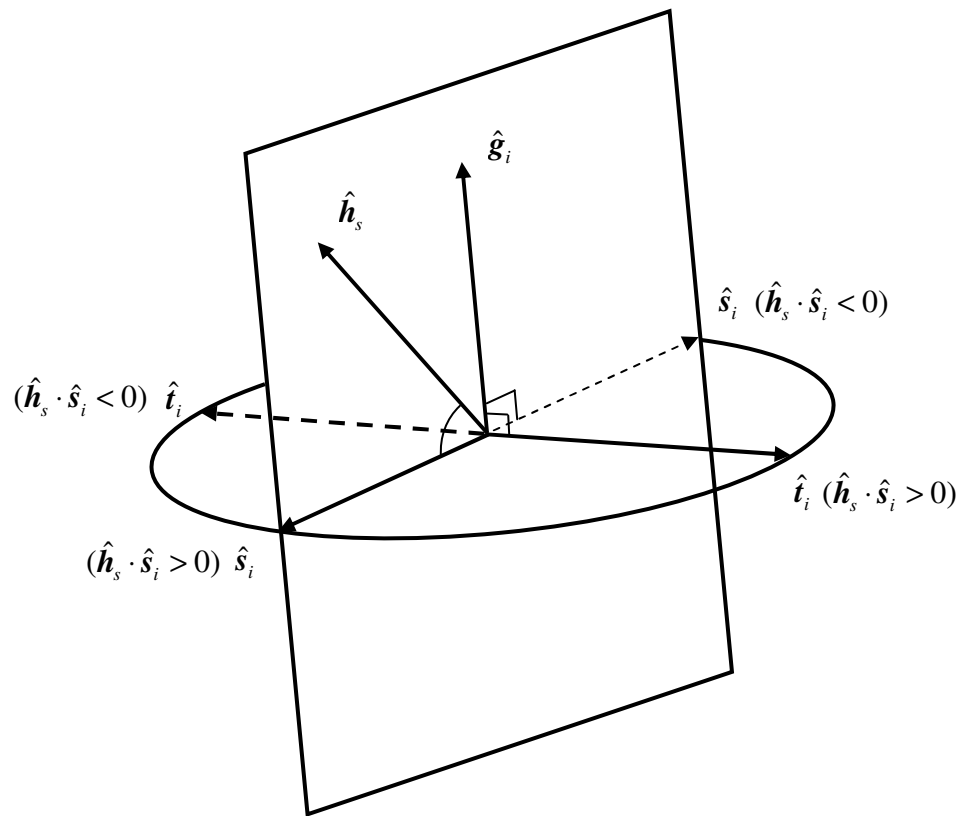


Fig. 4.2 Gimbal state with the direction \hat{h}_s considered as singular (Yoon, 2004)

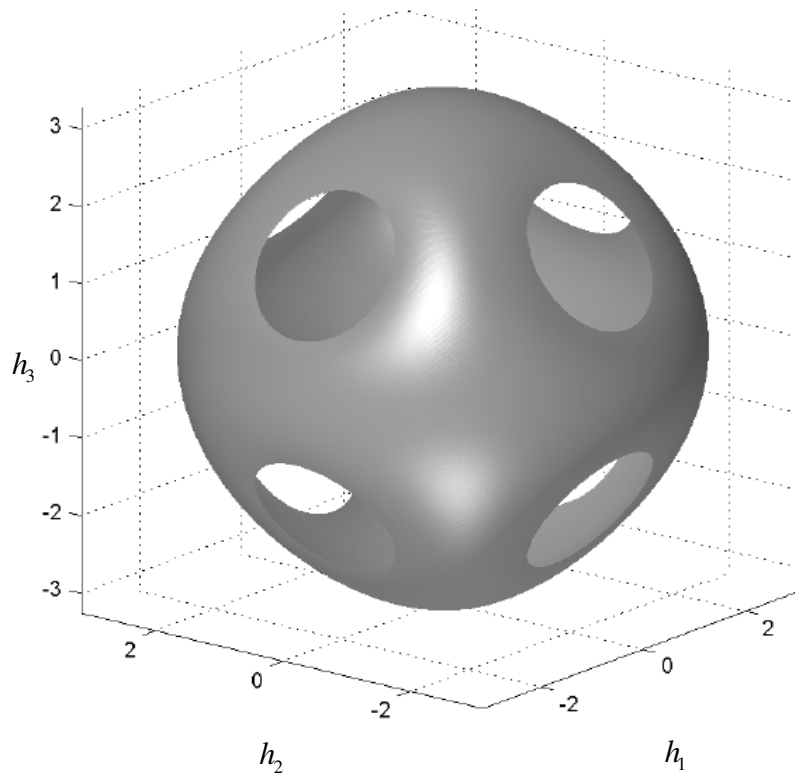


Fig. 4.3 Singular surface for pyramid-type CMG cluster with $\hat{h}_s \cdot \hat{s}_i > 0$ for $i=1,2,3,4$ (Yoon, 2004)

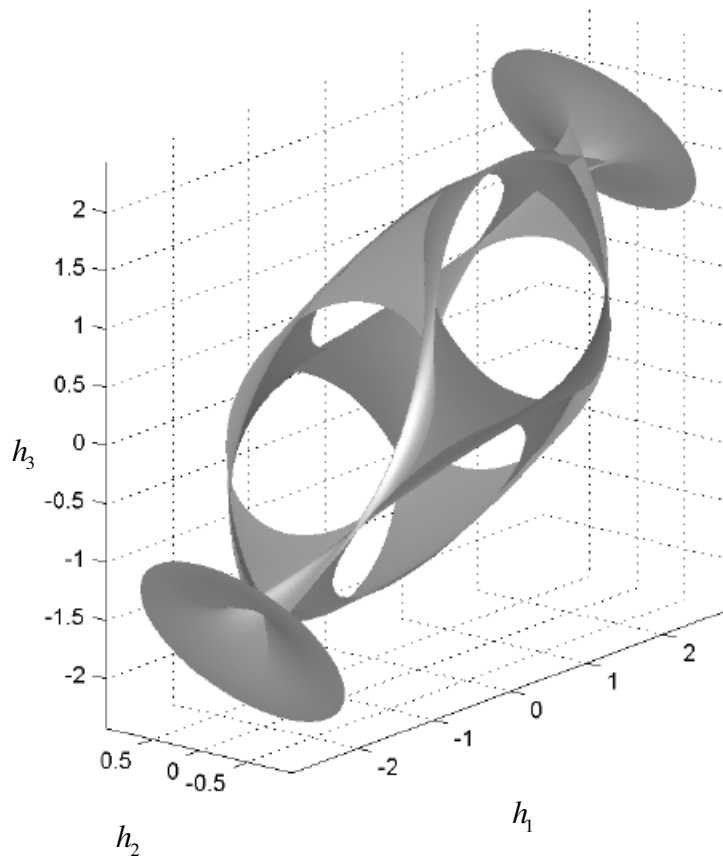


Fig. 4.4 Singular surface for pyramid-type CMG cluster with $\hat{h}_s \cdot \hat{s}_i > 0$ for $i = 2, 3, 4$ and $\hat{h}_s \cdot \hat{s}_1 < 0$ (Yoon, 2004)

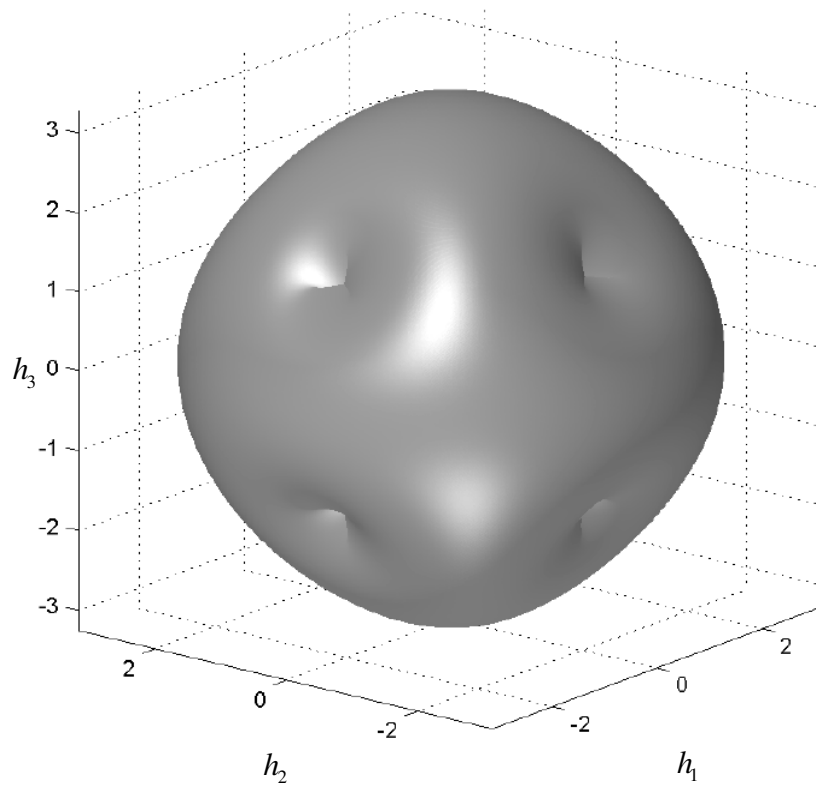


Fig. 4.5 Angular momentum envelope for pyramid-type CMG cluster (Yoon, 2004)

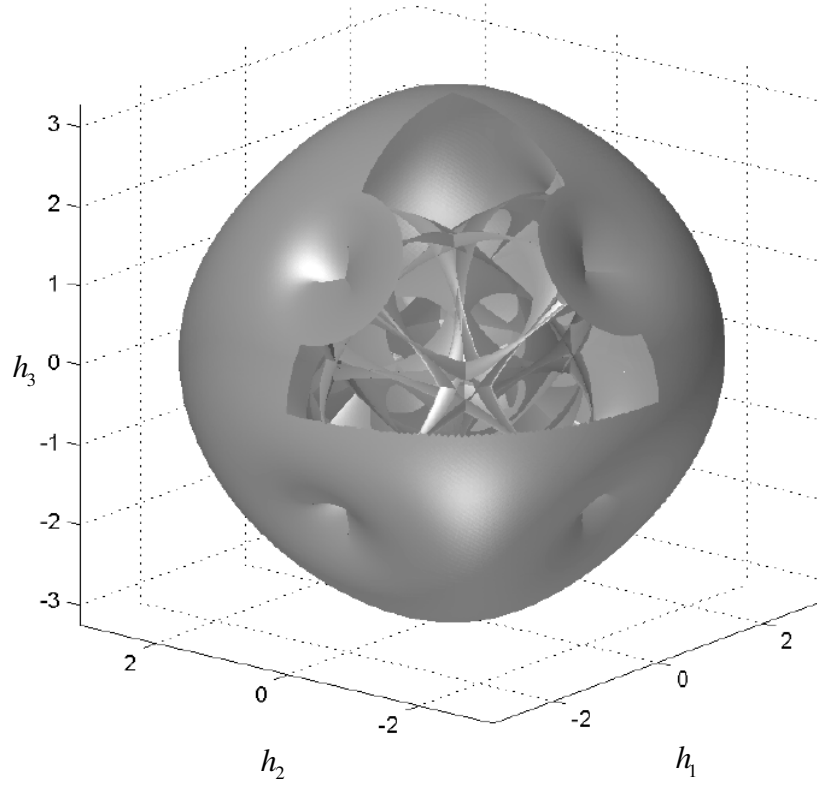


Fig. 4.6 Singular surface for pyramid-type CMG cluster with $\hat{\mathbf{h}}_s \cdot \hat{\mathbf{s}}_i > 0$ for all i (i.e. $i = 1, 2, 3, 4$) and with $\hat{\mathbf{h}}_s \cdot \hat{\mathbf{s}}_i > 0$ for all i except one value for which $\hat{\mathbf{h}}_s \cdot \hat{\mathbf{s}}_i < 0$ (Yoon, 2004)

The resulting angular momentum delivered by the cluster

$$\mathbf{h}_n = h_{CMG} \sum_{i=1}^4 \hat{\mathbf{s}}_i \quad (4.23)$$

is not parallel to $\hat{\mathbf{h}}_s$ where $\hat{\mathbf{s}}_i$ for $i = 1, 2, 3, 4$ are given by Eqs. (4.19). It is thus possible to split it into a desired component, parallel to $\hat{\mathbf{h}}_s$

$$\mathbf{h}_{nr} = (\mathbf{h}_n \cdot \hat{\mathbf{h}}_s) \hat{\mathbf{h}}_s \quad (4.24)$$

and an undesired one, perpendicular to it

$$\mathbf{h}_{np} = \mathbf{h}_n - \mathbf{h}_{nr} \quad (4.25)$$

In order to take advantage of the maximal total angular momentum available in the direction of \mathbf{h}_n , the gain s is tuned by imposing that $\mathbf{h}_s = \mathbf{h}_{nr}$. Hence, one is left with

$$s = \frac{\|\mathbf{h}_{nr}\|}{\|\mathbf{J}_B \tilde{\boldsymbol{\omega}}_s\|} \quad (4.26)$$

Using the above value of gain s , Eq. (4.13) takes the form

$$\tilde{\boldsymbol{\omega}}_s = -\frac{\|\mathbf{h}_{nr}\| \tilde{\mathbf{q}}_v}{\|\mathbf{J}_B \tilde{\boldsymbol{\omega}}_s\|} \quad (4.27)$$

There are two drawbacks related to the implementation of such a gimbal command law. Firstly, the undesired angular momentum component \mathbf{h}_{np} will perturb the resulting spacecraft attitude motion with respect to the desired eigen axis rotation and, secondly, the commanded angular momentum component does not drop towards zero as the spacecraft approaches the target attitude. This means that some other strategy must be implemented in order to stop the motion.

Numerical simulations demonstrate that the first issue does not harm closed-loop stability of the system, as $\|\mathbf{h}_{nr}\|$ is always significantly larger than $\|\mathbf{h}_{np}\|$ and the spacecraft is driven towards the desired attitude by the proposed command law, regardless of the initial value of the quaternion error vector. In order to circumvent the second problem, the maximum angular momentum command law is applied only until $\tilde{\mathbf{q}}_v^T \tilde{\mathbf{q}}_v > \sin^2(\Lambda_T/2)$, where Λ_T is a given threshold. When the initial pointing error is larger than Λ_T , the maximum angular momentum is exploited until this threshold is crossed. For the second part of the manoeuvre when $\tilde{\mathbf{q}}_v^T \tilde{\mathbf{q}}_v < \sin^2(\Lambda_T/2)$, the fixed value of the gain s , which is equal to the one attained at the threshold, is used. At the same time, the command law is switched to the approximate non-linear solution for the gimbal angles by Avanzini (2005) provided by Eq. (4.18).

Also, if the initial pointing error is less than Λ_T , that is, $\tilde{\mathbf{q}}_v(t_0)^T \tilde{\mathbf{q}}_v(t_0) < \sin^2(\Lambda_T/2)$, a suitably selected fixed value of the gain s is employed in conjunction with the solution of

Eq. (4.18). Note that, with the proposed approach, the gain s always results in an angular velocity/angular momentum command bounded by the angular momentum envelope of the cluster.

Aforementioned scheme can also be employed for the constrained slew manoeuvres considered in Chapter 3. In this case, the pseudo control law given by Eq. (3.10) can be written as

$$\tilde{\boldsymbol{\omega}}_s = -s(\tilde{\mathbf{q}}_v - BV_r \tilde{\mathbf{b}}_v) \quad (4.28)$$

where the quaternion $\tilde{\mathbf{b}} = [\tilde{\mathbf{b}}_v^T, \tilde{b}_4]^T$, $\tilde{\mathbf{b}}_v = [\tilde{b}_1, \tilde{b}_2, \tilde{b}_3]^T$ can be written as

$$\tilde{\mathbf{b}}_v = \tilde{q}_{c4} \tilde{\mathbf{q}}_v - \tilde{q}_4 \tilde{\mathbf{q}}_{cv} - \tilde{\mathbf{q}}_{cv} \times \tilde{\mathbf{q}}_v \quad (4.29)$$

$$\tilde{b}_4 = \tilde{\mathbf{q}}_{cv}^T \tilde{\mathbf{q}}_v + \tilde{q}_{c4} \tilde{q}_4 \quad (4.30)$$

with the quaternion $\tilde{\mathbf{q}}_c = [\tilde{\mathbf{q}}_{cv}^T, \tilde{q}_{c4}]^T$ defined as in Section 3.1 and V_r given by Eq. (3.8) while replacing the quaternion $\mathbf{b} = [\mathbf{b}_v^T, b_4]^T$ with $\tilde{\mathbf{b}} = [\tilde{\mathbf{b}}_v^T, \tilde{b}_4]^T$. The relation to tune the gain s for exploiting the maximum angular momentum available from the CMG cluster takes the form

$$s = \frac{\|\mathbf{h}_{nr}\|}{\|\mathbf{J}_B (\tilde{\mathbf{q}}_v - BV_r \tilde{\mathbf{b}}_v)\|} \quad (4.31)$$

Apparently, the gain s may diverge if $\tilde{\mathbf{q}}_v = BV_r \tilde{\mathbf{b}}_v$, but considering Eqs. (4.28) and (4.31) together as

$$\tilde{\boldsymbol{\omega}}_s = -\frac{\|\mathbf{h}_{nr}\| (\tilde{\mathbf{q}}_v - BV_r \tilde{\mathbf{b}}_v)}{\|\mathbf{J}_B (\tilde{\mathbf{q}}_v - BV_r \tilde{\mathbf{b}}_v)\|} \quad (4.32)$$

it is clear that the term $\|\mathbf{J}_B (\tilde{\mathbf{q}}_v - BV_r \tilde{\mathbf{b}}_v)\|$ is used to normalize the angular velocity command. Only if the condition $\tilde{\mathbf{q}}_v = BV_r \tilde{\mathbf{b}}_v$ is met exactly, the angular velocity command is singular. In order to meet the singularity condition, the vectors $\tilde{\mathbf{q}}_v$ and $BV_r \tilde{\mathbf{b}}_v$ should be

equal. This requires that, firstly, the vectors $\tilde{\mathbf{q}}_v$ and $\tilde{\mathbf{b}}_v$ are exactly parallel (which in turn means that from the current spacecraft attitude, the obstacle and the target attitudes are obtained by rotating the spacecraft through two angles $\Delta\theta$ and Λ , respectively, around exactly the same eigenaxis and, secondly, the angles Λ and $\Delta\theta$ satisfy the condition $\sin(\Lambda/2) = BV_r \sin(\Delta\theta/2)$ where the angle $\Delta\theta$ is given by Eq. (3.3) with the quaternion $\mathbf{b} = [\mathbf{b}_v^T, b_4]^T$ replaced with $\tilde{\mathbf{b}} = [\tilde{\mathbf{b}}_v^T, \tilde{b}_4]^T$ and the angle Λ is defined as

$$\Lambda = 2 \sin^{-1} \left[(\tilde{\mathbf{q}}_v^T \tilde{\mathbf{q}}_v)^{1/2} \right] \quad (4.33)$$

From the mathematical standpoint the two conditions can be met, and in simulation this may be possible if one forces the initial conditions to create such a configuration. Such a situation happens at a point of the state space where the angular velocity command given by Eq. (4.28) drops to zero as the gradient of the Lyapunov function vanishes here, regardless of any admissible control action. The presence of such local minima where the derivatives of the potential function vanish is typical of all the applications of the potential function method for obstacle avoidance. Being a saddle, the resulting local minimum is unstable. Moreover, in the present application, the parasite angular momentum \mathbf{h}_{np} acts as a perturbation to the exact implementation of the command avoiding the possibility of the system being trapped in the unstable local minimum of the potential function.

The architecture of the closed-loop system employing the aforementioned gimbal position command exploiting the maximum angular momentum deliverable by the CMG cluster is given by the block diagram reported as Fig. 4.7. The attitude error vector $\tilde{\mathbf{q}}$ is used in Eq. (4.13) or (4.28) to generate an angular velocity command $\tilde{\boldsymbol{\omega}}_s$ for the case of unconstrained or constrained large angle attitude manoeuvre, respectively. The gimbal position command law determines the value of the gimbal angles $\boldsymbol{\delta}_s$ as a solution of Eq. (4.19) or (4.18) for the ‘maximum available angular momentum transfer mode’ or the ‘convergence to the desired attitude mode’, respectively, of the attitude manoeuvre. The resulting value of $\boldsymbol{\delta}_s$ is tracked by means of a simple first-order system (Avanzini, 2005), such that the commanded gimbal rate comes out to be

$$\dot{\boldsymbol{\delta}} = K_{\delta}(\boldsymbol{\delta}_s - \boldsymbol{\delta}) \tag{4.34}$$

where K_{δ} is a positive constant. Dynamics of each gimbal is modelled by means of a second-order linear system as considered in (Wie, Heiberg and Bailey, 2001), featuring also a gimbal rate limit $\dot{\boldsymbol{\delta}}_{\max}$ for each CMG of the cluster. The resulting gyroscopic torque \mathbf{T}_B that forces the spacecraft attitude motion is then determined with the help of Eqs. (4.3–4.5) as a function of the gimbal position $\boldsymbol{\delta}$, the gimbal rate $\dot{\boldsymbol{\delta}}$ and the spacecraft angular velocity $\tilde{\boldsymbol{\omega}}$. The proposed scheme is based upon the attitude kinematics subsystem stabilization and still is practically viable as the response of the electric motors that drive the gimbals is usually sufficiently fast, so that the required angular momentum is transferred to the spacecraft platform in a relatively small amount of time, during which only minor variations of spacecraft attitude are expected, resulting in small corrections to angular velocity command.

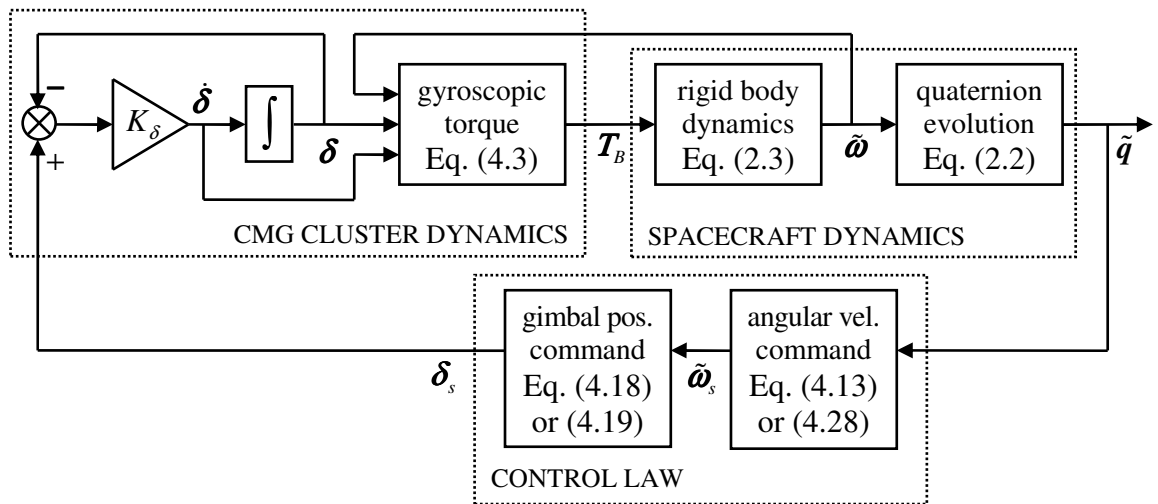


Fig. 4.7 Block diagram

4.5 Numerical Simulation

In this section, numerical simulations are used in order to assess the validity of the proposed CMG steering logic. Data for the rigid spacecraft equipped with a cluster of four single gimbal CMGs in a pyramid configuration is taken from (Wie, Bailey and Heiberg, 2001) and is provided as Table 4.1 whereas Table 4.2 provides information common among all the considered numerical examples. A skew angle μ of 53.13 deg features an almost spherical angular momentum envelope as shown in Fig. 4.5 (Oh and Vadali, 1991). A pure roll manoeuvre also acquired from (Wie, Bailey and Heiberg, 2001), where the 3-2-1 Euler angles θ_1 , θ_2 and θ_3 (describing the attitude of the body frame \mathbf{B} with respect to the inertial frame \mathbf{N}), at the start, are taken as 47, 0 and 0 deg, respectively, is used as a test benchmark for the numerical validation of the proposed gimbal position command generation algorithm. Moreover, the algorithm will also be employed for the said benchmark roll manoeuvre while avoiding a pointing constraint along the desired attitude path. For all the reported results, the total angular momentum \mathbf{H} is assumed to be zero.

Table 4.1 Data for the spacecraft equipped with pyramid-like cluster of four single-gimbal CMGs

Parameter	Value	Units
J_1	21400	kg.m ²
J_2	20100	kg.m ²
J_3	5000	kg.m ²
h_{CMG}	1000	kg.m ² .s ⁻¹
μ	53.13	deg
$\dot{\delta}_{\max}$	2	deg.s ⁻¹

Table 4.2 Data for the attitude manoeuvre examples for spacecraft equipped with pyramid-like cluster of four single-gimbal CMGs

Parameter	Value	Units
$\boldsymbol{\omega}(t_0)$	$[0 \ 0 \ 0]^T$	rad.s ⁻¹
K_δ	2	
A	0.5	
B	1000	

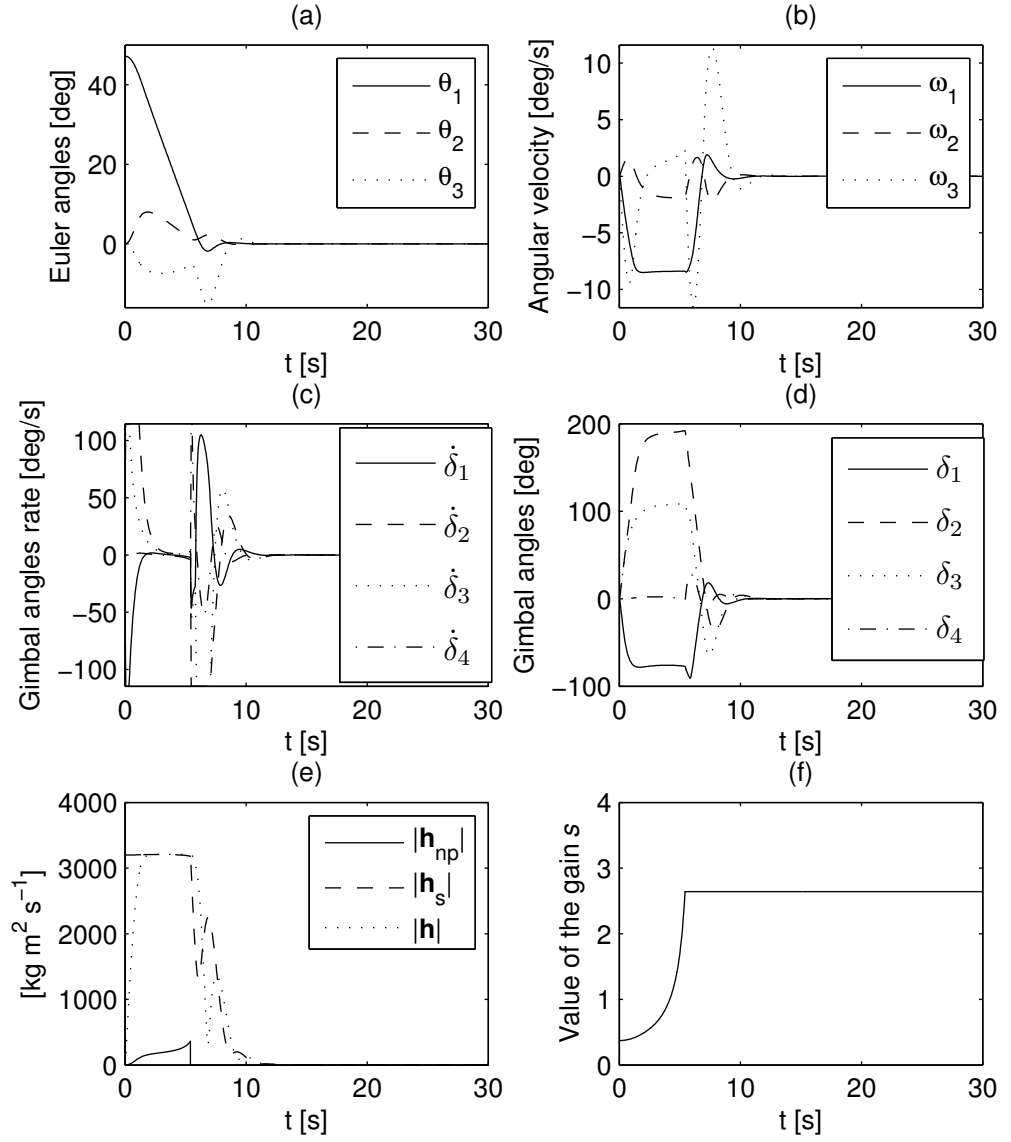


Fig. 4.8 Simulation results for the benchmark roll manoeuvre with the gimbal position steering logic exploiting the maximum available angular momentum

The features of the new gimbal position command exploiting the maximum angular momentum deliverable by the CMG cluster are first analysed for the constraint-free roll manoeuvre (Fig. 4.8). The manoeuvre is split into two sections, where the threshold for switching to the second section (the convergence mode) is at $\tilde{\mathbf{q}}_v^T \tilde{\mathbf{q}}_v = 0.005$, corresponding to an angular distance $\Lambda_T = 8$ deg from the target. Fig. 4.8 shows that the target attitude $\tilde{\mathbf{q}}_v = \mathbf{0}$ is achieved in approximately 11 seconds, i.e. little more than half of the time necessary when the gimbal position command described by Eq. (4.18) is used through out the manoeuvre (Fig. 4.9).

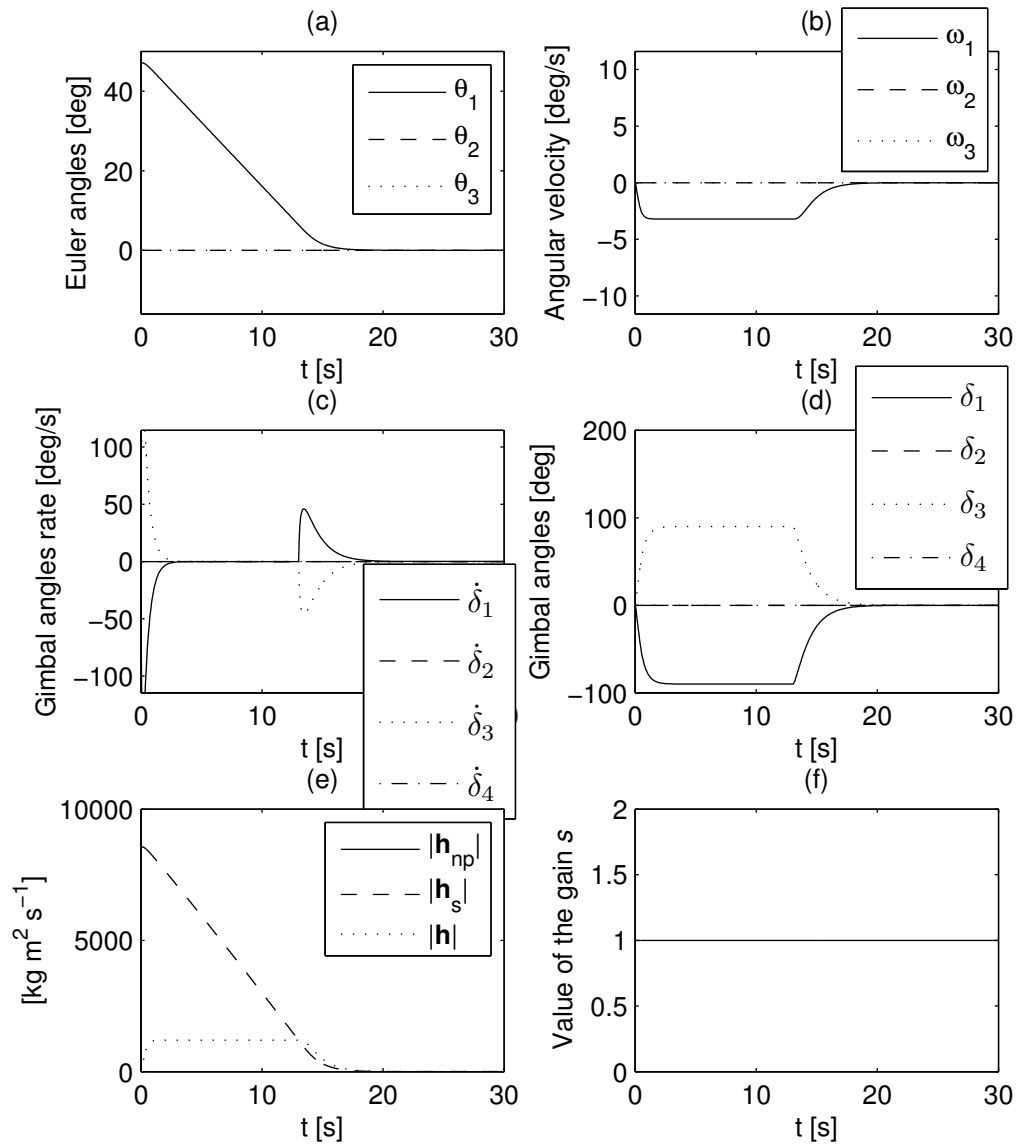


Fig. 4.9 Simulation results for the benchmark roll manoeuvre with nonlinear approximate gimbal position steering logic

Such a performance compares well with the quasi-optimal performance of the singularity robust pseudoinverse (Wie, Bailey and Heiberg, 2001), where the same rotation was performed in 8.5 seconds. It should be noted that the manoeuvre given by Fig. 4.8 is different from that presented as Fig. 4.9, in the sense that it is three-axial right from the beginning. Pitch and yaw angular velocity components are different from zero (and quite large, indeed, as shown in Fig. 4.8(b)). It is because of the fact that the maximal angular momentum gimbal position command rotates all the gimbals and delivers, together with the maximum angular momentum component along the desired rotation eigenaxis, also an

undesired angular momentum component in a perpendicular direction (Fig. 4.8(e)). Nonetheless, a very fast manoeuvre is achieved. Control activity (Fig. 4.8(c) and (d)) is smooth until the spacecraft crosses the threshold at $\Lambda_T = 8$ deg. A transient in Fig. 4.8(c) and (d) is clearly visible when the control law switches from the steering logic for maximum angular momentum to the gimbal position command of Eq. (4.18), and the angular velocity command gain s becomes constant (Fig. 4.8(f)).

In the next simulation scenario, the new gimbal position command exploiting the maximum angular momentum deliverable by the CMG cluster is employed in conjunction with the obstacle avoiding angular velocity command given by Eq. (4.28) to undergo large angle attitude manoeuvre while avoiding a prescribed pointing constraint. The aforementioned 47 deg roll manoeuvre is again used for indicating the viability of the approach. This time, a forbidden attitude is placed along the path towards the desired attitude at $\tilde{\mathbf{q}}_c = [0.0887 \ 0.0155 \ -0.0538 \ 0.9945]^T$, which corresponds to a position at 12 deg from the target attitude. The time history of the 3-2-1 Euler angles is reported in Fig. 4.10(a), and the effect of the presence of the obstacle along the angular path followed by the spacecraft is clearly visible: the decrease of θ_1 suddenly stops at $t = 4.5$ seconds, while at the same time θ_2 undergoes a sudden ‘bump’, which was not present in the previous, obstacle-free manoeuvre (Fig. 4.8(a)). The angular distance from the obstacle (Fig. 4.10(b)), which was rapidly decreasing along the nominal path, is stopped and the minimum distance kept higher than 5 deg. One of the interesting features of the proposed gimbal position command generation algorithm is that the control activity is very smooth for the unconstrained slew manoeuvre (Fig. 4.8) until the $\Lambda_T = 8$ deg threshold is reached. On the converse, for the case of constrained slew, the control activity becomes more intense as the forbidden attitude is approached (Fig. 4.10(c) and (d)), because of the requirement of making the roll angular velocity component as zero in order to avoid the obstacle (Fig. 4.10(e)). The said intensity of control effort is further enhanced by the almost simultaneous encounter with the $\Lambda_T = 8$ deg threshold, where the control law switches from the maximum angular momentum steering logic to the approximate non-linear gimbal position command given by Eq. (4.18). In spite of the presence of a gimbal

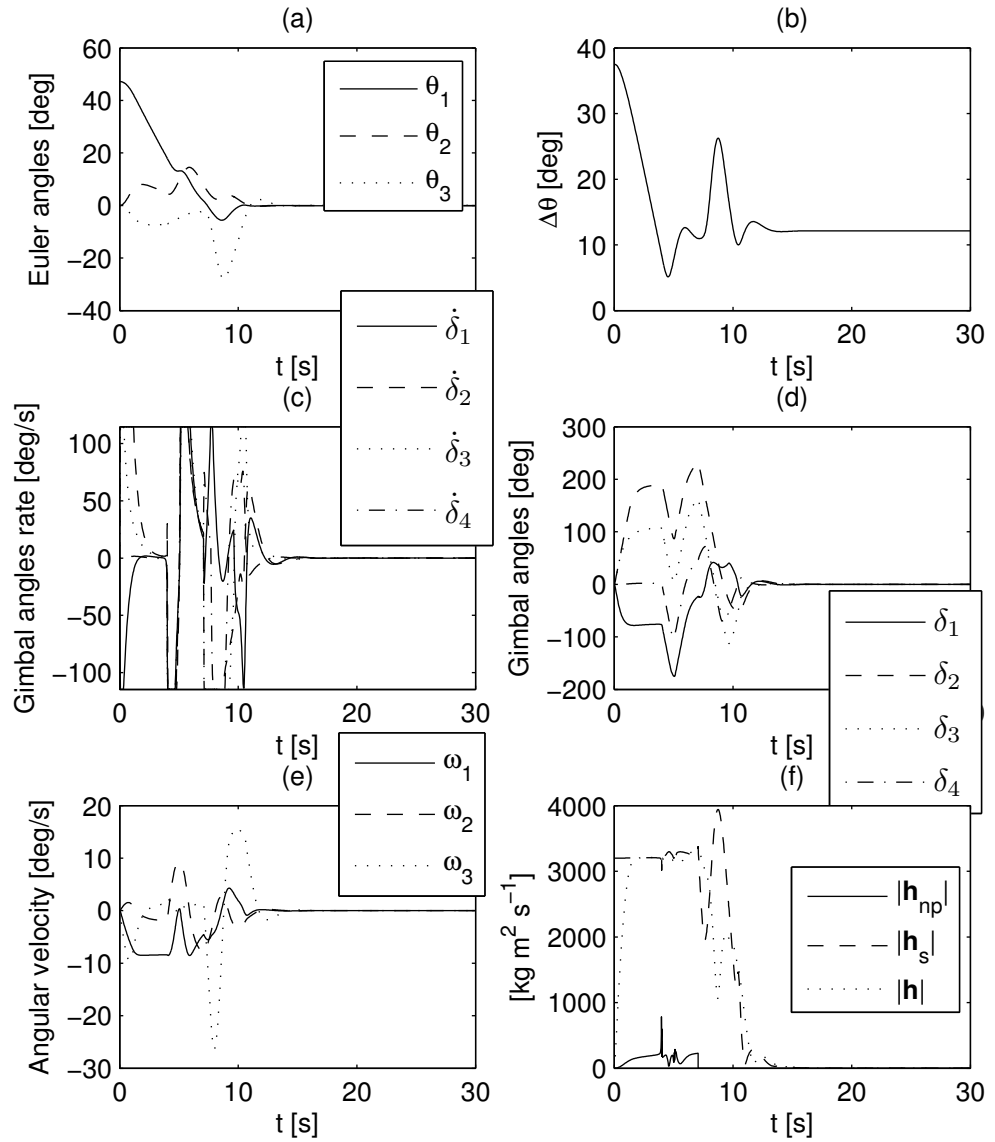


Fig. 4.10 Simulation results for the benchmark roll manoeuvre with the gimbal position steering logic exploiting the maximum available angular momentum while avoiding a pointing constraint

rate saturation limit of 2 rad/s clearly visible in Fig. 4.10(c), the closed-loop system remains stable and the manoeuvre is correctly tracked. By tuning the parameters of the repulsive potential function, it is possible to tailor the forbidden neighbourhood, keeping the attitude farther away from the obstacle or allowing closer passes with smaller angular separation. As expected, in spite of the singularity measure dropping close to 0, the proposed gimbal position command successfully implements the angular velocity command generated by the potential function approach. Control activity drops to 0 and the spacecraft is at rest after achieving the convergence to the target attitude in approximately less than 14 seconds. This represents a minor penalty, in terms of manoeuvre time, with respect to the results reported in Fig. 4.8 where the same manoeuvre was performed (without the presence of any obstacle) in approximately 11 seconds.

The results for the aforesaid constrained roll manoeuvre with the gimbal position command employing only the approximate nonlinear solution of Eq. (4.18) (Avanzini, 2005) are given by Fig. 4.11. In this case, the convergence to the final target attitude is achieved in approximately 21 seconds, when the spacecraft angular speed and the angular momentum drop back to zero (Fig. 4.11(e) and (f)). It should be noted that, because of the three dimensional nature of the simulation scenario, the obstacle for the manoeuvre given by Fig. 4.11 is not left in the same position as for the one presented in Fig. 4.10, as the angular distance from it gets only marginally smaller than 6.42 deg during the corresponding unconstrained manoeuvre reported in Fig. 4.9. For this reason, the forbidden attitude is moved to $\tilde{\mathbf{q}}_c = [0.2 \ 0.001 \ 0 \ 0.9798]^T$ which is approximately the position reached by the spacecraft at about $t = 7.85$ seconds during the previous manoeuvre with no obstacle as shown by Fig. 4.9. The results given by Fig. 4.11 show how the path towards the desired attitude is followed (Fig. 4.11(a)) until the angular distance from the obstacle, $\Delta\theta$ (reported in Fig. 4.11(b)), drops close to approximately 5 deg. At this point, the pure roll manoeuvre is traded for a tri-axial one, where minor displacements about the pitch and yaw axes allow to avoid the forbidden attitude (Fig. 4.11(a)).

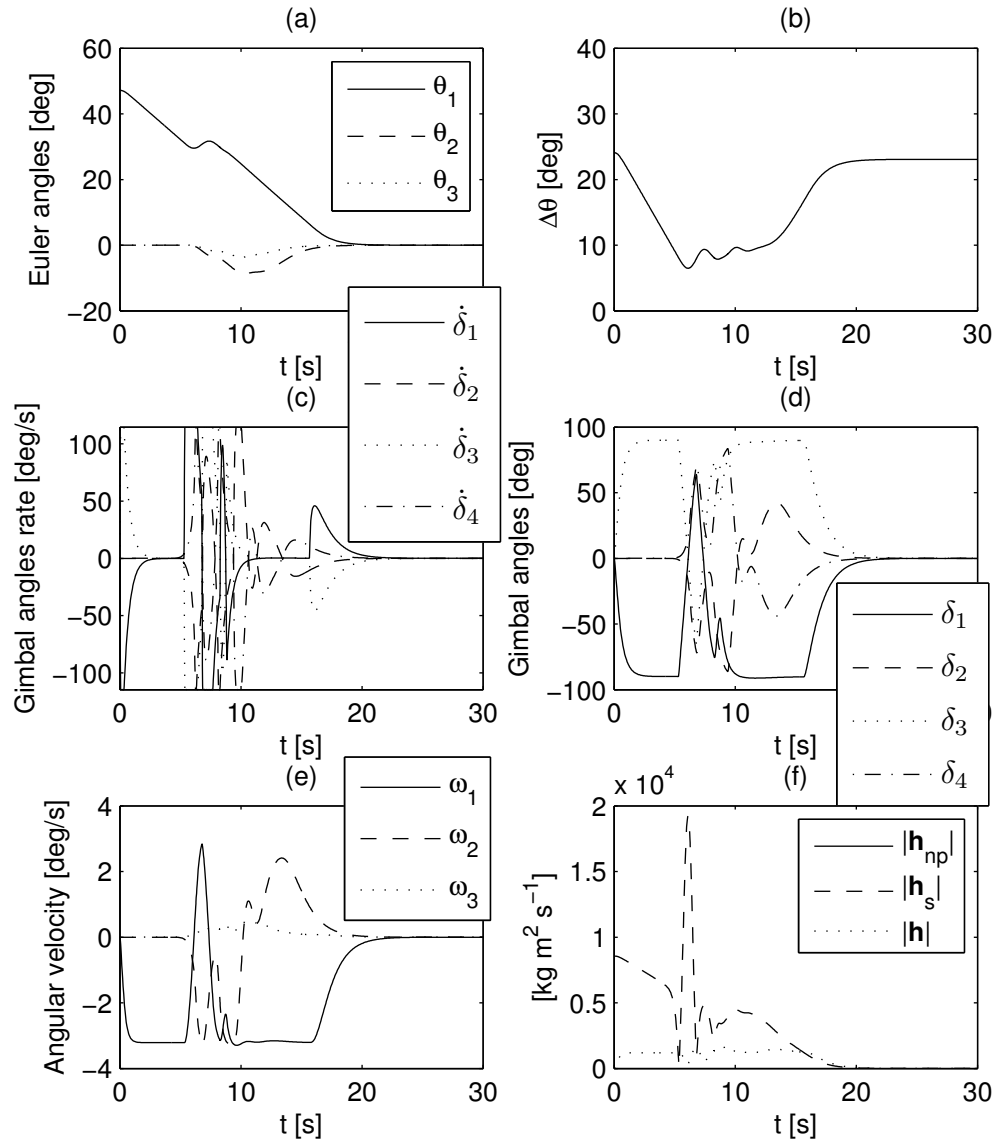


Fig. 4.11 Simulation results for the benchmark roll manoeuvre with nonlinear approximate gimbal position steering logic while avoiding a pointing constrain

Finally, we consider a slew manoeuvre of the spacecraft (with data given by Table 4.1) where the initial rest condition $\tilde{\mathbf{q}}(t_0)=[0.5 \ 0.5 \ 0.5 \ 0.5]^T$ requires a 120 deg rotation about an eigenaxis skewed by 60 deg with respect to all the body axes. Figure 4.12 shows the resulting manoeuvre when two obstacles are placed along the angular path followed during the nominal, obstacle-free case.

Again, the gimbal position command exploiting the maximum available angular momentum successfully stabilizes the spacecraft while avoiding all the forbidden attitudes, with a correction on the variation of the pitch and yaw angles, θ_2 and θ_3 (Fig. 4.12(a)), and angular velocity components (Fig. 4.12(e), where an abrupt change in the pitch and yaw angular rates is clearly visible). The first obstacle is avoided at $t = 4.5$ seconds and the minimum angular separation is kept larger than 5 deg. The deviation from the nominal angular path allows for avoiding the second one by means of a minor correction only, the second peak of the potential function in the neighbourhood of the second forbidden attitude being simply skimmed by the attitude variables at $t = 9$ seconds. The minor correction on the attitude path is hardly visible in the plots of Fig. 4.12, being evident only on the gimbal rate plot reported in Fig. 4.12(c).

The command law switches in 'convergence mode' at $t = 11.5$ seconds and the target attitude is achieved in approximately 16 seconds, when the angular velocity and the angular momentum components drop to zero (Fig. 4.12(e) and (f)). This manoeuvre time compares well with the nominal one, achieved for the obstacle free slew, when convergence on the target attitude is reached in approximately the same amount of time.

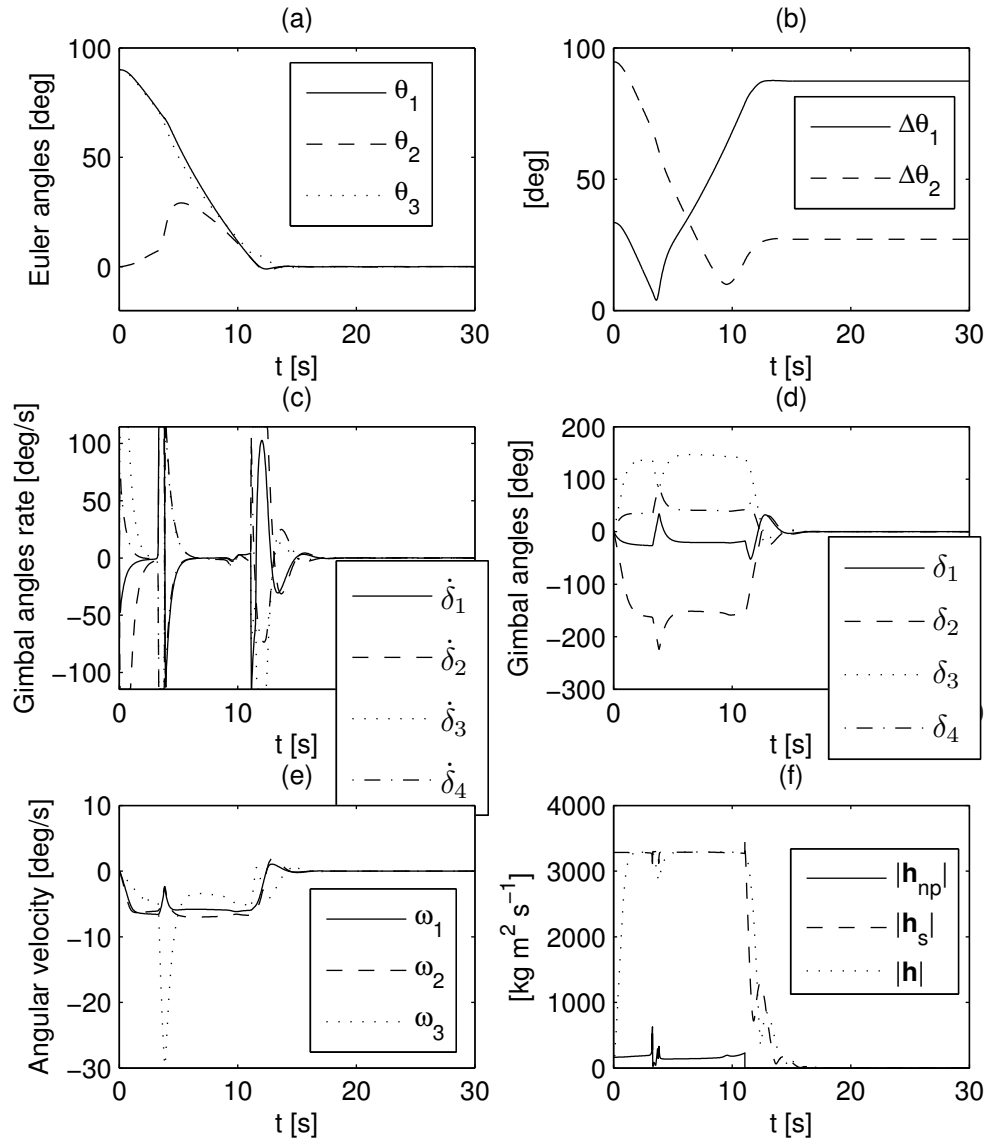


Fig. 4.12 Simulation results for the three-axis slew manoeuvre with gimbal position steering logic for maximum angular momentum while incorporating two pointing constraints

4.6 Summary

A novel gimbal position command generation algorithm has been proposed where large-angle slews are performed for the largest portion exploiting the maximum angular momentum available. In spite of the presence of an undesired angular momentum component in the direction perpendicular to the desired angular momentum command, the spacecraft is successfully driven towards the desired target attitude, final convergence being achieved by switching to a more conventional inverse kinematic solution. Numerical simulations showed that the resulting control logic allows for suboptimal performance in the obstacle-free case, where the final attitude is achieved in a total time only marginally higher than the best published results on a test benchmark pure roll manoeuvre. When an obstacle is present, minor corrections allow for keeping the forbidden attitude sufficiently far from the spacecraft angular path with minor penalties (if any) on the total manoeuvre time.

Chapter 5

Conclusions and Future Work

Here, we conclude the results from the previous chapters and identify the possible directions for the future research.

- Actuator saturation is an important issue to be addressed while designing feedback control systems. There are two general ways of circumventing this problem. The one caters for the issue a posteriori like anti-windup control methodologies. The other is to compensate the saturation a priori where the controller is designed such that the system has certain guarantees of stability and performance with the additional aim that the control action avoids reaching saturation in the presence of all anticipated bounded external disturbances and parametric uncertainties. We have exploited integrator backstepping based control design to develop a scheme pertaining to the latter category to address the said issue in the context of spacecraft attitude control problem. Reduction of the peak control torque for the spacecraft attitude stabilization and tracking manoeuvres has been achieved by introducing a new positive constant gain within the framework of conventional backstepping control method. The bounds for the control torque components are derived analytically as a function

of the initial attitude and angular velocity errors and the gains involved in the control design procedure. The proposed scheme has also been blended with the artificial potential function method for the case of large angle slew manoeuvres with constraints on the admissible attitude. It has been shown to perform adequately in the numerical simulations where we demonstrated that, for a given settling time specification, the analytical bound can be used effectively for tuning the control parameters so that the guaranteed maximum torque upper bound is minimized. The obtained values of the analytical torque bound are comparable even with the simulation values of the peak control torque reported in the literature (Wie and Barba, 1985; Krstić and Tsiotras, 1999; Joshi, Kelkar and Wen, 1995; Kim and Kim, 2003). Further, the analytical bound for the control torque has been developed for a control law that is similar in shape to the one already existing in the literature (Seo and Akella, 2007).

- The methodology can be turned to further advantage by exploiting it to avoid the cancelation of ‘good’ nonlinearities, if any, in the system (Krstić, Kanellakopoulos and Kokotovic, 1995). It may be helpful to decrease both the peak control torque from the simulation and its analytical bound.
- As we used a simple local optimization algorithm, the torque bound may also be improved further with some global optimization techniques.
- A higher control torque rate at the start is a common element among the attitude manoeuvres, reported in Chapters 2 and 3, for which the control gains have been tuned for minimizing the analytical bound of the control torque norm. This observation is specially pronounced for the manoeuvres of Chapter 3 where robustness against uncertainties in spacecraft moments of inertia and external disturbances has also been ensured. It identifies the need of also addressing the control torque rate saturation.
 - The scheme can be explored for its extension to address the problem of actuation rate saturation.

- Considering the scheme as a more general theoretical contribution, applications other than the spacecraft attitude control can be sought.
- Many other applications of artificial potential function method as available in the literature including the space applications such as proximity manoeuvring (Roger and McInnes, 2000), spacecraft guidance and control (McInnes, 1995a), formation flying (Badawy and McInnes, 2009; McQuade, Ward and McInnes, 2002), autonomous and distributed motion planning for satellite swarm (Izzo and Pettazi, 2007), on-orbit assembly of large and complex space structures (Badawy and McInnes, 2008; Izzo, Pettazzi and Ayre, 2005; McQuade and McInnes, 1997), and terminal descent on a planetary surface (McInnes, 1995b) can also be explored in conjunction with the proposed scheme.
- The scheme talks of a general class K_∞ function but a very simple form of this function has been utilized. More sophisticated forms of class K_∞ function can also be explored in pursuit of less conservative control input bound and improved robustness against bounded external disturbances and parametric uncertainties.
- While blending the scheme with artificial potential function method, only Gaussian function based repulsive potential has been considered. This choice for repulsive potential results in higher values for the analytical torque bound. This is caused by a high value of a gain associated with the Gaussian function as square and cube of this gain are involved in the calculation of analytical bound for control torque norm, an issue being typical of the Gaussian function based repulsive potential for the spacecraft slew manoeuvre problem with unit quaternion used as attitude parameterization. Larger values of the settling time have been found useful for compensating for the high value of the said Gaussian function-related gain.
 - Other forms of repulsive potentials can also be explored in conjunction with the scheme.

- The scheme can be explored as baseline framework for spacecraft failure detection and identification and reconfigurable control.
- The proposed gimbal position command generation algorithm (Chapter 4), for a major part of the spacecraft large angle reorientation manoeuvre, exploits the maximum angular momentum deliverable by the pyramid-type cluster of four single-gimbal CMGs corresponding to the direction of the commanded angular momentum. It has caused a significant reduction in the manoeuvre time when compared with the approximate nonlinear inverse kinematic solution-based gimbal position command by Avanzini (2005). However, such an implementation of gimbal position command law can be improved further in the following possible ways.
 - Firstly, the undesired angular momentum component associated with this algorithm, which perturbs the spacecraft attitude motion with respect to the desired eigen axis rotation, can to be removed.
 - Secondly, the CMG cluster angular momentum caused by this gimbal position scheme does not drop to zero as the spacecraft approaches the target attitude and some other strategy, like the approximate nonlinear gimbal position command by Avanzini (2005), has to be employed in order to bring the spacecraft at rest at the desired final attitude. The proposed algorithm can be modified so that the convergence onto the desired target attitude in the final part of the spacecraft attitude manoeuvre may be achieved without switching to a different scheme.
 - Lastly, the proposed scheme is based upon the attitude kinematics subsystem stabilization and is viable as the response of the electric motors that drive the gimbals is usually sufficiently fast, so that the required angular momentum is transferred to the satellite platform in a relatively small amount of time, during which only minor variations of spacecraft attitude are expected, resulting in small corrections to angular

velocity command. However, a more complete stability proof involving the spacecraft and actuator dynamics can also be sought.

Appendix

Backstepping Control Overview

Let us consider the following cascaded system[‡]

$$\dot{\boldsymbol{\eta}} = F(\boldsymbol{\eta}) + G(\boldsymbol{\eta})\boldsymbol{\xi} \quad (\text{a1})$$

$$\dot{\boldsymbol{\xi}} = F_a(\boldsymbol{\eta}, \boldsymbol{\xi}) + G_a(\boldsymbol{\eta}, \boldsymbol{\xi})\mathbf{u} \quad (\text{a2})$$

where $\boldsymbol{\eta} \in \mathfrak{R}^n$, $\boldsymbol{\xi} \in \mathfrak{R}^m$, $\mathbf{u} \in \mathfrak{R}^m$, $F(\mathbf{0}) = \mathbf{0}$ and $F_a(\mathbf{0}, \mathbf{0}) = \mathbf{0}$. The functions $F(\boldsymbol{\eta})$ and $F_a(\boldsymbol{\eta}, \boldsymbol{\xi})$ are continuous and the $m \times m$ matrix G_a is invertible.

The subsystem described by Eq. (a1) is stabilized first using the control law $\boldsymbol{\xi} = -f(\boldsymbol{\eta})$ and then the resultant control \mathbf{u} is developed so that the overall system described by Eqs. (a1) and (a2) is stabilized. The backstepping control design scheme can be briefly described by the following theorems.

[‡] Notation of the appendix is independent of that for the rest of the thesis.

Theorem 1: Using a candidate Lyapunov function $V(\boldsymbol{\eta})$, the subsystem described by Eq. (a1) can be stabilized by the control law $\boldsymbol{\xi} = -f(\boldsymbol{\eta})$ that satisfies the following condition

$$\frac{\partial V}{\partial \boldsymbol{\eta}} [F(\boldsymbol{\eta}) - G(\boldsymbol{\eta})f(\boldsymbol{\eta})] \leq -W(\boldsymbol{\eta}) \quad (\text{a3})$$

where $W(\boldsymbol{\eta})$ is a positive definite function.

Proof: see (Khalil, 2002)

Theorem 2: Assume that Eq. (a3) is satisfied, the overall system described by Eqs. (a1) and (a2) is stabilized by the control input given by Eq. (a6) with the augmented Lyapunov function of Eq. (a4) and its time derivative as Eq. (a5):

$$U(\boldsymbol{\eta}, \boldsymbol{\xi}) = V(\boldsymbol{\eta}) + \frac{1}{2} [\boldsymbol{\xi} + f(\boldsymbol{\eta})]^T [\boldsymbol{\xi} + f(\boldsymbol{\eta})] \quad (\text{a4})$$

$$\dot{U}(\boldsymbol{\eta}, \boldsymbol{\xi}) = \frac{\partial V}{\partial \boldsymbol{\eta}} [F - Gf] + \frac{\partial V}{\partial \boldsymbol{\eta}} G [\boldsymbol{\xi} + f] + [\boldsymbol{\xi} + f]^T \left[F_a + G_a \mathbf{u} + \frac{\partial f}{\partial \boldsymbol{\eta}} [F + G\boldsymbol{\xi}] \right] \quad (\text{a5})$$

$$\mathbf{u} = G_a^{-1} \left[-\frac{\partial f}{\partial \boldsymbol{\eta}} [F + G\boldsymbol{\xi}] - \left(\frac{\partial V}{\partial \boldsymbol{\eta}} G \right)^T - F_a - g [\boldsymbol{\xi} + f] \right] \quad (\text{a6})$$

where $g > 0$.

Proof: see (Khalil, 2002)

References

- [1] Ahmed, A., Alexander, J., Boussalis, D., Breckenridge, W., Macala, G., Mesbahi, M., San Martin, M., Singh, G., and Wong, E. (1998). *Cassini Control Analysis Book*. Jet Propulsion Laboratory, USA.
- [2] Ahmed, J., Coppola, V., and Bernstein, D. (1998). Adaptive Asymptotic Tracking of Spacecraft Attitude Motion with Inertia Matrix Identification. *Journal of Guidance, Control, and Dynamics*, **21**(5), 684–691.
- [3] Akella, M. R., Valdivia, A., and Kotamraju, G. R. (2005). Velocity-Free Attitude Controllers Subject to Actuator Magnitude and Rate Saturations. *Journal of Guidance, Control, and Dynamics*, **28**(4), 659–666.
- [4] Ali, I., and Radice, G. (2008). Autonomous Attitude Control Using Potential Function Method Under Control Input Saturation. In *The 59th International Astronautical Congress*, Glasgow, UK.

- [5] Ali, I., Radice, G. and Kim, J. (2010). Backstepping Control Design with Actuator Torque Bound for Spacecraft Attitude Manuever. *Journal of Guidance, Control, and Dynamics*, **33**(1), 254–259.
- [6] Allgöwer, F., Findeisen, R., and Nagy, Z. K. (2004). Nonlinear Model Predictive Control: From Theory to Application. *Journal of the Chinese Institute of Chemical Engineers*, **35**(3), 299-315.
- [7] Anderson, M. J., and Grantham, W. J. (1989). Lyapunov Optimal Feedback Control of a Nonlinear Inverted Pendulum. *Journal of Dynamic Systems, Measurement, and Control*, **111**, 554–558.
- [8] Angeli, D. (2004). An Almost Global Notion of Input-to-state Stability, *IEEE Transactions on Automatic Control*, **49**(6), 866–874.
- [9] Arambel, P. O., Manikonda, V., and Mehra, R. K. (2000). Spacecraft Attitude Tracking in the Presence of Input Magnitude Constraints. In *Proceedings of the American Control Conference*, Inst. of Electrical and Electronics Engineers, Piscataway, NJ, pp. 4082–4086.
- [10] Avanzini, G. (2005). Gimbal-Position Command Generation for a Cluster of Control Moment Gyroscopes. In *AAS/AIAA Astrodynamics Specialist Conference*, Lake Tahoe, CA, USA.
- [11] Avanzini, G. and Palmas, A. C. (2007). Singularity-free control moment gyroscope steering law by a potential function approach. In *Proceedings of the XIX Conference of the Italian Association for Aeronautics and Astronautics (AIDAA)*, Forlì, Italy.
- [12] Avanzini, G., Radice, G., and Ali, I. (2009). Potential Approach for Constrained Autonomous Manoeuvres of a Spacecraft Equipped with a Cluster of Control Moment Gyroscopes. *Proceedings of the Institution of Mechanical Engineers, Part G: Journal of Aerospace Engineering*, **223**(3), 285-296.
- [13] Badawy, A., and McInnes, C. R. (2008). On-Orbit Assembly Using Superquadric Potential Fields. *Journal of Guidance, Control, and Dynamics*, **31**(1), 30–43.

- [14] Badawy, A., and McInnes, C. R. (2009). Small Spacecraft Formation Using Potential Functions. *Acta Astronautica*, **65**, 1783–1788.
- [15] Bang, H., Tahk, M.-J., and Choi, H.-D. (2003). Large Angle Attitude Control of Spacecraft with Actuator Saturation. *Control Engineering Practice*, **11**, 989–997.
- [16] Bauer, F. H., Femiano, M. D., and Mosier, G. E. (1992). Attitude Control System Conceptual Design for the X-Ray Timing Explorer. In *Proceedings of the AIAA Guidance, Navigation and Control Conference* (pp. 236–249). AIAA, Washington DC.
- [17] Bedrossian, N. S., Paradiso, J., Bergmann, E. V., and Rowell, D. (1990a). Steering Law Design for Redundant Single-Gimbal Control Moment Gyroscopes. *Journal of Guidance, Control, and Dynamics*, **13**(6), 1083–1089.
- [18] Bedrossian, N. S., Paradiso, J., Bergmann E. V., and Rowell, D. (1990b). Redundant Single Gimbal Control Moment Gyroscopes Singularity Analysis. *Journal of Guidance, Control and Dynamics*, **13**(6), 1096–1101.
- [19] Bhat, S. P., and Bernstein, D. S. (2000). A Topological Obstruction to Continuous Global Stabilization of Rotational Motion and the Unwinding Phenomenon. *Systems and Control Letters*, **39**(1), 63–70.
- [20] Bilimoria, K., and Wie, B. (1993). Time-Optimal Three-Axis Reorientation of a Rigid Spacecraft. *Journal of Guidance, Control, and Dynamics*, **16**(3), 446–452.
- [21] Bošković, J. D. (1997). A Multiple Model-Based Controller for Nonlinearly-Parametrized Plants. In *Proceedings of American Control Conference (ACC)* (pp. 2140–2144). Evanston, IL.
- [22] Bošković, J. D., Li, S.-M., and Mehra, R. K. (1999). Globally Stable Adaptive Tracking Control Design for Spacecraft Under Input Saturation. *Proceedings of the 1999 IEEE Conference on Decision and Control*, Vol. 2, IEEE Press, Piscataway, NJ, pp. 1952–1957.

- [23] Bošković, J. D., Li, S.-M., and Mehra, R. K. (2001). Robust Adaptive Variable Structure Control of Spacecraft Under Control Input Saturation. *Journal of Guidance, Control and Dynamics*, **24**(1), 14–22.
- [24] Bošković, J. D., Li, S.-M., and Mehra, R. K. (2004). Robust Tracking Control Design for Spacecraft Under Control Input Saturation. *Journal of Guidance, Control and Dynamics*, **27**(4), 627–633.
- [25] Bryson, A. E. (1994). *Control of Spacecraft and Aircraft*. Chap. 9, Princeton, NJ: Princeton University Press.
- [26] Caccavale, F., and Villani, L. (1999). Output Feedback Control for Attitude Tracking. *Systems and Control Letters*, **38**(2), 91–98.
- [27] Casasco, M., and Radice, G. (2004). Autonomous Slew Manoeuvring and Attitude Control Using the Potential Function Method. *Advances in the Astronautical Sciences*, **116**, 1745–1765.
- [28] Casasco, M., and Radice, G. (2005a). Time-Varying Potential Function Control for Constrained Attitude Tracking. *Advances in the Astronautical Sciences*, **119**, 555–575.
- [29] Casasco, M., and Radice, G. (2005b). Optimal Results for Autonomous Attitude Control Using the Potential Function Method. *Advances in the Astronautical Sciences*, **119**, 1369–1389.
- [30] Chaturvedi, N., Bloch, A., and McClamroch, N. (2006) Global Stabilization of a Fully Actuated Mechanical System on a Riemannian Manifold Including Control Saturation Effects, In *Proceedings of the 45th IEEE Conference on Decision and Control*, pp. 6116–6121.
- [31] Chaturvedi, N., and McClamroch, N. (2007). Attitude Stabilization of the Inverted 3D Pendulum on TSO(3) with Control Saturation. In *Proceedings of the 46th IEEE Conference on Decision and Control*, pp. 1910–1915.

- [32] Chaturvedi, N., McClamroch, N., and Bernstein, D. (2007). Stabilization of a Specified Equilibrium in the Inverted Equilibrium Manifold of the 3D Pendulum. In *Proceedings of the American Control Conference*, pp. 2485–2490.
- [33] Choi, H. D., Bang, H., and Kim, Z. C. (1999). Design Methods for Rocket Attitude Control Systems Subject to Actuator Saturation. *Journal of Guidance, Control, and Dynamics*, **22**(1), 183–185.
- [34] Collaudim, B., and Passvogel, Th. (1998). The FIRST and Planck Carrier Missions: Description of Cryogenic Systems. In *1998 Space Cryogenics Workshop*, ESTEC, Noordwijk, Netherlands.
- [35] Cortes, J. (2008). Discontinuous Dynamic Systems. *IEEE Control Systems Magazine*, **28**(3), 36–71.
- [36] Crassidis, J. L., and Markley, F. L. (1996). Sliding Mode Control Using Modified Rodrigues Parameters. *Journal of Guidance, Control, and Dynamics*, **19**(6), 1381–1383.
- [37] Crassidis, J. L., Markley, F. L., Anthony, T. C., and Andrews, S. F. (1997). Nonlinear Predictive Control of Spacecraft. *Journal of Guidance, Control, and Dynamics*, **20**(6), 1096–1103.
- [38] Crassidis, J. L., Vadali, S. R., and Markley, F. L. (2000). Optimal Variable-Structure Control Tracking of Spacecraft Maneuvers. *Journal of Guidance, Control, and Dynamics*, **23**(3), 564–566.
- [39] Creamer, G., Delahunt, P., Gates, S., and Levenson, M. (1996). Attitude Determination and Control of Clementine during Lunar Mapping. *Journal of Guidance, Control, and Dynamics*, **19**(3), 505–511.
- [40] Cristi, R., and Burl, J. (1993). Adaptive Eigenaxis Rotations. In *European Control Conference*, Groningen, Netherlands.

- [41] DeCarlo, R. A., Zak, S. H., and Matthews, G. P. (1988). Variable Structure Control of Nonlinear Multivariable Systems: A Tutorial. *Proceedings of the IEEE*, **76**(3), 212–232.
- [42] Di Gennaro, S. (1997). Stabilization of Rigid Spacecraft with Uncertainties and Input Saturation in a Central Gravitational Field. In *Proceedings of the 36th Conference on Decision and Control*, Vol. 5, IEEE Press, Piscataway, NJ, pp. 4204–4209.
- [43] Dwyer, T. A. W., III (1984). Exact Nonlinear Control of Large Angle Rotational Maneuvers. *IEEE Transactions on Automatic Control*, **AC-29**(9), 769–774.
- [44] Dwyer, T. A. W., III (1986). Exact Nonlinear Control of Spacecraft Slewing Maneuvers with Internal Momentum Transfer. *Journal of Guidance, Control, and Dynamics*, **9**(2), 240–247.
- [45] Dwyer, T. A. W., III, and Sira-Ramirez, H. (1988). Variable-Structure Control of Spacecraft Attitude Maneuvers. *Journal of Guidance, Control, and Dynamics*, **11**(3), 262–270.
- [46] Egeland, O., and Godhavn, J. M. (1994). Passivity-Based Adaptive Attitude Control of a Rigid Spacecraft. *IEEE Transactions on Automatic Control*, **39**, 842–846.
- [47] Emelyanov, S. V. (1967). *Variable Structure Control Systems*. (in Russian), Nauka, Moscow.
- [48] Esfandiari, F., and Khalil, H. K. (1992). Output Feedback Stabilization of Fully Linearizable Systems. *International Journal of Control*, **56**(5), 1007–1037.
- [49] Fjellstad, O.-E., and Fossen, T. I. (1994). Comments on “The Attitude Control Problem”. *IEEE Transactions on Automatic Control*, **39**(3), pp. 699–700.
- [50] Ford, K. A., and Hall, C. D. (2001). Singular Direction Avoidance Steering for Control-Moment Gyros. *Journal of Guidance, Control and Dynamics*, **23**(4), 648–656.

- [51] Frakes, J. P., Henretty, D. A., Flatley, T. W., Markley, F. L., San, J. K., and Lightsey, E. G. (1992). SAMPEX Science Pointing with Velocity Avoidance. In *AAS/AIAA Spaceflight Mechanics Meeting 1992*, Colorado Springs, CO, USA.
- [52] Franklin, G. F., Powell, J. D., and Emami-Naeini, A. (1994). *Feedback Control of Dynamic Systems*, (pp. 196–199, 304–310). Menlo Park, CA: Addison–Wesley.
- [53] Frazzoli, E., Dahleh, M. A., Feron, E., and Kornfeld, R. (2001). A Randomized Attitude Slew Planning Algorithm for Autonomous Spacecraft. In *AIAA Guidance, Navigation, and Control Conference*, Montreal, Quebec, Canada.
- [54] Friedland, B. (1996). *Advanced Control System Design*, (Chap. 6). Englewood Cliffs, NJ: Prentice–Hall.
- [55] Ge, S. S., and Cui, Y. I. (2002). Dynamic Motion Planning for Mobile Robots Using Potential Field Method. *Autonomous Robots*, **13**(3), 207–222.
- [56] Hablani, H. B. (1999). Attitude Commands Avoiding Bright Objects and Maintaining Communication with Ground Station. *Journal of Guidance, Control, and Dynamics*, **22**(6), 759–767.
- [57] Hanu, R., Kinnaert, M., and Henrotte, J. L. (1987). Conditioning Technique, A General Anti-windup and Bumpless Transfer Method. *Automatica*, **23**, 729–739.
- [58] Heiberg, C. J., Bailey, D., and Wie, B. (1997). Precision Pointing Control of Agile Spacecraft Using Single Gimbal Control Moment Gyros. In *AIAA Guidance, Navigation, and Control Conference*, New Orleans, LA, USA.
- [59] Huang, Y., and Lu, W.-M. (1996). Nonlinear Optimal Control: Alternative to Hamilton-Jacobi Equations. *Proceedings of the 35th IEEE Conference on Decision and Control*, IEEE Press, Piscataway, NJ, pp. 3942–3947.
- [60] Hughes, P. C. (1986). *Spacecraft Attitude Dynamics*. New York: Wiley.
- [61] Hung, J. Y., Gao, W., and Hung, J. C. (1993). Variable Structure Control: A Survey. *IEEE Transactions on Industrial Electronics*, **40**(1), 2–22.

- [62] Izzo, D., and Pettazi, L. (2007). Autonomous and Distributed Motion Planning for Satellite Swarm. *Journal of Guidance, Control, and Dynamics*, **30**(2), 449–459.
- [63] Izzo, D., Pettazzi, L., and Ayre, M. (2005). Mission Concept for Autonomous on Orbit Assembly of a Large Reflector in Space. In *56th International Astronautical Congress*, Fukuoka, Japan.
- [64] Jacot, A. D., and Liska, D. J. (1966). Control Moment Gyros in Attitude Control. *Journal of Spacecrafts and Rockets*, **3**(9), 1313–1320.
- [65] Joshi, S. M., Kelkar, A. G., and Wen, J. T. (1995). Robust Attitude Stabilization of Spacecraft Using Nonlinear Quaternion Feedback. *IEEE Transactions on Automatic Control*, **40**(10), 1800–1803.
- [66] Junkins, J. L., Akella, M. R., and Robinett, R. D. (1997). Nonlinear Adaptive Control of Spacecraft Maneuvers. *Journal of Guidance, Control, and Dynamics*, **20**(6), 1104–1110.
- [67] Junkins, J. L., and Bang, H. (1993a). Lyapunov Optimal Control Law for Flexible Space Structure Maneuver and Vibration Control. *Journal of the Astronautical Sciences*, **41**(1), 91–118.
- [68] Junkins, J. L., and Bang, H. (1993b). Maneuver and Vibration Control of Hybrid Coordinate Systems Using Lyapunov Stability Theory. *Journal of Guidance, Control, and Dynamics*, **16**(4), 668–676.
- [69] Junkins, J. L., and Kim, Y. (1993). *Introduction to Dynamics and Control of Flexible Structures*, AIAA Education Series. Washington, DC: AIAA.
- [70] Junkins, J. L., and Turner, J. D. (1980). Optimal Continuous Torque Attitude Maneuvers. *Journal of Guidance, Control, and Dynamics*, **3**(3), 210–217.
- [71] Kalman, R. E., and Bertram, J. E. (1960a). Control Systems Analysis and Design via the Second Method of Lyapunov: Continuous Time Systems. *Journal of Basic Engineering*, pp. 371–393.

- [72] Kalman, R. E., and Bertram, J. E. (1960b). Control Systems Analysis and Design via the Second Method of Lyapunov: Discrete Time systems. *Journal of Basic Engineering*, pp. 394–400.
- [73] Kanellakopoulos, I., Kokotovic, P.V., and Morse, A. S. (1992). A Toolkit for Nonlinear Feedback Design. *Systems and Control Letters*, **18**, 83–92.
- [74] Karlgaard, C. D. (2006). Robust Reorientation and Power Controller Using Flywheels and Control Moment Gyroscopes. *Journal of Guidance, Control, and Dynamics*, **29**(1), 217–220.
- [75] Khalil, H. K. (2002). *Nonlinear Systems*. 3rd Ed., Chap. 14, Upper Saddle River, NJ: Prentice–Hall.
- [76] Khatib, O. (1986). Real-Time Obstacle Avoidance for Manipulators and Mobile Robots. *International Journal of Robotics Research*, **5**(1), 90–98.
- [77] Kim, K.-S., and Kim, Y. (2003). Robust Backstepping Control for Slew Maneuver Using Nonlinear Tracking Function. *IEEE Transactions on Control Systems Technology*, **11**(6), 822-829.
- [78] Kim, Y., and Mesbahi, M. (2004). Quadratically Constrained Attitude Control via Semidefinite Programming. *IEEE Transactions on Automatic Control*, **49**(5), 731-735.
- [79] Kim, Y., Mesbahi, M., Singh, G., and Hadaegh, F.Y. (in press) On the Convex Parameterization of Spacecraft Orientation in Presence of Constraints and its Application. *IEEE transactions on Aerospace and Electronic Systems*.
- [80] Koditschek, D. E. (1988). The Application of Total Energy as a Lyapunov Function for Mechanical Control Systems, Dynamics and Control of Multibody Systems. In *Proceedings of the AMS-IMS-SIAM Joint Summer Research Conference at Bowdin College, Maine*, edited by J. E. Marsden, P. S. Krishnaprasad, and J. C. Simo, Vol. 97, American Mathematical Society, Providence, RI, pp. 131–157.

- [81] Kokotovic, P. V. (1992). Bode lecture: The Joy of Feedback. *IEEE Control System Magazine*, **3**, 7–17.
- [82] Kothare, M. V., Campo, P. J., Morari, M., and Nett, C. N. (1994). A Unified Framework for the Study of Anti-windup Designs. *Automatica*, **30**, 1869–1883.
- [83] Krikelis, N. J. (1980). State Feedback Integral Control with Intelligent Integrators. *International Journal of Control*, **32**, 465–473.
- [84] Krstić, M., Kanellakopoulos, I., and Kokotovic, P. (1995). *Nonlinear and Adaptive Control Design*. New York: Wiley Interscience.
- [85] Krstić, M., and Tsiotras, P. (1999). Inverse Optimal Stabilization of a Rigid Spacecraft. *IEEE Transactions on Automatic Control*, **44**(5), 1042–1049.
- [86] Kurokawa, H. (1997). Constrained Steering Law of Pyramid-Type Control Moment Gyros and Ground Tests. *Journal of Guidance, Control, and Dynamics*, **20**(3), 445–449.
- [87] Kurokawa, H. (2007). Survey of Theory and Steering Laws of Single-Gimbal Control Moment Gyros. *Journal of Guidance, Control, and Dynamics*, **30**(5), 1331–1340.
- [88] Lai, L.-C., Yang, C.-C., and Wu, C.-J. (2007). Time-Optimal Maneuvering Control of a Rigid Spacecraft. *Acta Astronautica*, **60**, 791–800.
- [89] Lappas, V., and Wie, B. (2009). Robust Control Moment Gyroscope Steering Logic with Gimbal Angle Constraints. *Journal of Guidance, Control, and Dynamics*, **32**(5), 1662–1666.
- [90] Lee, B., and Grantham, W. J. (1989). Aeroassisted Orbital Maneuvering Using Lyapunov Optimal Feedback Control. *Journal of Guidance, Control, and Dynamics*, **12**(2), 237–242.
- [91] Li, Z.-X., and Wang, B.-L. (2006). Several Problems on Rejecting Disturbances Acting on Rigid Spacecraft. *The IMACS Multi-conference on Computational*

Engineering in Systems Applications, Vol. 1, Tsinghua University Press, Beijing, pp. 663–669.

- [92] Li, Z.-X., and Wang, B.-L. (2007). Robust Attitude Tracking Control of Spacecraft in the Presence of Disturbances. *Journal of Guidance, Control and Dynamics*, **30**(4), 1156–1159.
- [93] Lizarralde, F., and Wen, J. T. (1996). Attitude Control without Angular Velocity Measurement: A Passivity Approach. *IEEE Transactions on Automatic Control*, **41**, 468–472.
- [94] Lo, S.-C., and Chen, Y.-P. (1995). Smooth Sliding-Mode Control for Spacecraft Attitude Tracking Maneuvers. *Journal of Guidance, Control, and Dynamics*, **18**(6), 1345–1349.
- [95] Loria, A., and Nijmeijer, H. (1998). Bounded Output Feedback Tracking Control of Fully Actuated Euler–Lagrange Systems. *Systems and Control Letters*, **33**(3), 151–161.
- [96] Luo, W., Chu, Y.-C., and Ling, K.-V. (2005a). H_∞ Inverse Optimal Attitude-Tracking Control of Rigid Spacecraft. *Journal of Guidance, Control, and Dynamics*, **28**(3), 481–493.
- [97] Luo, W., Chu, Y.-C., and Ling, K.-V. (2005b). Inverse Optimal Adaptive Control for Attitude Tracking of Spacecraft. *IEEE Transactions on Automatic Control*, **50**(11), 1639–1654.
- [98] Lyapunov, A. M. (1892). The General Problem of the Stability of Motion (in Russian). Kharkov Mathematical Society (250 pp.), Collected Works II, 7. Republished by the University of Toulouse 1908 and Princeton University Press 1949 (in French), republished in English by *International Journal of Control* 1992.
- [99] Lyapunov, A. M. (1992). The General Problem of the Stability of Motion (translated into English by A. T. Fuller). *International Journal of Control*, **55**, 531–773. Also published as a book by Taylor & Francis, London.

- [100] Marandi, S. R., and Modi, V. J. (1987). A Preferred Coordinate System and the Associated Orientation Representation in Attitude Dynamics. *Acta Astronautica*, **15**(11), 833–843.
- [101] Margulies, G., and Aubrun, J. N. (1978). Geometric Theory of Single-Gimbal Control Moment Gyro System. *Journal of the Astronautical Sciences*, **26**(2), 159–191.
- [102] Mazenc, F., and Iggidr, A. (2004). Backstepping with Bounded Feedbacks. *Systems and Control Letters*, **51**, 235–245.
- [103] McDuffie, J. H., and Shtessel, Y. B. (1997). A Sliding Mode Controller and Observer for Satellite Attitude Control. In *AIAA Guidance, Navigation, and Control Conference*, New Orleans, LA, USA.
- [104] McInnes, C. R. (1994). Large Angle Slew Maneuvers with Autonomous Sun Vector Avoidance. *Journal of Guidance, Control, and Dynamics*, **17**(4), 875–877.
- [105] McInnes, C. R. (1995a). Potential Function Methods for Autonomous Spacecraft Guidance and Control. In *Astrodynamics 1995: AAS/AIAA Astrodynamics Conference*, Halifax, Nova Scotia, Canada.
- [106] McInnes, C. R. (1995b). Path Shaping Guidance for Terminal Lunar Descent. *Acta Astronautica*, **36**(7), 367–377.
- [107] McQuade, F., and McInnes, C. R. (1997). Autonomous Control for On-Orbit Assembly Using Potential Function Methods. *The Aeronautical Journal*, **101**(1008), 255–262.
- [108] McQuade, F., Ward, R., and McInnes, C. R. (2002). The Autonomous Configuration of Satellite Formations Using Generic Potential Functions. In *International Symposium: Formation Flying Missions and Technologies*, Centre National d'Etudes Spatiales, Toulouse Space Centre, France.

- [109] Mengali, G., and Quarta, A. A. (2004). Spacecraft Control with Constrained Fast Reorientation and Accurate Pointing. *The Aeronautical Journal*, **108**(1080), 85–91.
- [110] Meyer, G. (1966). On the Use of Euler’s Theorem on Rotations for the Synthesis of Attitude Control Systems. NASA TN D-3643.
- [111] Meyer, G. (1971). Design and Global Analysis of Spacecraft Attitude Control Systems. NASA TR R-361.
- [112] Mulder, E. F., Tiwari, P. Y., and Kothare, M. V. (2009). Simultaneous Linear and Anti-Windup Controller Synthesis Using Multiobjective Convex Optimization. *Automatica*, **45**, 805–811.
- [113] Nakamura, Y., and Hanafusa, H. (1986). Inverse Kinematic Solutions with Singularity Robustness for Robot Manipulator Control. *Journal of Dynamic Systems, Measurement, and Control*, **108**, 163–171.
- [114] Narendra, K. S., and Annaswamy, A. (1989). *Stable Adaptive Systems*. Englewood Cliffs, NJ: Prentice–Hall.
- [115] Narendra, K. S., and Bošković, J. D. (1990). Robust Adaptive Control Using a Combined Approach. *International Journal of Adaptive Control and Signal Processing*, **4**(2), 111–131.
- [116] Narendra, K. S., and Bošković, J. D. (1992). A Combined Direct, Indirect and Variable Structure Method for Robust Adaptive Control. *IEEE Transactions on Automatic Control*, **37**(2), 262–268.
- [117] Oh, H. S., and Vadali, S. R. (1991). Feedback Control and Steering Laws for Spacecraft Using Single Gimbal Control Moment Gyros. *Journal of the Astronautical Sciences*, **39**(2), 183–203.
- [118] Paielli, R. A., and Bach, R. E. (1993). Attitude Control with Realization of Linear Error Dynamics. *Journal of Guidance, Control, and Dynamics*, **16**(1), 182–189.

- [119] Paradiso, J. A. (1992). Global Steering of Single Gimbal Control Moment Gyroscopes Using a Directed Search. *Journal of Guidance, Control, and Dynamics*, **15**(5), 1236–1244.
- [120] Pechev, A. N. (2007). Feedback-Based Steering Law for Control Moment Gyros. *Journal of Guidance, Control, and Dynamics*, **30**(3), 848–855.
- [121] Radice, G., and Casasco, M. (2007). On different parameterisation methods to analyse spacecraft attitude manoeuvres in the presence of attitude constraints. *The Aeronautical Journal*, **111**(1119), 335–342.
- [122] Radice, G., and McInnes, C. R. (1999). Constrained On-Board Attitude Control Using Gas Jet Thrusters. *The Aeronautical Journal*, **103**(1030), 549–556.
- [123] Radice, G., and McInnes, C. R. (2001). Multiple Target Selection and Obstacle Avoidance Using Potential Function Guidance Method. *Advances in the Astronautical Sciences*, **109**, 1721–1733.
- [124] Reyhanoglu, M., van der Schaft, A., McClamroch, N., and Kalmanovsky, I. (1999). Dynamics and Control of a Class of Underactuated Mechanical Systems. *IEEE Transactions on Automatic Control*, **AC-44**(9), 1663–1671.
- [125] Robinett, R. D., Parker, G. G., Schaub, H., and Junkins, J. L. (1997a). Lyapunov Optimal Saturated Control for Nonlinear Systems. In *35th Aerospace Sciences and Meeting*, Reno, NV, USA.
- [126] Robinett, R. D., Parker, G. D., Schaub, H., and Junkins, J. L. (1997b). Lyapunov Optimal Saturated Control for Nonlinear Systems. *Journal of Guidance, Control, and Dynamics*, **20**(6), 1083–1088.
- [127] Roger, A. B., and McInnes, C. R. (2000). Passive-Safety Constrained Free-Flyer Path-Planning with Laplace Potential Guidance at the International Space Station. *Journal of Guidance, Control, and Dynamics*, **23**(2), 332–338.

- [128] Sanyal, A., Fosbury, A., Chaturvedi, N., and Bernstein, D. S. (2009). Inertia-Free Spacecraft Attitude Tracking with Disturbance Rejection and Almost Global Stabilization. *Journal of Guidance, Control, and Dynamics*, **32**(4), 1167–1178.
- [129] Sastry, S., and Bodson, M. (1989). *Adaptive Control: Stability, Convergence and Robustness*. Upper Saddle River, NJ: Prentice–Hall.
- [130] Schaub, H., Akella, M. R., and Junkins, J. L. (2000). Adaptive Realization of Linear Closed Loop Tracking Dynamics in the Presence of Large System Model Errors. *Journal of the Astronautical Sciences*, **48**(4), 537–551.
- [131] Schaub, H., Akella, M. R., and Junkins, J. L. (2001). Adaptive Control of Nonlinear Attitude Motions Realizing Linear Closed Loop Dynamics. *Journal of Guidance, Control and Dynamics*, **24**(1), 95–100.
- [132] Schaub, H., and Junkins, J. L. (1996). Stereographic Orientation Parameters for Attitude Dynamics: A Generalization of the Rodrigues Parameters. *Journal of the Astronautical Sciences*, **44**(1), 1–19.
- [133] Schaub, H., and Junkins, J. L. (2000). Singularity Avoidance Using Null Motion and Variable-Speed Control Moment Gyros. *Journal of Guidance, Control and Dynamics*, **23**(1), 11–16.
- [134] Schaub, H., and Junkins, J. L. (2003). *Analytical Mechanics of Space Systems*, AIAA Education Series. Chap. 8, AIAA.
- [135] Schaub, H., Robinett, R. D., and Junkins, J. L. (1996). Globally Stable Feedback Laws for Near-Minimum-Fuel and Near-Minimum-Time Pointing Maneuvers for a Landmark-Tracking Spacecraft. *Journal of the Astronautical Sciences*, **44**(4), 443–466.
- [136] Schaub, H., Robinett, R. D., and Junkins, J. L. (1997). New Penalty Functions for Optimal Control Formulation for Spacecraft Attitude Control Problems. *Journal of Guidance, Control, and Dynamics*, **20**(3), 428–434.

- [137] Scrivener, S. L., and Thompson, R. C. (1994). Survey of Time-Optimal Attitude Maneuvers. *Journal of Guidance, Control and Dynamics*, **(17)**2, 225-233.
- [138] Seo, D., and Akella, M. R. (2007). Separation Property for the Rigid-Body Attitude Tracking Control Problem. *Journal of Guidance, Control, and Dynamics*, **30**(6), 1569–1576.
- [139] Seywald, H. (2001). Globally Asymptotically Stable Reorientation Controller with Control Constraint and Slew Rate Limit. *Journal of the Astronautical Sciences*, **48**(1), 45–67.
- [140] Sharma, R., and Tewari, A. (2004). Optimal Nonlinear Tracking of Spacecraft Attitude Maneuvers. *IEEE Transactions on Control Systems Technology*, **12**(5), 677-682.
- [141] Shen, H., and Tsiotras, P. (1999). Time-Optimal Control of Axisymmetric Rigid Spacecraft Using Two Controls. *Journal of Guidance, Control, and Dynamics*, **22**(5), 682–694.
- [142] Shuster, M. D. (1993). A Survey of Attitude Representations. *Journal of the Astronautical Sciences*, **41**(4), 439–517.
- [143] Singh, G., Macala, G., Wong, E., and Rasmussen, R. (1997). A Constraint Monitor Algorithm for the Cassini Spacecraft. In *AIAA Guidance, Navigation and Control Conference*, Reston, VA, USA.
- [144] Singh, S. A., and Iyer, A. (1989). Nonlinear Decoupling Sliding Mode Control and Attitude Control of Spacecraft. *IEEE Transactions on Aerospace and Electronic Systems*, **25**(5), 621–633.
- [145] Skaar, S. B., and Kraige, L. G. (1984). Large Angle Spacecraft Attitude Maneuvers Using an Optimal Reaction Wheel Power Criterion. *Journal of Astronautical Sciences*, **32**(1), 47–61.

- [146] Slotine, J. E., and Li, W. (1991). *Applied Nonlinear Control*. pp. 12–85, Englewood Cliffs, NJ: Prentice–Hall.
- [147] Sontag, E. D., and Sussmann, H. J. (1989). Further Comments on the Stabilizability of the Angular Velocity of a Rigid Body. *Systems and Control Letters*, **12**, 213–217.
- [148] Sorenson, A. M. (1993). ISO Attitude Maneuver Strategies. In *Spaceflight dynamics 1993: AAS/NASA 8th International Symposium*, Greenbelt, MD, USA.
- [149] Tatsch, A., Xu, Y., and Fitz-Coy, N. (2005). A Nonlinear Controller via Artificial Potential Functions for Spacecraft Attitude Maneuvers. *Advances in the Astronautical Sciences*, **121**, 107–123.
- [150] Tayebi, A. (2008). Unit Quaternion-Based Output Feedback for the Attitude Tracking Problem. *IEEE Transactions on Automatic Control*, **53**(6), 1516–1520.
- [151] Teel, A. R. and Kapoor, N. (1997). The L_2 Anti-windup Problem: Its Definition and Solution. In *European Control Conference*. Brussels, Belgium.
- [152] Teel, A. R., and Praly, L. (1995). Tools for Semiglobal Stabilization by Partial State and Output Feedback. *SIAM Journal of Control and Optimizations*, **33**(5), 1443–1488.
- [153] Terui, F. (1998). Position and Attitude Control of a Spacecraft by Sliding Mode Control. In *Proceedings of the American Control Conference (ACC)* (pp. 217–221). Philadelphia, PA, USA.
- [154] Tewari, A. (2002). Optimal Nonlinear Spacecraft Attitude Control through Hamilton-Jacobi Formulation. *Journal of the Astronautical Sciences*, **50**(1), 99–112.
- [155] Tsiotras, P. (1996). Stabilization and Optimality Results for the Attitude Control Problem. *Journal of Guidance, Control, and Dynamics*, **19**(4), 772–779.
- [156] Tsiotras, P. (1998). Further Passivity Results for the Attitude Control Problem. *IEEE Transactions on Automatic Control*, **43**(11), 1597–1600.

- [157] Tsiotras, P., and Doumchenko, V. (2000). Control of Spacecraft Subject to Actuator Failures—State-of-the-Art and Open Problems. *Journal of the Astronautical Sciences*, **48**(2–3), 337–358.
- [158] Tsiotras, P., and Luo, J. (2000). Control of Under-actuated Spacecraft with Bounded Inputs. *Automatica*, **36**(8), 1153–1169.
- [159] Utkin, V. I. (1997). Variable Structure Systems with Sliding Modes. *IEEE Transactions on Automatic Control*, **22**(2), 212–222.
- [160] Vadali, S. R. (1986). Variable-Structure Control of Spacecraft Large-Angle Maneuvers. *Journal of Guidance, Control, and Dynamics*, **9**(2), 235–239.
- [161] Vadali, S. R., and Junkins, J. L. (1984). Optimal Open Loop and Stable Feedback Control of Rigid Spacecraft Attitude Maneuvers. *Journal of the Astronautical Sciences*, **32**(2), 105–122.
- [162] Vadali, S. R., and Krishnan, S. (1995). Suboptimal Command Generation for Control Moment Gyroscopes and Feedback Control of Spacecraft. *Journal of Guidance, Control, and Dynamics*, **18**(6), 1350–1354.
- [163] Vadali, S. R., Oh, H., and Walker, S. (1990). Preferred Gimbal Angles for Single Gimbal Control Moment Gyroscopes. *Journal of Guidance, Control, and Dynamics*, **13**(6), 1090–1095.
- [164] Wallsgrove, R. J., and Akella, M. R. (2005). Globally Stabilizing Saturated Attitude Control in the Presence of Bounded Unknown Disturbances. *Journal of Guidance, Control and Dynamics*, **28**(5), 957–963.
- [165] Wan, C.-J., and Bernstein, D. S. (1995). Nonlinear Feedback Control with Global Stabilization. *Dynamics and Control*, **5**(4), 321–346.
- [166] Wen, J. T.-Y., and Kreutz-Delgado, K. (1991). The Attitude Control Problem. *IEEE Transactions on Automatic Control*, **36**(10), 1148–1162.

- [167] Wie, B. (1998). *Space Vehicle Dynamics and Control, AIAA Education Series*. Chap. 7, Reston, VA: AIAA.
- [168] Wie, B. (2004). Singularity Analysis and Visualization for Single-Gimbal Control Moment Gyro Systems. *Journal of Guidance, Control, and Dynamics*, **27**(2), 271–282.
- [169] Wie, B. (2005). Singularity Escape/Avoidance Steering Logic for Control Moment Gyro Systems. *Journal of Guidance, Control, and Dynamics*, **28**(5), 948–956.
- [170] Wie, B., and Barba, P. M. (1985). Quaternion Feedback for Spacecraft Large Angle Maneuvers. *Journal of Guidance, Control, and Dynamics*, **8**(3), 360–365.
- [171] Wie, B., Heiberg, C. J., and Bailey, D. (2001). Singularity Robust Steering Logic for Redundant Single-Gimbal Control Moment Gyros. *Journal of Guidance, Control, and Dynamics*, **24**(5), 865–872.
- [172] Wie, B., Heiberg, C. J., and Bailey, D. (2002). Rapid Multi-Target Acquisition and Pointing Control of Agile Spacecraft. *Journal of Guidance, Control, and Dynamics*, **25**(1), 96–104.
- [173] Wie, B., and Lu, J. (1995). Feedback Control Logic for Spacecraft Eigenaxis Rotations Under Slew Rate and Control Constraints. *Journal of Guidance, Control, and Dynamics*, **18**(6), 1372–1379.
- [174] Wie, B., Weiss, H., and Arapostathis, A. (1989). Quaternion Feedback Regulator for Spacecraft Eigenaxis Rotations. *Journal of Guidance, Control, and Dynamics*, **12**(3), 375–380.
- [175] Wu, B., Cao, X., and Li, Z. (2009). Multi-Objective Output-feedback Control for Microsatellite Attitude Control: An LMI Approach. *Acta Astronautica*, **64**, 1021–1031.
- [176] Ximénez de Ferrán, S. (1991). The ISO Spacecraft. *ESA Bulletin*, **67**, 17–24.

[177] Yoon, H. (2004). *Spacecraft Attitude and Power Control Using Variable Speed Control Moment Gyros*. Ph.D. thesis, Georgia Institute of Technology, USA.